SRI International

Final Report • March 1992

LOW PRESSURE THERMAL DECOMPOSITION STUDIES SELECTED NITRAMINE AND DINITRAMINE ENERGETIC MATERIALS

M. J. Rossi, D. F. McMillen, and D. M. Golden

SRI Project 8999
Contract No. N00014-90-C-0115
MP 91-281

Prepared for:

Office of Naval Research
Code 1132P
800 North Quincy Street
Arlington, VA 22217

Attn: Dr. Richard Miller

333 Ravenswood Avenue • Menlo Park, CA 94025-3493 • (415) 326-6200 • FAX (415) 326-5512 • Telex: 334486

Final Report • March 1992

LOW PRESSURE THERMAL DECOMPOSITION STUDIES SELECTED NITRAMINE AND DINITRAMINE ENERGETIC MATERIALS

M. J. Rossi, D. F. McMillen, and D. M. Golden

SRI Project 8999
Contract No. N00014-90-C-0115
MP 91-288

Prepared for:

Office of Naval Research
Code 1132P
800 North Quincy Street
Arlington, VA 22217

Attn: Dr. Richard Miller

Approved:

D. S. Ross, Director
Chemistry Laboratory

David M. Golden
Vice President
Physical Sciences Division

Statement A per telecon
Dr. Richard Miller ONR/Code 432
Arlington, VA 22217-5000

NWW 3/26/92

SRI International 333 Ravenswood Avenue • Menlo Park, CA 94025-3493 • (415) 326-6200 • FAX. (415) 326-5512 • Telex: 334486

LOW PRESSURE THERMAL DECOMPOSITION STUDIES OF SELECTED NITRAMINE AND DINITRAMINE ENERGETIC MATERIALS

Michel J. Rossi, Donald F. McMillen and David M. Golden
Chemistry Laboratory, SRI International, Menlo Park CA 94025-3434

EXECUTIVE SUMMARY

Under sponsorship of the Office of Naval Research (Contract No. N00014-90-C-0115), SRI International conducted a study of the thermal decomposition of a newly developed energetic material ammonium dinitramide (ADN), as well as, for comparison, two related materials ammonium nitrate (AN), and nitramide (NH_2NO_2). Brief studies were also performed with RDX and with $AgN(NO_2)CH_2CN$, which was tested as a potential source of the suspected RDX intermediate $CH_2 = NNO_2$. The former portion of the work has resulted in a manuscript, which is being submitted for publication and is included as an appendix to this final report. A summary of the work and its principal findings is given below, beginning with the results for ADN itself.

Pyrolysis of ADN under low pressure showed acid-base dissociation like AN, but it also resulted in some decomposition to N_2O, NO, and water. The onset of evolution of these species was at 90°C, and as in the case of AN, an "explosive" event was noted at 174°C, which is about 80°C higher than the melting point of ADN and 15°C higher than thermal decomposition in a DSC. When the cryostat window was left at ambient temperature, only dinitramine, HDN, condensed on it, along with some water as determined by FTIR. However, if the window was cooled to -190°C, ADN was formed again.

The experiment with the cryostat at ambient temperature provided us the opportunity to examine the properties of the acid component of ADN, namely HDN, which has not been previously obtained in the pure form. FTIR of the film showed the characteristic N-H stretch at 3250 cm^{-1}. Also some of the other major bands were shifted from the corresponding bands in ADN, a result that is consistent with the formation of the free acid. Interestingly enough, when we bled ammonia into the system containing HDN, we did not observe the formation of the salt. This result is puzzling and should be pursued in a future research effort.

To test whether the decomposition products seen in ADN pyrolysis were a result of HDN decomposition, we subjected the HDN film to thermal stress. HDN decomposed very readily, the

gentlest of warming (cryostat temperature >60°C) produced peaks corresponding to H_2O, NO, and N_2O. Most significantly, no peaks were observed at m/z 46 or 62 (ion fragments of HDN), which implies that the HDN film decomposed but did not evaporate. Using FTIR, we determined that the HDN was completely depleted from the KCl window by 140°C. The finding that no HDN evaporated intact from the HDN film even at temperatures as low as 70°C means that HDN in the bulk condensed state is much less stable than that formed as an isolated species during ADN pyrolysis. This finding is significant and suggests that care should be exercised to avoid buildup of HDN during storage of ADN. Furthermore, we speculate that the decomposition of condensed phase HDN occurs more rapidly than that of various dinitramide salts because the very high acidity of HDN makes an acid-catalyzed, self-protonation pathway readily accessible. This conclusion is consistent with the recent finding that acids destabilize ADN.

Slow heating of ammonium nitrate (AN) in our system produced only ammonia and nitric acid—an acid-base dissociation—and no nitrous oxide. The sample was completely depleted by the time it was heated to 200°C. Evidently nitrous oxide, which is the commonly observed product of thermal decomposition under atmospheric pressure, is produced by a secondary reaction of nitric acid with itself (or possibly with its decomposition products or with excess AN) at higher temperatures. The evolved nitric acid and ammonia condensed on the cold cryostat window to re-form AN, whose identity was verified by FTIR. If the window was left at ambient temperature, the gases did not condense to form a film.

The temperature-programmed pyrolysis of AN always exhibited an "explosive" event, characterized by a sudden temporary increase of the mass spectral signal as well as of the background pressure. This event took place around 182°C. However, even during and following this event, we observed only ammonia and nitric acid, which are the products of an *endothermic* dissociation. Hence, we suspect that the event was a result of the sample melting into a thin film with a substantially larger surface area and better thermal contact with the sample container. This event is nominally about 12°C higher than the melting point of AN, 170°C; however, there are significant uncertainties in the temperature measurement, because we expect the sample temperature to lag somewhat behind the thermocouple reading.

The behavior of nitramide was substantially different. Even at ambient temperature, there was considerable gas evolution. The mass spectrum of the evolving gases showed peaks due to nitramide or its decomposition products. These peaks are not entirely due to fragment ions from nitramide, because the relative intensities of the peaks changed with time; most notably, the peaks at m/z 18 (H_2O) and 44 (N_2O) increased and persisted even after the peak at m/z 62 (parent nitramide) was gone. We suggest that autocatalytic decomposition of nitramide in the condensed phase competes with its sublimation even at ambient temperatures. FTIR of the material condensed

on the cold window (-190°C) showed nitramide and some water. Gradual warming of the window first released the water with a T_{max} at -113°C. The rate of water evolution declined above -113°C, but again increased above -82°C. The second rise in water signal is a result of additional nitramide decomposition as evidenced by a rise in the intensity of peaks at m/z 30, 44, 46, and 62. The relative intensity of the peak at m/z 62 decreased with time (and increasing temperature), as decomposition into N_2O and H_2O became prominent.

A shorter series of experiments was performed with RDX and $AgN(NO_2)CH_2CN$, a specially synthesized potential precursor to N-nitromethyleneimine (CH_2=NNO_2), a long-suspected intermediate in the decomposition of RDX. Only very limited success was obtained in these experiments, with the apparent early decomposition of RDX being traced primarily to changes in ion fragmentation routes due to changes in RDX pressure in the mass spectrometer ion source. Experiments with $AgN(NO_2)CH_2CN$ revealed some decomposition to CH_2O and N_2O, the secondary decomposition products of CH_2=NNO_2, but substantial production of free silver, indicating failure to form the "designed" elimination product AgCN in high yield.

All of the above thermal decomposition studies were conducted in a vacuum chamber with provisions for continuous monitoring of the evolving gases by a quadrupole mass spectrometer, and for trapping condensibles on a cryostatically cooled window for examination by FTIR. Typically about 1 mg of the sample was taken in a melting point capillary and placed inside a heatable direct insertion probe. The sample was heated at 0.3 to 200°C/min in the low pressure chamber. Since decomposition generally leads to volatile gases, which are immediately removed from the sample, our experimental set up minimizes secondary reactions and provides an opportunity for examining the early stages of thermal decomposition.

The above findings for ADN decomposition can be summarized as follows:

- ADN is much more stable than NH_4NO_2 with respect to decomposition and is similar to NH_4NO_3 with respect to acid-base dissociation.
- True decomposition of ADN appears to take place through secondary reactions of the free acid (HDN), probably through self-protonation.
- Secondary decomposition of HDN is more facile than that of HNO_3: ADN shows real decomposition at temperatures and pressures where NH_4NO_3 undergoes only acid/base dissociation.
- Isolated HDN molecules are stable to ~140°C; condensed phase HDN is found to exist primarily in the N-H form and begins decomposing below ~70°C.
- These results lead to the projection that limitation of hydrolysis/dissociation of ADN to HDN is key to maintaining the storage stability and insensitivity of ADN.

Recommendations

Since dissociation of ADN to its acid-base components occurs at moderate temperature in vacuum, and since the condensed-phase free dinitraminic acid is much less stable than ADN or other dinitramide salts, the reactions of HDN almost certainly play a key role in determining the storage stability and combustion behavior of ADN. Moreover, the high acidity of HDN suggests that self-protonation reactions control decomposition of neat HDN, and also means that limiting the hydrolysis of dinitramide salts is key to maintaining the storage stability of ADN. Therefore, the interplay of acid-catalyzed and "thermal" (i.e., non-ionic) decomposition of ADN is an area that warrants a concerted effort. For example, in the present study, we found that slowing the heating rate during vacuum thermal decomposition of ADN to ~0.3°C/min resulted in intact HDN molecules no longer being delivered into the gas phase at 94°C. However, other work by Schmitt and coworkers shows that holding the ADN melt more than 10°C higher (107°C) in flowing N_2 for 22 hours resulted in less than 8% "evaporation" of ADN and in *no* autoacceleratory process. This apparent discrepancy may well result from differing degrees of removal of the base component NH_3 at the two different pressures. We recommend that the decomposition behavior of ADN be thoroughly characterized as a function temperature, acidity, and concentration in aqueous and non-aqueous liquid phase environments. We believe in this case that such studies are even more important than the gas-phase thermal decomposition measurements, which are themselves a baseline for understanding the thermal condensed phase behavior.

CONTENTS

LIST OF FIGURES

INTRODUCTION AND BACKGROUND

This report describes the results of our experiments on the thermal decomposition of $NH_4N(NO_2)_2$, NH_4NO_3, NH_2NO_2, RDX, and $AgN(NO_2)CH_2CN$ in an apparatus described in the next section. Our results delineate the possible pathways in the thermal decomposition of those energetic materials as well as some similarities between them and thus provide a guide to future experiments in the more relevant high heating rate regime

Bottaro and Schmitt of SRI's Chemistry Laboratory recently synthesized for the first time[1] several examples in a family of novel energetic materials, namely, salts of the previously unknown compound dinitramide acid $HN(NO_2)_2$. A typical member of the family is the ammonium dinitramide, $NH_4N(NO_2)_2$ ("SRI-12"or ADN). This energetic material shows considerable promise for fulfilling the requirement of a new alternative to existing solid high energy/high density material. It is a representative of a potential new class of energetic materials that is free of chlorine. This and other desirable features lead us to wish to learn more about the modes of thermal decomposition and detonation. The facts gathered in this investigation should guide the intuition for the optimization of synthesis procedures for ADN itself, for synthesis of similar yet improved organic energetic molecules, or for potential modification of storage stability, sensitivity, or burn rate parameters.

In view of the absence of any detailed information on the thermal decomposition of dinitramide, we conducted baseline thermal decomposition experiments and compared its behavior under thermal stress with that of NH_4NO_3 and NH_2NO_2. By comparing the behavior of this series of compounds, we obtained insight into the relationship between evaporation/sublimation and thermal decomposition. In view of the unique experimental capability described below, we also undertook some thermal baseline experiments on the decomposition of RDX under our experimental conditions and contrasted its behavior to that recently observed in a molecular beam by Y. T. Lee and coworkers.[2] In the course of this latter effort, an attempt was made to thermally generate methylene nitramine, CH_2=NNO_2. Because CH_2 = NNO_2 is an expected (albeit so far elusive) reactive intermediate that can be formed and consumed by several different reaction

pathways during the thermal decomposition of RDX and related nitramines, independent information about its behavior may be critical to a real understanding of what controls burning rates during nitramine-based propellant combustion.

We appreciate full well that the most desirable kind of experiments on the kinetics of decomposition of energetic materials include thermal stress experiments under high heating rate conditions, and such experiments are the logical end result of the present preliminary investigations. Rapid rate thermal experiments, performed for example by shock heating or laser heating, come closest to the relevant regimes of combustion and/or initiation of detonation of energetic material. However, in the near complete absence of experimental data for the potentially interesting novel energetic material ADN, we thought it appropriate to focus our investigations on some "base-line" slow thermal decomposition experiments that are preparatory to experiments under high heating rate conditions and may provide useful indications of the mode(s) of decomposition under higher heating rate conditions.

In fact, the present investigations reveal at least two more competing pathways in the low heating rate thermal decomposition of ADN and strongly suggest that investigations at high heating rates be undertaken. The kinetic behavior will thus be controlled by the branching ratio and the rates of the different decomposition pathways prevailing under the conditions of use. Homogeneous as well as heterogeneous kinetic processes are probably both important and revolve around the question in which phase the energy release takes place. Answers to these types of detailed questions may ultimately lead to the possibility of sensitivity modification and burn rate control of the dinitramide-based materials.

In addition, we undertook experiments on the decomposition behavior of NH_4NO_3 and NH_2NO_2 under the same experimental conditions in separate reference experiments because of their obvious close relationship with ADN. (We will usually refer to ammonium dinitramide by the acronym ADN, and for consistency to the free acid as HDN or dinitraminic acid. In deference to common usage, we will use the name nitramide for NH_2NO_2)

In a formal sense, ADN is the dimer of nitramide, NH_2NO_2:

$$NH_4N(NO_2)_2 \rightarrow 2\ NH_2NO_2 \qquad (1)$$

Nitramide, in turn, is related to NH_4NO_3, because the latter decomposes thermally via nitramide as an intermediate according to (2):

$$NH_4NO_3 \rightarrow H_2O + NH_2NO_2 \quad (2)$$

Reaction (2) has been corroborated by experiment,[3] and two competing pathways have been found, both involving NH_2NO_2 (or its protonated form) as an intermediate. These similarities suggest that one of the thermal decomposition pathways for ADN might lead to H_2O and N_2O [see the hypothetical reaction (1)] according to reaction (3):

$$NH_4N(NO_2)_2 \rightarrow 2H_2O + 2N_2O \quad (3)$$

This possible connection between ADN and NH_4NO_3 via NH_2NO_2 as a common intermediate provides useful leading questions as to the modes of thermal decomposition of ADN, even though the mechanism for thermal decomposition may not involve NH_2NO_2 at all. In addition to the irreversible thermal decomposition reactions (1), (2) and (3), we must consider, as with other ammonium salts, simple reversible sublimation according to reactions (4) and (5)

$$NH_4N(NO_2)_2 \rightarrow NH_3 + HN(NO_2)_2 \quad (4)$$

$$NH_4NO_3 \rightarrow NH_3 + HONO_2 \quad (5)$$

In addition to the thermal decomposition of $NH_4N(NO_2)_2$, NH_2NO_2, and NH_4NO_3, this report also describes the results of a shorter series of experiments with RDX and $AgN(NO_2)CH_2CN$ using the same thin-film diagnostic apparatus. The goal in these latter studies was to use the combined mass spectral and FTIR monitoring capabilities to obtain new information on the possible intermediacy of N-nitromethyleneimine in the decomposition of RDX and other cyclic nitramines.

EXPERIMENTAL APPARATUS AND PROCEDURES

THIN-FILM DIAGNOSTIC APPARATUS.

The experimental apparatus is designed around a high vacuum chamber housing a cryogenically cooled optically transparent substrate. The sample is put in a heatable melting tube capillary that is positioned opposite the cooled substrate. The observables in this experiment are both the FTIR absorption spectrum of the condensed pyrolysate on a KCl window and the mass spectral signature of the gaseous pyrolysis products that did not condense under our experimental conditions. Information is also provided by the mass spectrum of gaseous products generated when the KCl window is heated This process is essentially a temperature-programmed desorption (TPD), although the heating rate control is not yet precise. The mass spectrometer is operated as a residual gas analyzer whose vacuum chamber walls are heated to slightly above ambient, so that to minimize background signals, various parts of the chamber walls range from about 50° to 70°C. The cryostat is cooled using liquid N_2, but the lowest temperature of the KCl window that could be achieved was about 95 K because the cryostat was not heat-shielded by a shroud. Therefore, certain gases such as N_2, NO, and N_2O, whose vapor pressures at that temperature exceed the ultimate pressure in the vacuum system, do not condense on the KCl window.

Figure 1 presents a schematic of the apparatus used in the present investigations. The high vacuum chamber (base pressure of 10^{-8} Torr) is pumped by a 2000 L/s oil diffusion pump and equipped with the cryogenic KCl window (liquid N_2 cooled), a heatable sample probe (lower left of Figure 1), and a quadrupole mass spectrometer (Balzers QMG 511, left of Figure 1) operated in residual gas analysis mode. The mass spectrometry chamber is pumped by a turbomolecular pump and is automatically isolated from the deposition/pyrolysis chamber by a gate valve in case the pressure becomes too high in the mass spectral analysis chamber. The material requirements for pyrolysis are minimal in that 0.5 to 2 mg of solid sample are put in a melting point capillary and inserted in the probe tip. The probe is introduced into the vacuum chamber through an air-lock fitted with 1/2 in Cajon fittings. The probe tip itself, shown in Figure 2,.consists of a double-walled quartz tube, whose inner wall (i.d. 2-mm) forms a well that accepts the capillary sample holder with only about 20-mil clearance. The annular space between the two walls contains the loops of a Ni-Cr wire heater. A type "K" thermocouple is butted against the bottom of the well, so

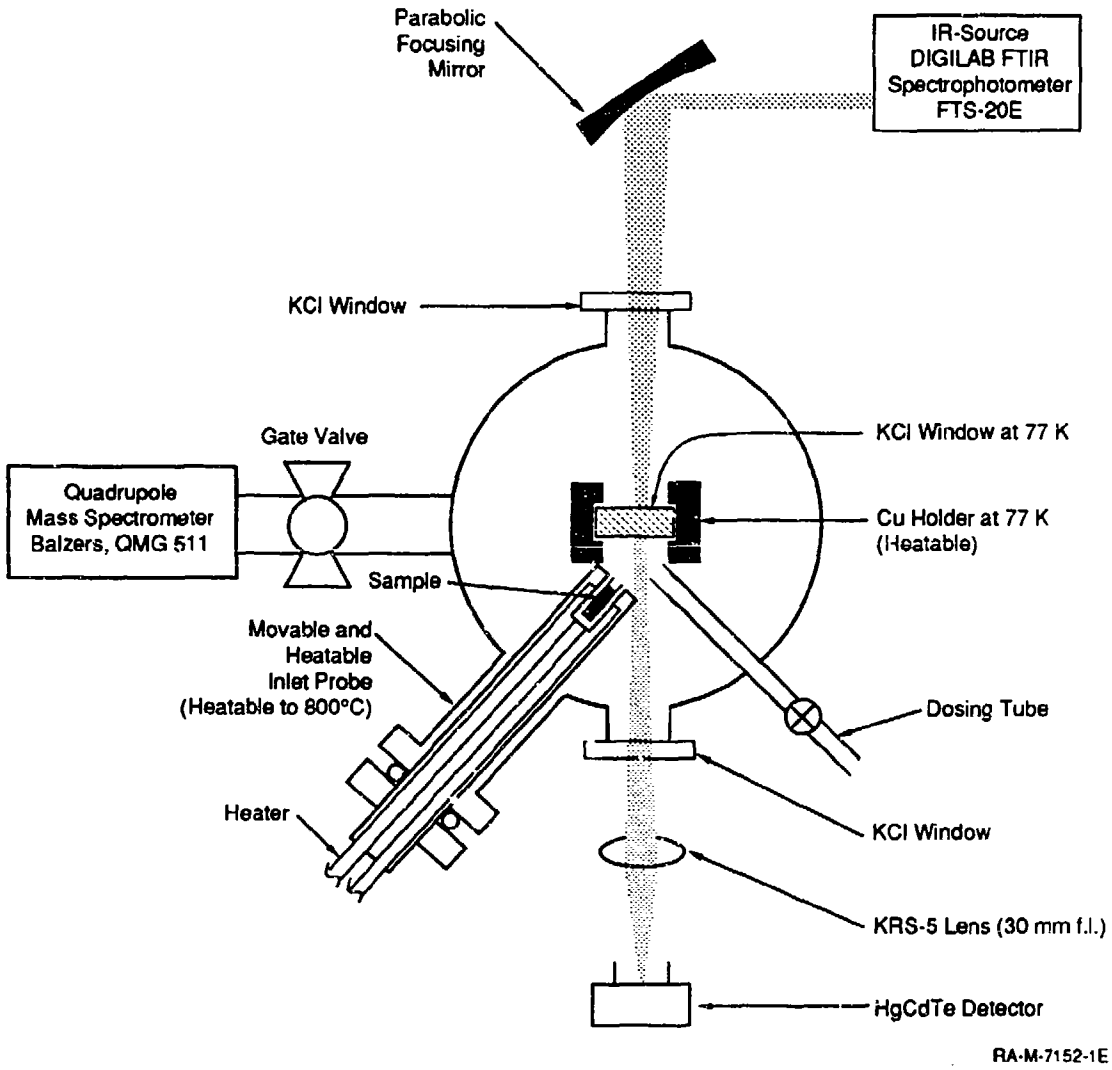

Figure 1. Thin film diagnostic apparatus using FTIR-absorption and mass spectrometry.

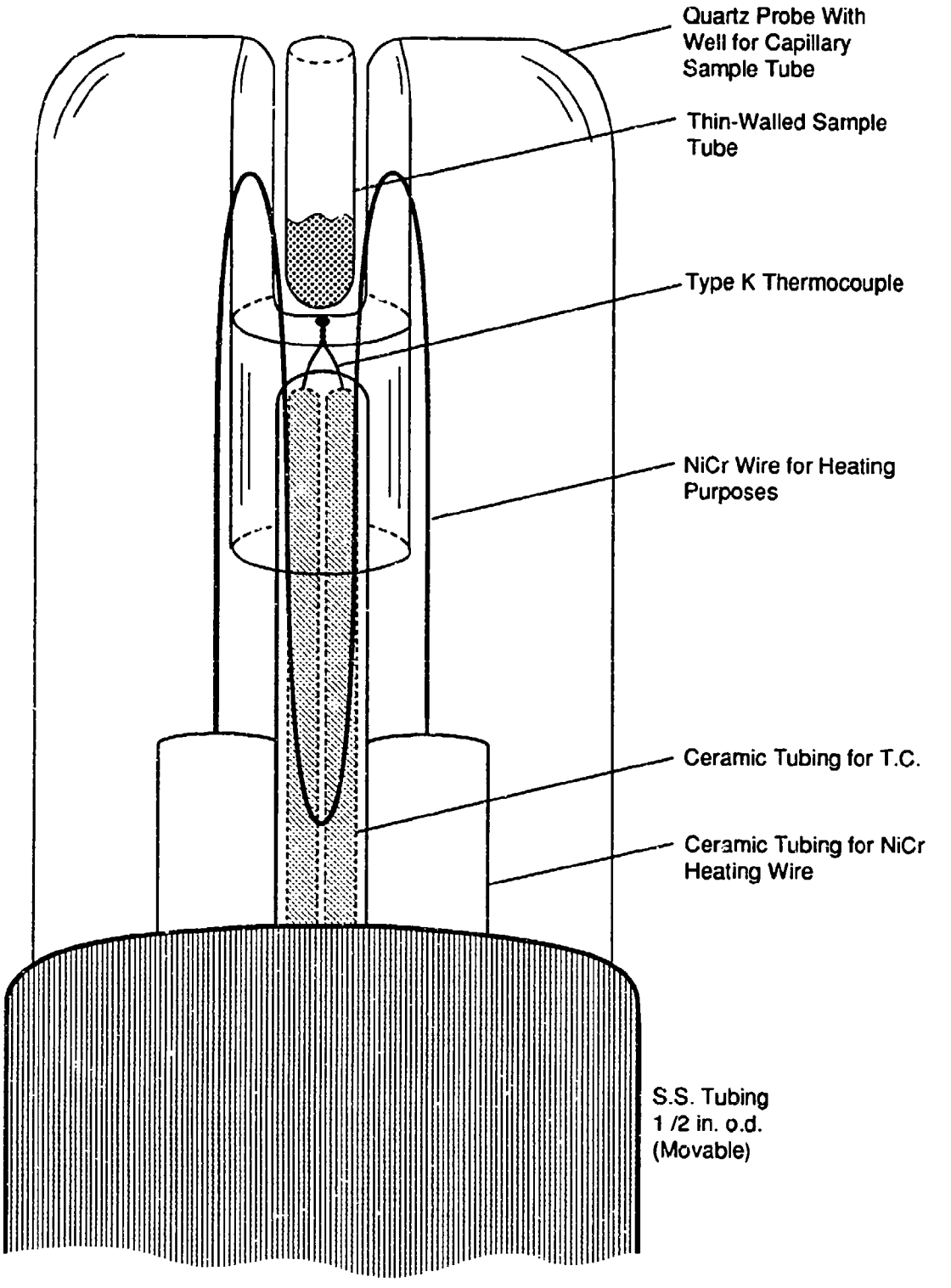

Figure 2. Schematic cross section of the resistively heated fused silica probe tip for holding capillary sample tubes.

that it makes good thermal contact with the capillary tube sample holder. When the heating rates are on the order of a few degrees Celsius per minute, this type of probe provides temperature readings that are within ~10 °C of the true temperature.

With sample sizes of 0.5 to 2 mg , mass spectra and FTIR spectra of thin films of μm thickness have been obtained with excellent signal-to-noise ratios (≥100). A typical experimental sequence of events consists of increasing the probe temperature while collecting the pyrolysate on either the cold (77 K) or ambient temperature IR transmission window. The temperature of the cryostat is monitored at the tip farthest from the liquid nitrogen using either type "E" or "T" thermocouples.

DECOMPOSITION EXPERIMENTS.

During the thermal decomposition, FTIR spectra are obtained as the pyrolysis products collect on the cryogenic window, while the mass spectrometer monitors the gas evolution of material that is not condensed on the cryogenic window. We obtain either a scan of the complete mass spectrum at a given temperature or a time-dependent, and therefore temperature-dependent, trace of a particular fragment ion when the temperature of the probe is increased in some monotonic fashion.

Two types of experiments were conducted. In the first type we cooled the KCl window to essentially liquid nitrogen temperature and started the pyrolysis by turning on the heater coil in the sample probe. A mass spectral scan or mass spectral record at a particular mass was taken as a function of probe temperature. This type of measurement addresses primarily those gaseous components that do not condense at the low temperature of the cryostat. Furthermore, because the gas phase components are recorded in terms of residual gases analysis, the parent neutrals have interacted with the large internal surface of the reaction vessel. After the sample had been completely decomposed/evaporated, the cryostat was raised to ambient temperature, either by letting it warm up by itself (radiative heating from the usually warm vacuum chamber walls) or by heating it with the heating element wrapped around the thermostat. After the KCl window reached ambient temperature, the cryostat was further heated either until complete IR transmission of the KCl window was restored or until the temperature reached approximately 300°C. During the warming periods, both mass scans or FTIR absorption spectra were repeatedly taken as a function of temperature of the cryostat. In this way a record was obtained of both the desorbed gaseous component (mass spectrometry) as well as the condensed component not yet desorbed, hence sticking to the KCl window (FTIR absorption spectroscopy).

The second type of experiments simply consisted of starting the pyrolysis with the cryogenic window at ambient temperature, which traps only the less volatile products of the pyrolysis. By comparing both sets of experiments, we gained useful insight into the nature of the pyrolysis products as will be shown below.

Once the material in the probe is exhausted, the cryogenic window (originally at any temperature from 95 K to ambient) is heated to desorb the condensate, and then mass spectra are recorded with increasing window temperature in the same way as before until the cryogenic window is again "clean." In some of the experiments "cryostat" temperatures up to 300°C were required to rid the KCl window of any absorptions in the IR. In this way mass spectra are obtained of all the components of the pyrolysate, whereas FTIR spectra are recorded only for those components that can be collected on the cryogenic window.

FTIR spectra were recorded using a DIGILAB FTS-20E spectrometer, whose external beam was not purged. Therefore, the resulting IR spectra show some residual presence of atmospheric absorbers, even after nominal spectral subtraction of the known atmospheric constituents (H_2O, CO_2) using a background spectrum recorded at the start of the experiment. IR radiation leaving the optics bench of the FTIR spectrometer was directed using two flat first -surface Al mirrors onto a 3-in.-diameter-first surface Al focusing mirror (fl = ~5 in.). The vacuum system was sealed by two 2-in. flat KCl windows. After passage through the cryogenic KCl window and before detection, the diverging IR beam was again focused using a 1-in. focal length KRS-5 lens onto a wide band-width HgCdTe detector (5000-500 cm^{-1}).

MATERIAL PREPARATION.

ADN [$NH_4N(NO_2)_2$], NH_2NO_2, and $AgN(NO_2)CH_2CN$ were synthesized by Bottaro, Penwell, and Schmitt of SRI's Chemistry Laboratory.[1] In experiments with ADN, we observed small contributions at m/e = 55 and 57 that originate from a small impurity of n-C_4H_9OH, which was used to recrystallize ADN. The RDX samples were obtained from SRI's Poulter Laboratory, and NH_4NO_3 was used as obtained from a commercial source after ball-milling it for 2 minutes.

Some difficulties were encountered with degradation of vacuum pump oil, notwithstanding the very small amounts of nitrocompounds being decomposed. We observed that the hydrocarbon "white" oil became extremely viscous (just like honey) after only minute contamination with RDX and/or its decomposition products. Since the Balzers turbomolecular pump (TPH 270) was lubricated with Fomblin oil and experienced no difficulty, we switched to the use of a fluorocarbon oil (KRYTOX; Du pont) in the Leybold D-30A forepump and had no apparent trouble since.

RESULTS AND DISCUSSION

A. NH_4NO_3

The thermal decomposition of NH_4NO_3, which was previously studied under more confined conditions[3,4] was followed by mass spectrometry to provide a baseline for examination of nitramide and ammonium dinitramide, the other two members of this "family." Both NH_3 and HNO_3 were observed as the only products evolving to similar extents at a given temperature (congruous evaporation). Figure 3 presents a mass scan at the average temperature of 163°C (158°C at the start, to 169°C at the end of the scan).

The mass spectrum was taken with the cryostat at -190°C. Figure 3 unambiguously shows the presence of NH_3 at m/e 16 and 17 and HNO_3 at m/e 63 (small but significant relative to a background spectrum), as well as at 46 and 30. Even though the equilibrium vapor pressure of both components is below 10^{-8} Torr at -190°C, the residual mass spectrum shows the presence of these two gases. Thus trapping is not 100% efficient even though the tip of the probe (in protracted position) is less than 3 cm from the surface of the KCl window. Another possible reason for the presence of gas phase NH_3 and $HONO_2$ could be that some portion of the plume emanating from the sample capillary "misses" the cryogenic surface, leading to a small but finite partial pressure in the vacuum system. The maximum of the gas evolution was measured in the mass scan from 177° to 187°C, that is, slightly above the melting point of 169.6°C.

Figures 4 and 5 display the FTIR transmission spectrum after the sample has been fully evaporated from the probe, that is, after the probe temperatures reached 203°C. Figure 4 is the absorption spectrum with the cryostat at -190°C. Figure 5 displays the spectrum obtained from that same sample after the the cryostat had warmed to -50°C. The latter spectrum is identical to a pure NH_4NO_3 absorption spectrum, whereas the spectrum displayed in Figure 4 is a composite of NH_4NO_3 with a small amount of NH_3 (note the bending mode at 958 cm^{-1}). Conspicuously absent from the lower temperature spectrum in Figure 4, however, is any indication of the presence of HNO_3, which would manifest itself through the very intense absorption at 1710 cm^{-1} and 870 cm^{-1}. We conclude that, in the temperature range from -188° to -50°C, NH_3 evaporates, after which pure NH_4NO_3 remains. The characteristic broad N-H stretch at 3150 cm^{-1}, the asymmetric and symmetric NO_2 stretch at 1440 and 1400 cm^{-1}, and the sharp 825 cm^{-1} absorptions displayed in Figure 4 are all characteristic features of NH_4NO_3. When the cryostat was at ambient

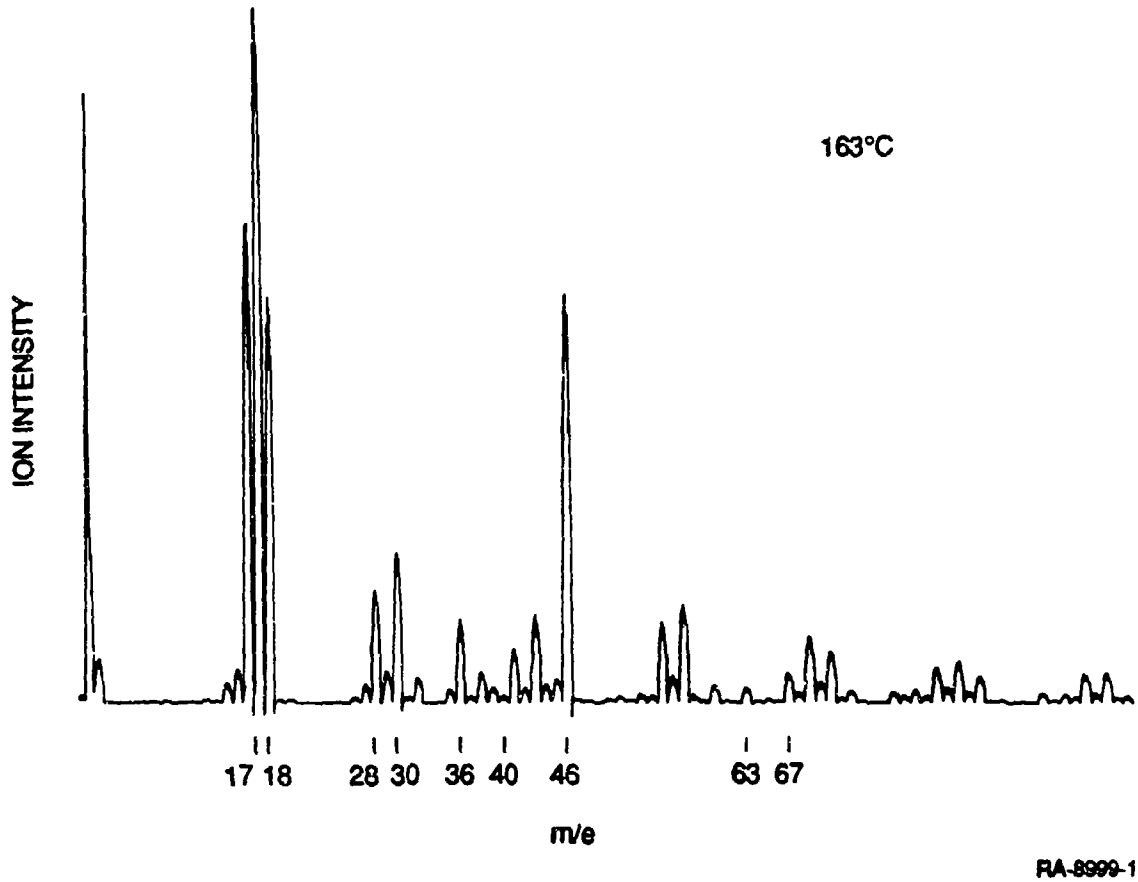

Figure 3. Mass spectrum recorded during NH_4NO_3 decomposition at 163°C with the cryostat at -190°C.

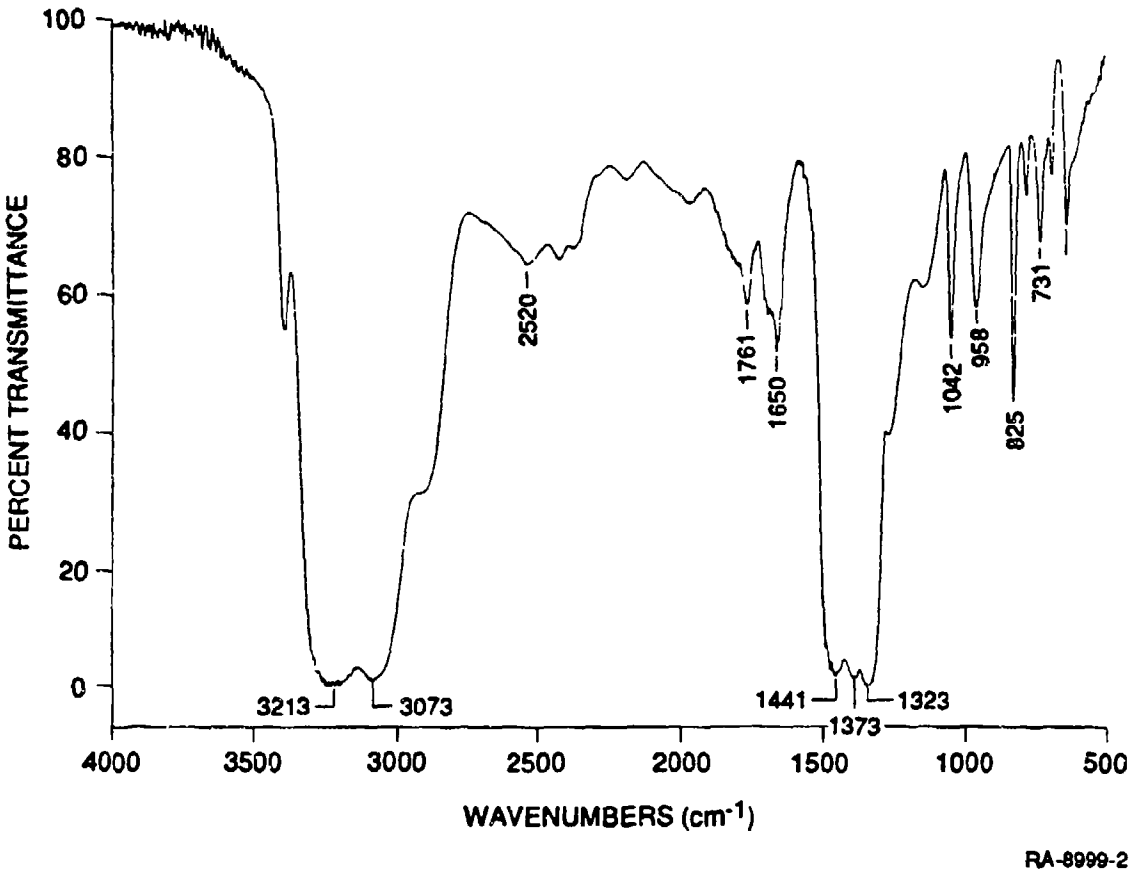

Figure 4. FTIR transmission spectrum after complete evaporation of NH_4NO_3 (probe T = 203°C) and with the cryostat maintained at -188°C.

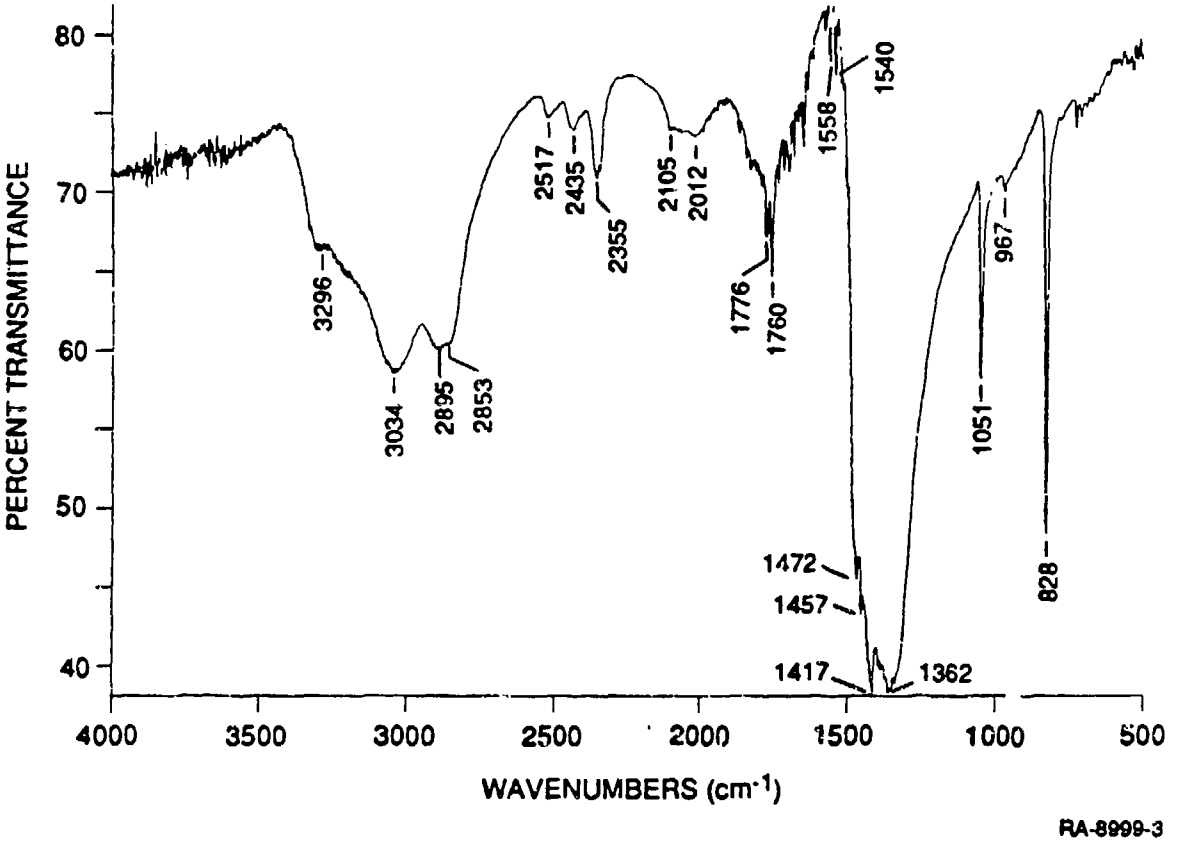

Figure 5. FTIR transmission spectrum after complete evaporation of NH_4NO_3 (probe T = 203°C) after the cryostat has been warmed to -50°C.

temperature, only a small amount of NH_4NO_3 was deposited during complete evaporation of the sample. As expected, the above results are consistent with dissociation of NH_4NO_3 into the free volatile acid and base, whereupon both components travel independently across the gas phase and recombine on the cold surface due to a large sticking coefficient of at least one component. The slight excess of NH_3 observed could be due to a small degree of catalytic decomposition of HNO_3 on some surface. The decomposition of HNO_3 on surfaces at ambient or slightly higher temperatures is an often encountered phenomenon, occurs even on Teflon surfaces, and is related to the fact that HNO_3 is thermodynamically unstable in the gas phase around ambient temperatures.

In subsequent experiments with NH_4NO_3, single masses were followed mass spectrometrically as a function of time at a somewhat higher heating rate (2-3°C/sec as opposed to 5-10°C/min) with the cryogenic window hot at approximately 160°C. The evolution of NH_3 was observed at m/e = 17 (Figure 6) and HNO_3 was monitored at m/e = 46 and 63 (Figure 7).

Although the individual curves of ion current versus temperature vary, sometimes significantly, as to their precise shapes, their characteristic parameters such as onset, width, and maximum agree remarkably well within certain limits. For every sample the onset of decomposition (sublimation) was measured at approximately 75°C, and the maximum evolution of both constituents, observed as a single sharp spike, was measured at 182 ± 5°C . In each case, this single "explosive" event expended the remaining sample. This explosive decomposition was also observed by monitoring the total pressure (ion gauges).

The observed T_{max} of 182 ± 5°C is nominally about 10°C higher than the measured melting point at 169.9°C. From previous calibrations with this particular probe design, we judge that there will probably be a lag in temperature of about 10°C between the thermocouple in contact with the bottom of the sample capillary holder and the inside of the capillary itself (see Figure 2). Consequently, we conclude that the rapid dissociation of NH_4NO_3 under these conditions takes place within a few degrees of its melting point. Thus, the sudden increase in dissociation (an endothermic event) in the absence of any substantial amount of exothermic reaction to drive it very likely results simply from improved heat transfer from the hot capillary walls upon melting of the NH_4NO_3. This phenomenon is common with materials that show a distinct melting point.

No N_2O was observed mass spectrometrically. Evidently, the HNO_3 pressure and/or the temperature was too low for decomposition either by self-protonation or by free radical formation of NH_2NO_2, the two mechanisms discussed by Brower, et al.[3] Considering the present results and those reported by Brower et al. from their batch reactor studies, the heating rate would have to be very high to result in true decomposition under these high vacuum conditions.

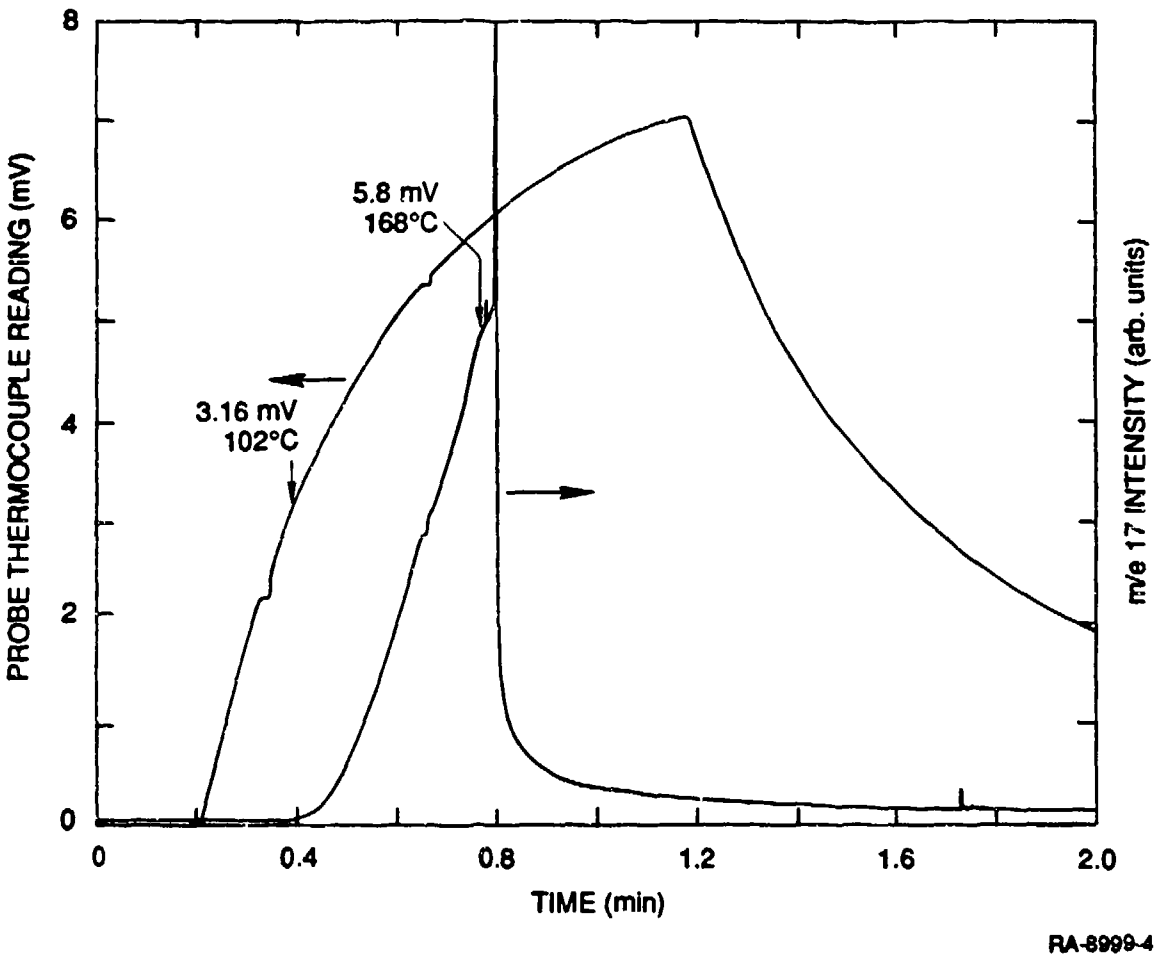

Figure 6. The evolution of NH_3 during NH_4NO_3 decomposition (monitored at m/e 17), as a function of temperature.

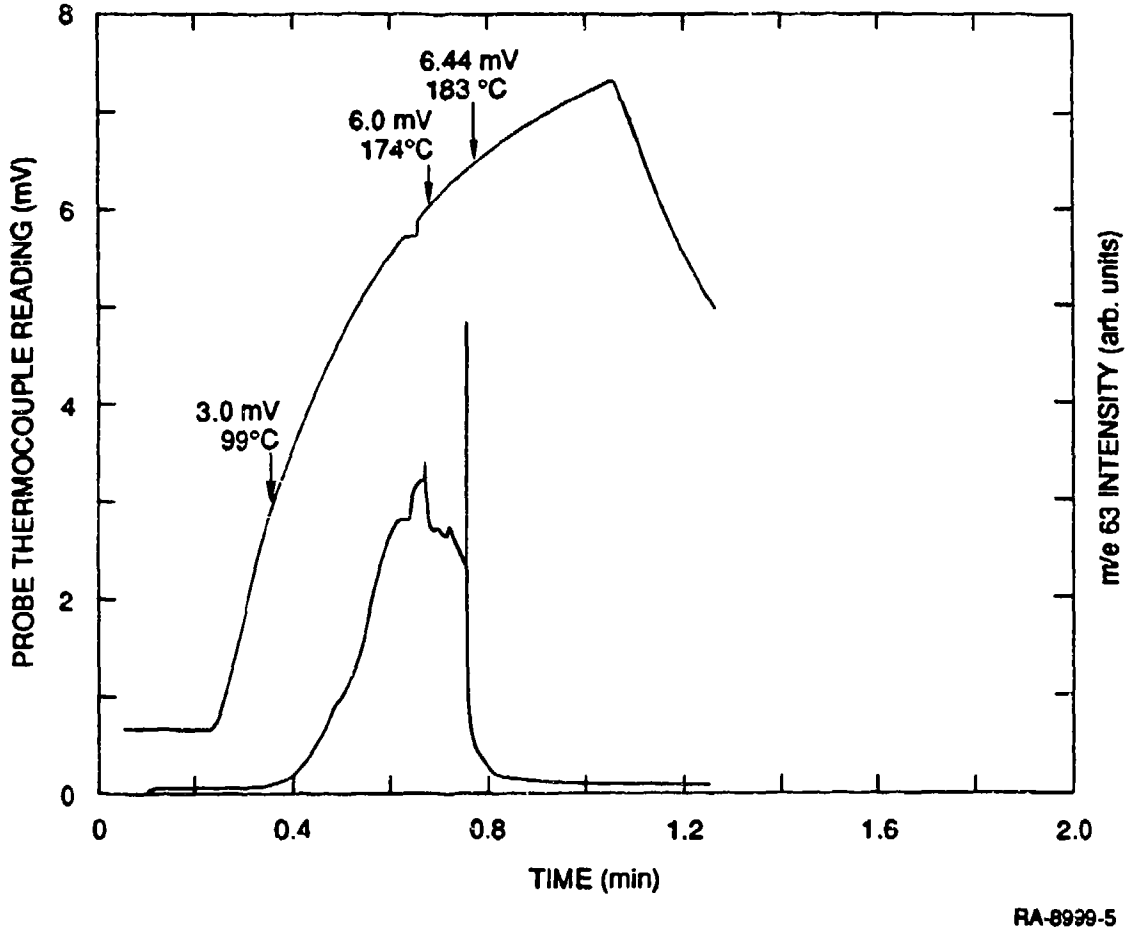

Figure 7. The evolution of HNO_3 (monitored at m/e 46 and 63) during NH_4NO_3 decomposition, as a function of temperature.

B. NH_2NO_2

Nitramide is the key intermediate that has been shown to play a role in the decomposition of NH_4NO_3 and may do so in the case of $NH_4N(NO_2)_2$ (ADN). Therefore, it was deemed necessary to examine the behavior of NH_2NO_2 under our experimental conditions, especially in the absence of pertinent kinetic data. Nitramide is a deliquescent material that must be kept in the freezer for storage. Figure 8 displays a mass spectral scan of material kept at ambient temperature (probe temperature) with the cryogenic window at approximately -180°C. In contrast to NH_4NO_3, nitramide has a high vapor pressure, potentially precluding the observation of thermal decomposition under our low pressure conditions. However, as we shall see below, decomposition of NH_2NO_2 according to reaction (6) takes place (along with evaporation) even at the lowest temperatures used here, namely, 30°C.

$$NH_2NO_2 \rightarrow N_2O + H_2O \qquad (6)$$

The mass spectrum essentially consists of the peaks at m/e 17, 18, 28, 30, and 44 and weaker peaks at 46 and 62, the latter representing the molecular ion. It is unusual for a closed-shell species to show masses in its electron-impact fragmentation mass spectrum at even mass numbers such as 18 and 44 corresponding to ions H_2O^+ and N_2O^+. Therefore, we suspected that the parents for ions m/e 18 and 44 were indeed neutral H_2O and N_2O arising from condensed-phase/heterogeneous decomposition of NH_2NO_2 at the temperature of evaporation. Interestingly enough, the (residual) mass spectrum of nitramide did not change when a sample was evaporated from an ambient temperature probe with the cryogenic window at ambient temperature, rather than at -180°C. Specifically, the intensity ratio of the peaks at m/e 44 and 62 did not change, so we conclude that the nitramide that survives its ambient temperature residence in, and transport from, the sample capillary does not decompose upon striking the KCl substrate surface. The precise amount of nitramide that survives the wall interactions is uncertain because the fragmentation pattern of "pure" NH_2NO_2 vapor could not be determined, but the maximum level of m/e 62 was usually between 2.5% and 3% of m/e 44.

In an attempt to record an authentic FTIR absorption spectrum of nitramide uncomplicated by any decomposition that might occur during sublimation,we dissolved a sample in absolute ethanol and then applied it to an ambient temperature KCl window. After evaporation of the solvent, we obtained the spectrum displayed in Figure 9, which does not bear any resemblance to the published IR spectrum of a thin solid film of nitramide. Since this spectrum was not further investigated, we can offer no detailed interpretation at this time. However, decomposition apparently occurred during preparation of the film.

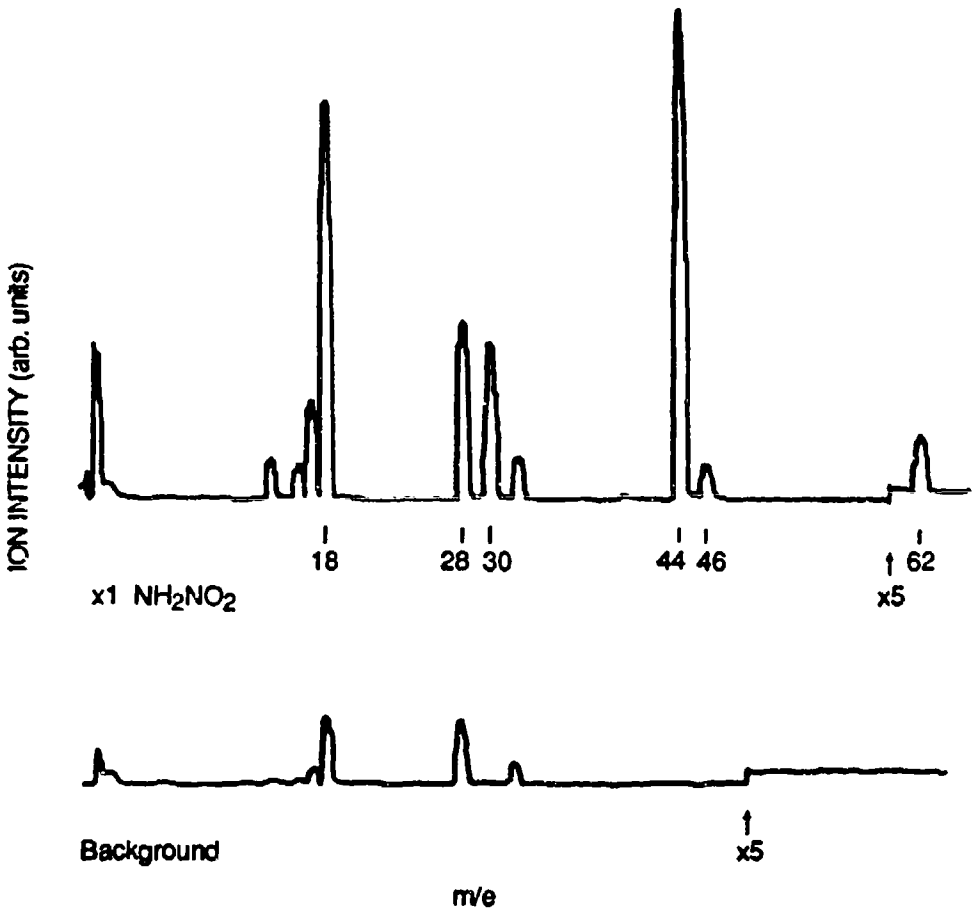

Figure 8. Mass spectrum of material desorbing/decomposing from an ambient temperature probe containing NH_2NO_2, with the cryogenic window held at -180°C.

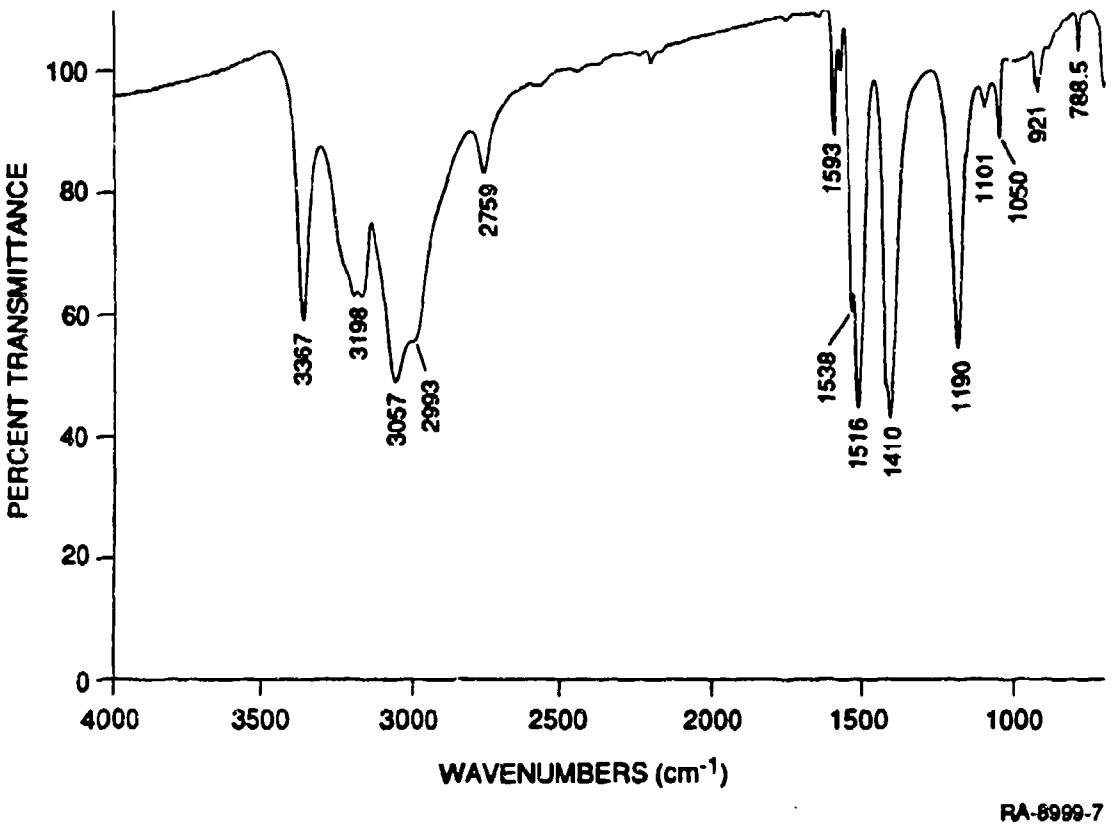

Figure 9. FTIR transmission spectrum of NH_2NO_2 decomposition products obtained from a thin film deposited from ethanol solution.

To obtain an authentic nitramide IR absorption spectrum, we evaporated a sample onto the cooled cryogenic window (approx. -190°C) with the probe at ambient temperature. Figure 10 displays the resulting very characteristic FTIR absorption spectrum, which agrees well with the IR absorption spectrum in the literature.[5] The characteristic features are the asymmetric and symmetric NH_2 stretches at 3435 and 3291 cm^{-1} as well as the strong asymmetric and symmetric NO_2 stretches at 1535, 1491 (doublet) and 1396. The agreement with the literature values is good, especially considering that Davies and Jonathan recorded an absorption spectrum of a crystalline film at room temperature,[5] whereas our conditions correspond to a low temperature amorphous film. There can be little doubt that the FTIR absorption spectrum displayed in Figure 10 corresponds to pure nitramide.

The time, and hence temperature, dependence of several mass spectrometric peaks during NH_2NO_2 decomposition was recorded with the cryostat both at ambient temperature and cold. The peaks investigated were m/e 18, 44, and 62; a typical intensity-time trace is given in Figure 11. The time behavior of the ion intensity is generally erratic (from one experiment to the next) at all masses, such that we could not, with our quadrupole instrument, study the parent-daughter relationship from the study of the temperature dependence. Irregular release of gas monitored through the ion current can sometimes be encountered when small volume elements in the bulk material have already decomposed, and this "bursting of the bubble" or the explosion of pockets of decomposed material occurs from time to time as the sample is progressively evaporated/decomposed. Such prior decomposition of parts of the sample makes it more difficult to obtain information about the decomposition kinetics under the time-temperature conditions of a given experiment. The observed peaks in ion intensity always coincided with a pressure burst observed with either of the two ionization gauges. The only significant difference between runs at ambient-temperature and low-temperature cryostat conditions is the slope of the rising portion of the ion current, which is much steeper for the ambient temperature cryostat, in part because a significant portion of the NH_2NO_2 is no longer being trapped on the liquid nitrogen cooled cryostat.

In another series of experiments, we evaporated nitramide onto the cold KCl window with the probe tip at ambient temperature. If heterogeneous decomposition occurs during evaporation, the FTIR absorption spectrum of the condensate should consist of undecomposed NH_2NO_2 and H_2O, with N_2O being pumped away. In fact, the resulting FTIR absorption spectrum displayed in Figure 9 above shows nitramide and water, but no other absorbers. Upon warming the cryostat, we monitored large amounts of H_2O at -113°C cryostat temperature. This H_2O must have originated from the previous evaporation/decomposition of nitramide, because upon further

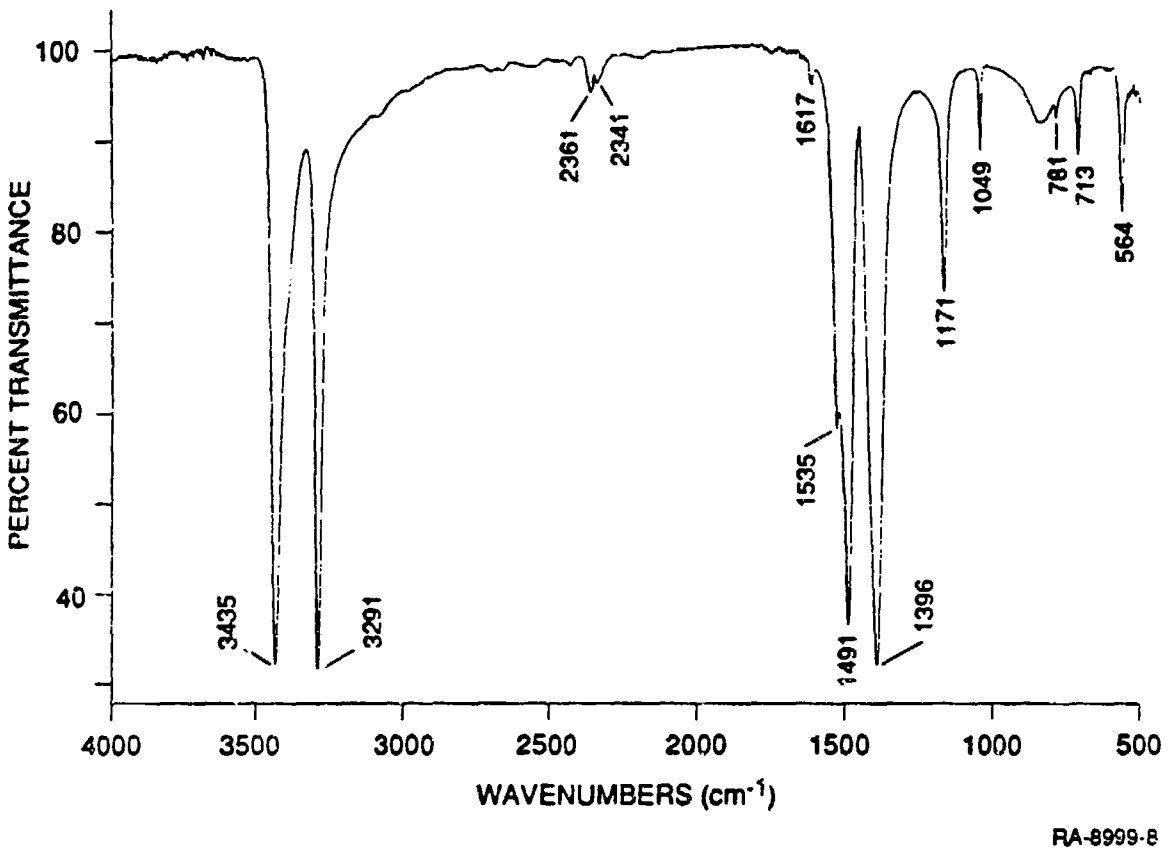

Figure 10. FTIR transmission spectrum of NH_2NO_2 obtained from a thin film deposited onto a -190°C KCl window by evaporation from an ambient temperature probe.

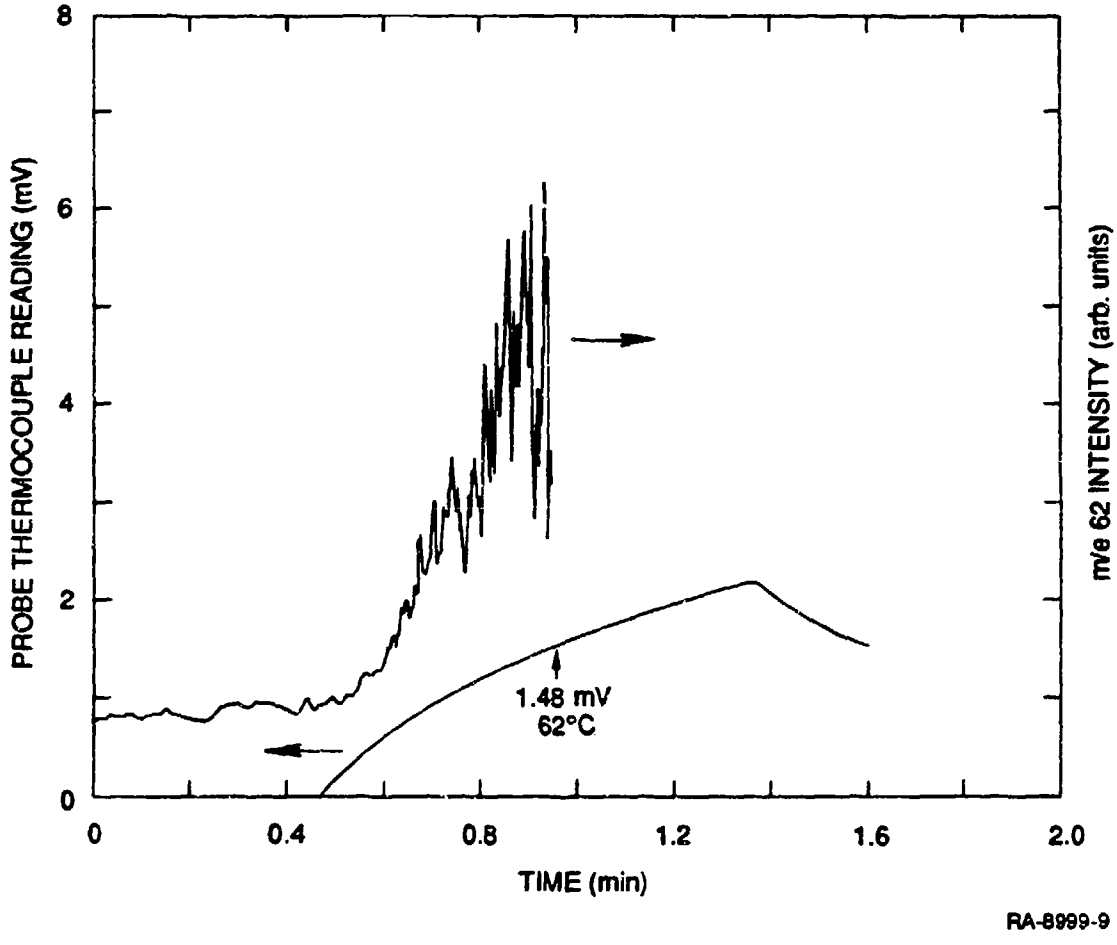

Figure 11. The evolution of mass 62 during NH_2NO_2 decomposition as a function of temperature.

warming of the cryostat, the rate of H_2O release became smaller. At -82°C the H_2O release became a minimum, with m/e 30, 44, 46, and 62 steadily increasing. Upon further warming, masses at 17, 18, 28, 30, 44, 46, and 62 increased dramatically until the cryostat reached -46°C, at which point the rate of decomposition evidently reached a maximum. Noteworthy is the ratio of 62 ($NH_2NO_2^+$) to m/e 46 (NO_2^+), which is smaller at -46°C than at -56°C and decreases even further by -38°C, beyond which m/e 62 is virtually non-existent. At -29°C, m/e 62 has completely disappeared, while m/e 44 is still present .

These observations led us to conclude that nitramide is unstable relative to presumably heterogeneous decomposition, either before evaporating or as a gas colliding with some surface. We know that nitramide has a molecular ion (m/e 62) that can easily be observed at low levels, but the residual gas mass spectrum is dominated by masses corresponding to the decomposition products N_2O and H_2O. While m/e 62 is a marker for the presence of NH_2NO_2, the origin of m/e 46 is not clear. If m/e 46 were only a fragment peak of nitramide, the ratio of m/e 62 to 46 should remain constant under all conditions, which it does not . M/e 46 could also be a decomposition product of a minor reaction channel of nitramide according to the stoichiometry shown in reaction (7)

$$NH_2NO_2 \rightarrow 0.5\ N_2O + 0.5\ HNO_3 + 0.5\ NH_3 \qquad (7)$$

M/e 46 is the base peak for HNO_3, and small amounts of NH_3 could be masked by the large amounts of H_2O generated.

In conclusion, we believe that the decomposition of NH_2NO_2 has some limited relevance to the decomposition of $NH_4N(NO_2)_2$: in both cases (see below), N_2O is presumably produced from an aci-nitro form in which two nitrogen atoms are already doubly bonded. In both cases, then, some reaction increases electron density on one of the nitrogens, facilitating formation of the triply bonded species. However, in the case of nitramide, this is most likely a base-catalyzed reaction (removal of the remaining proton from the amine nitrogen) as described in the literature for condensed phase decomposition,[6,7] whereas in the case of ammonium dinitramide, it is much more likely to be an acid-catalyzed reaction. On balance, we believe that the absence of any evidence that NH_2NO_2, or an NH_2NO_2-like species is an intermediate in ADN decomposition suggests that further study of dinitramide itself will not be very helpful in understanding the behavior of ammonium dinitramide.

C. $NH_4N(NO_2)_2$ (ADN)

In a formal sense, at least three reaction paths can be formulated for the thermal decomposition of ADN:

$$NH_4N(NO_2)_2 \rightarrow NH_3 + HN(NO_2)_2 \rightarrow NH_3 + HNO_3 + N_2O \quad (8a)$$

$$NH_4N(NO_2)_2 \rightarrow (2NH_2NO_2) \rightarrow 2N_2O + 2H_2O \quad (8b)$$

$$NH_4N(NO_2)_2 \rightarrow NH_4NO_3 + N_2O \quad (8c)$$

Note that Equations (8-a), (8-b), and (8-c) describe only potential stochiometric relationships; the actual occurrence of the reactions must be identified by experiment. By outlining the results of several types of ADN decomposition experiments, we show that neither pathway (8-b) nor (8-c) plays a significant role in the decomposition under the conditions explored here. Instead, reaction (8-a) is followed by heterogeneous decomposition of HNO_3 to NO, H_2O, and presumably O_2. Also of prime interest here is the behavior of the free dinitraminic acid $HN(NO_2)_2$ (HDN): its stability and the factors affecting its decomposition. We describe in turn the results of each category of experiment performed with ADN and the conclusions drawn from these results. These conclusions are then compiled into a scenario for ADN decomposition under the present slow-heating, vacuum conditions.

Pyrolysis with a Cold Cryostat. This series of experiments consisted of conducting the ADN pyrolysis in the melting capillary when the cryostat is at low temperature, usually between -180° and -160°C. The equilibrium vapor pressures of NO and N_2O are such that we do not expect them to condense on the cryostat, even if it were cooled all the way to 77 K. NH_3 is a borderline case, with 10^{-6} Torr at 102 K and 10^{-7} Torr at 96 K. It appears that NH_3 by itself does not condense on the cryostat, even at the lowest temperatures reached under our conditions, but will be trapped only if a salt can be formed. As in the above discussion of the NH_4NO_3 results, we will use "dissociation" to refer to separation into the volatile acid and base component, and "decomposition" to refer only to reaction that involves further decomposition of one or both of these components.

Throughout most of the temperature range in which dissociation/decomposition of ADN took place, the ion at m/e 17 (mainly NH_3, some H_2O) was the most abundant. However, under some conditions, we observed bursts of H_2O at lower temperatures even before the onset of continuous NH_3 release, which occurred at about 90°C. The prominence of these bursts seemed to

correlate with the quality and age of the sample, with the effect being more marked when more thermal decomposition had taken place in the sample before the experiment.

At 90°C, NH_3 (m/e 16, 17) is the dominant feature, together with N_2O. In addition some NO (m/e 30) and a small but significant mass 46 emerge. At 130°C, NH_3 and, to a lesser degree N_2O are still dominant. In addition, H_2O begins to appear as a steady product. Along with the NO, this H_2O could originate from the heterogeneous decomposition of HNO_3. At 130°C, the transmission of the KCl window also begins to drop. As discussed below, this indicates deposition of an amorphous H_2O film, together with ADN. At ~150°C, NH_3 and N_2O are still dominant, and H_2O and NO are significant. The maximum intensity for both H_2O and NH_3 is typically observed at 150° to 160°C. In this temperature range also, new masses at m/e 46 and 60 begin to appear. We suggest that m/e 46 and 60 indicates the dissociation of ADN and vapor transport of free $HN(NO_2)_2$, ultimately leading to re-deposition of ADN on the cold cryogenic substrate.

Although H_2O should be deposited quantitatively on the cryogenic surface, we observe significant quantities in the gas phase. This means either that the effective surface temperature of the KCl window during the deposition is significantly warmer than indicated by the thermocouple (located farthest from the liquid nitrogen well, at the warmest end of the cryostat) or that we are merely seeing the fringes of the pyrolysis plume that miss the cryogenic trap.

At 170°C, both NH_3 and NO are dominant features, with N_2O and H_2O also being significant. At this temperature both m/e 46 and 60 attain their maximum. Some of the m/e 46 may reflect the presence of small amounts of HNO_3, because the latter has contributions at m/e 46 and 30, both of which are seen. Under the present conditions, m/e 63, which is the parent ion of HNO_3, is not expected to be seen because it should be at most a percent or so of the HNO_3 base peak at m/e 46. In earlier experiments, when the vacuum chamber was unheated, m/e 46 was even larger and a small m/e 63 was visible.

At 200°C, the dominant species are still NH_3 and H_2O, with N_2O and NO still present in significant quantities, together with an unidentified species with fragment mass m/e 28. By contrast, both m/e 46 and 60 have significantly decreased. Above 200° to 220°C, the sample is spent and the background mass spectrum show some lingering N_2O, NO, and additional contribution at m/e 28, whereas NH_3 has completely disappeared.

These observations indicate that ADN dissociates into its acid and base components and that, depending on temperature, the acid HDN in turn decomposes into N_2O and HNO_3, which further decomposes into H_2O, NO, and, evidently, O_2.

$$NH_4N(NO_2)_2 \rightarrow NH_3 + HN(NO_2)_2 \qquad (4)$$

$$HN(NO_2)_2 \rightarrow N_2O + HNO_3 \quad (9)$$

$HNO_3 \rightarrow\rightarrow$(heterogeneous decomposition leading ultimately to $NO + H_2O + O_2$)

Support for generation of the intact free acid comes also from the FTIR observations described below. The free acid $HN(NO_2)_2$ shows partial decomposition (and partial survival) over a surprisingly wide temperature range. There is some decomposition (of HDN) at the lowest temperatures at which dissociation occurs (ca. 90°C), but some HDN survives intact even at probe temperatures of 200°C.

FTIR Spectrum of the Film Deposited on the Cold Cryostat. Figure 12 presents a FTIR absorption spectrum of the pyrolysate (probe at 196°C) condensed on the cold cryogenic window. The IR spectrum of condensed products did not change during programmed temperature pyrolysis, and a comparison with an authentic polycrystalline sample of ADN (dissolved in absolute ethanol and spread over a KCl window), shown in Figure 13, establishes that the condensate consisted exclusively of vapor-deposited ADN. In comparing the amorphous vapor-deposited compound with the polycrystalline phase, we observe that the relative intensity of many absorption bands is significantly changed, but the band position is usually identical within experimental error. The comparison of the reference spectrum of Figure 13 with an analogous one obtained by making a KBr pellet reveals qualitatively the same differences. The most prominent bands in ADN are the NH_4^+ N-H stretching fundamentals around 3200 cm^{-1} as well as the symmetric and asymmetric NO_2 stretch bands, which are split because there are two NO_2 groups interacting through a common atom.

Figure 14 displays the FTIR spectrum obtained from a film deposited over the entire ambient to 200°C temperature range of dissociation/decomposition. This spectrum, which is a superposition of amorphous H_2O and recondensed ADN, is similar to that of Figure 12, but with much more intense peaks, and less indication of co-condensed H_2O.

The recondensation of ADN on a cold cryostat is totally analogous to the case of the unreactive sublimation of NH_4NO_3 discussed before, in which the two components, NH_3 and HNO_3, travel individually to the cold substrate and reform the ammonium salt *in situ*. Because NH_3 probably does not condense by itself, the microscopic process of regeneration of ADN occurs by NH_3 hitting a molecule of $HN(NO_2)_2$ immobilized on the cold surface, thus regenerating the ammonium salt. As we will see below, apparently not all the condensed $HN(NO_2)_2$ has the opportunity to be reconverted to ADN. This result is somewhat unexpected in view of an excess of NH_3 , due to decomposition of a substantial fraction of the free $HN(NO_2)_2$ according to equation (8-a). (This result is however, consistent with the difficulty, described below, in

converting an already-deposited HDN film to ADN.) Our experiments do not tell us in which phase this decomposition occurs. Several scenarios are possible. For instance, $HN(NO_2)_2$ could heterogeneously decompose while still on the surface of the sample after NH_3 evaporates. Another possibility would be the heterogeneous decomposition of gas-phase $HN(NO_2)_2$ on the walls of the melting tube capillary or some ambient temperature surface. The only way to answer this question in a systematic way is to vary the surface-to-volume ratio of the sample capillary. Although such a study was outside the scope of the present investigation, the results discussed below suggest that decomposition by self-protonation (which must be either condensed phase or on a surface) is likely the principal route of HDN decomposition.

Changes observed upon Heating of the Cold Cryostat film. One exception to this 1:1 correspondence between the low-temperature condensates (Figures 12 and 14) and the reference spectrum (Figure 13) becomes clear when we consider the changes that occur in the FTIR spectrum during deposition and removal of the ADN film. There is a group of absorption bands around 3500 cm^{-1} in the low-temperature condensate (Figures 12 and 14) that we interpret as due to the presence of H_2O, because warming of the cryostat between -100°C and -30°C generates large amounts of H_2O, as observed by mass spectrometry, and yields the spectrum shown in Figure 15 (from the film that gave the spectrum in Figure 12). The H_2O desorption behavior actually seems to reveal two kinds of hydrogen-bonded H_2O. The first kind is an amorphous H_2O layer characterized by a broad peak at approximately 3250 cm^{-1} and two shoulders at 3360 and 3150 cm^{-1}. In the original deposition, this weak absorption grows in right after the start of the pyrolysis at relatively low probe temperatures. At higher pyrolysis temperatures, starting at about 130°C, a similar broad absorption is monitored at 3500 cm^{-1} together with the somewhat lower frequency absorptions associated with the presence of the NH^{4+} ion. We judge that here the vapor deposition of ADN is providing an "anchor" for the more strongly adsorbed H_2O.

We come to the above judgment for the following reasons. If the cryostat is subsequently warmed slowly, a H_2O burst is observed at around -100°C cryostat temperature, without much indication of change in the FTIR absorption spectrum. This behavior stems from the fact that amorphous H_2O is a relatively weak absorber in the IR. [It is an interesting question as to how this amorphous underlayer of H_2O can evaporate so easily while having to migrate through a solid phase of frozen ADN and $HN(NO_2)_2$.] The next "wave" of H_2O is released in the temperature range -80° to -60°C, and is accompanied by the disappearance of the IR absorption at 3500 cm^{-1}.

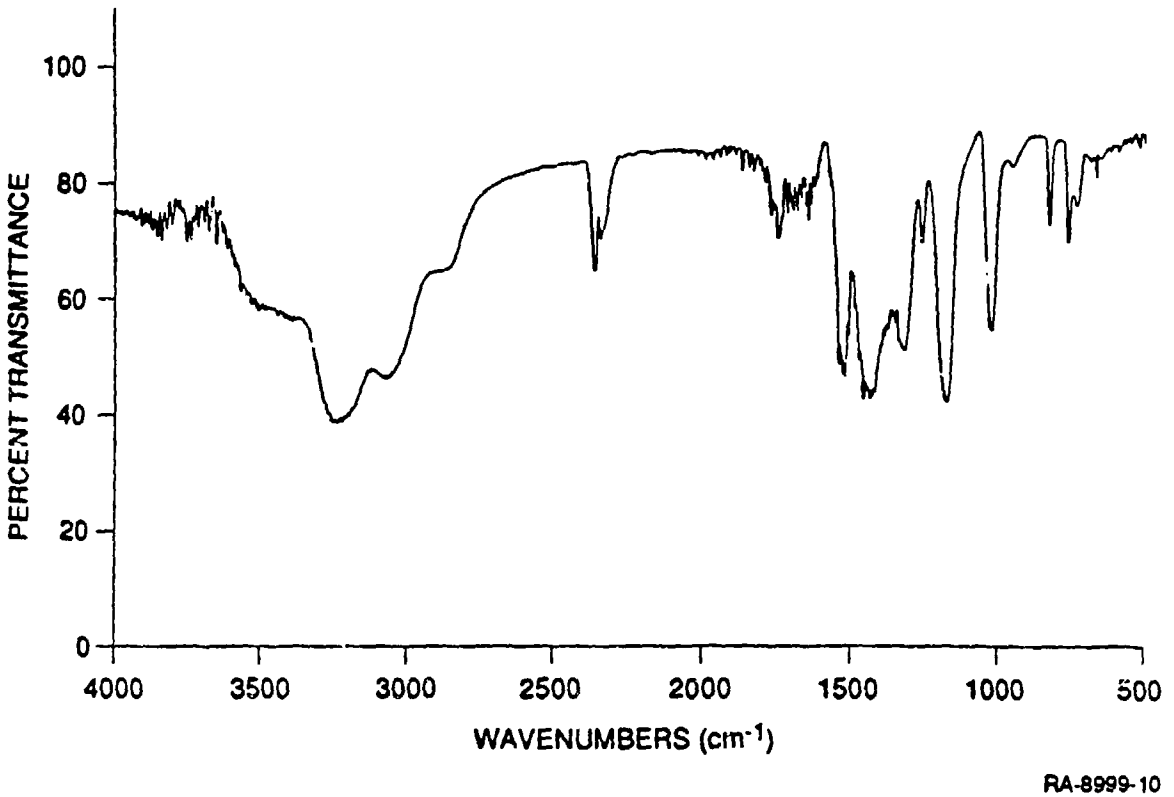

Figure 12. FTIR transmission spectrum of the pyrolysate from $NH_4N(NO_2)_2$ generated from a probe at 196°C, and deposited onto a -160°C KCl window.

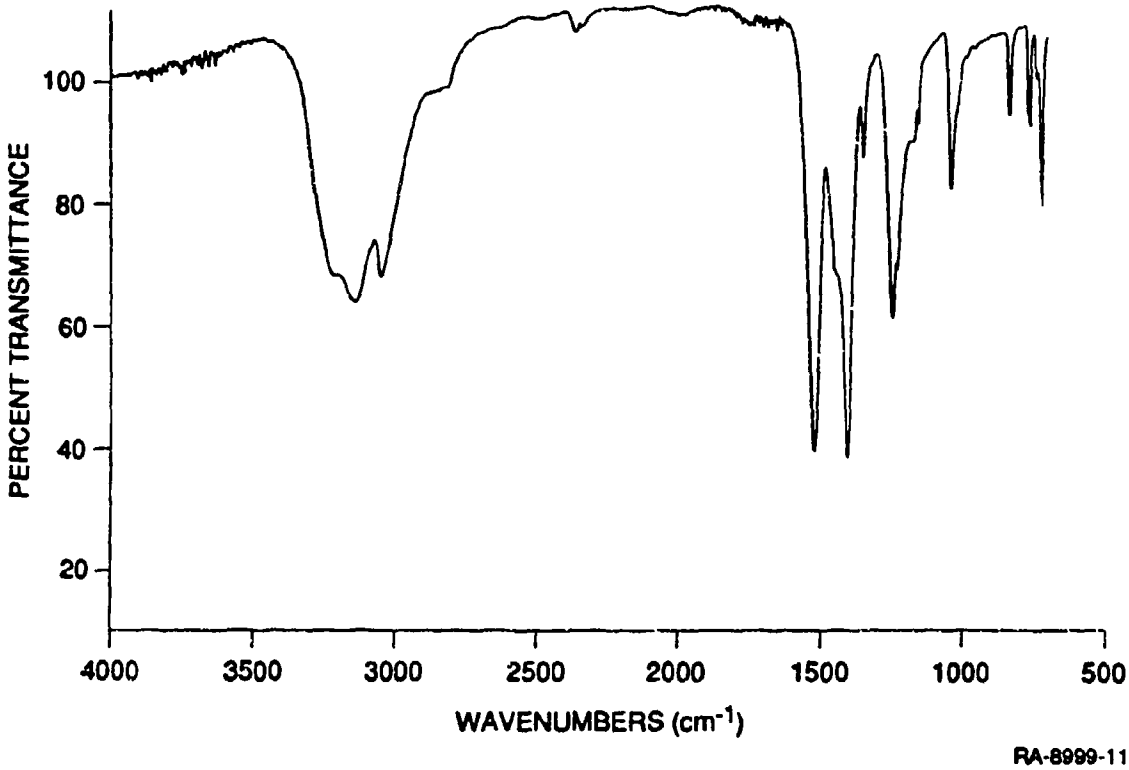

Figure 13. FTIR transmission spectrum of a polycrystalline thin film of $NH_4N(NO_2)_2$ deposited from an ethanol solution.

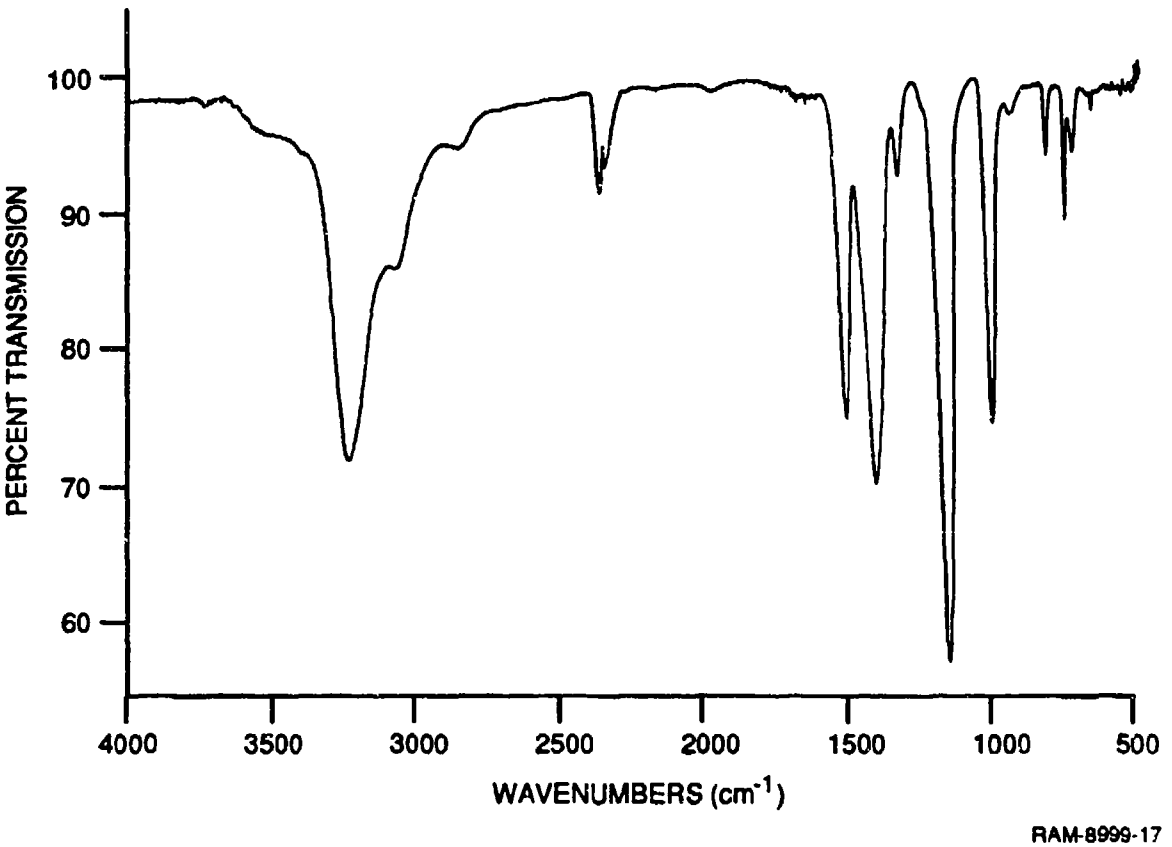

Figure 14. FTIR absorption spectrum of -160°C condensate resulting from evaporation/ desorption of SRI-12 with the probe temperature programmed from ambient to 200°C.

This change can be seen in Figure 16, which shows FTIR spectra taken with the film at -170°C and of that remaining at -16°C.

During H_2O desorption described above, the FTIR absorption spectrum does not change substantially except for the disappearance of the broad 3500 cm^{-1} band. However, in some spectra, (i.e., that in Figure 15, but not in Figure 16b) the baseline progressively slopes downwards (when plotted in the transmission mode) toward the high frequency end of the IR spectrum, indicating an increased scattering by the absorber. This is not surprising at all in view of the substantial H_2O desorption from the bulk of the medium, after which we might anticipate the residue to have a pitted and rough, (highly scattering) surface. We thus conclude that the low temperature trapping of the pyrolysate of ADN consists mainly of dissociated and reformed SRI-12 along with H_2O, some of which was pre-existing in the original SRI-12 and some of which came from the pyrolysis. The other obvious pyrolysis product, N_2O, cannot be trapped under our experimental conditions, even if the cryostat achieved the temperature of liquid nitrogen (-196°C).

As the cryostat is further warmed from about -30°C to ambient, little mass spectrometric intensity arises. However, because the warming of the cryostat takes so long, the integral of the mass flux over time could still be significant. The more significant masses observed during this time are m/e 16, 17, 46, and 60, corresponding to NH_3 and $HN(NO_2)_2$. By the same token, the optical density at 3250 cm^{-1} contributing intensity to the complex band shape around 3000 cm^{-1} decreases noticeably, and as the cryostat temperature approaches ambient, the evaporation of NH_3 and N_2O pick up. Once the cryostat heater is turned on, the products already described for the probe pyrolysis [i.e., NH_3, H_2O, NO, N_2O, $HN(NO_2)_2$, and an ion at m/e 28] emerge at increased intensities. By 200°C, the flux of $HN(NO_2)_2$ (m/e 60) has already decreased substantially, as discussed above for the pyrolysis of SRI-12 in the melting tube capillary. As gaseous products are progressively evolved with increasing KCl substrate temperature, the FTIR absorption spectra become weaker. The biggest change in the spectra seems to occur at 3250 cm^{-1} even up to higher temperatures. This suggests perhaps, that as long as HDN is part of the acid-base pair (i.e., exists as ADN), it does not undergo substantial decomposition.

The low temperature changes in the condensed ADN film do not arise entirely from loss of water. In fact, from about -30°C to ambient cryostat temperature, the only products evaporating are NH_3 and HDN, at a small rate. Since ADN itself does not begin to dissociate until about +90°C, we conclude that those changes result from loss of isolated ADN and HDN in the matrix. Associated with the loss of NH_3 and HDN are a band sharpening with partial splitting and a decrease in the optical density at 3250 cm^{-1}. We attribute this to an annealing process that accompanies loss of NH_3 and HDN from the ADN film. Quantitative studies seem warranted at this stage and could be performed using the existing experimental apparatus.

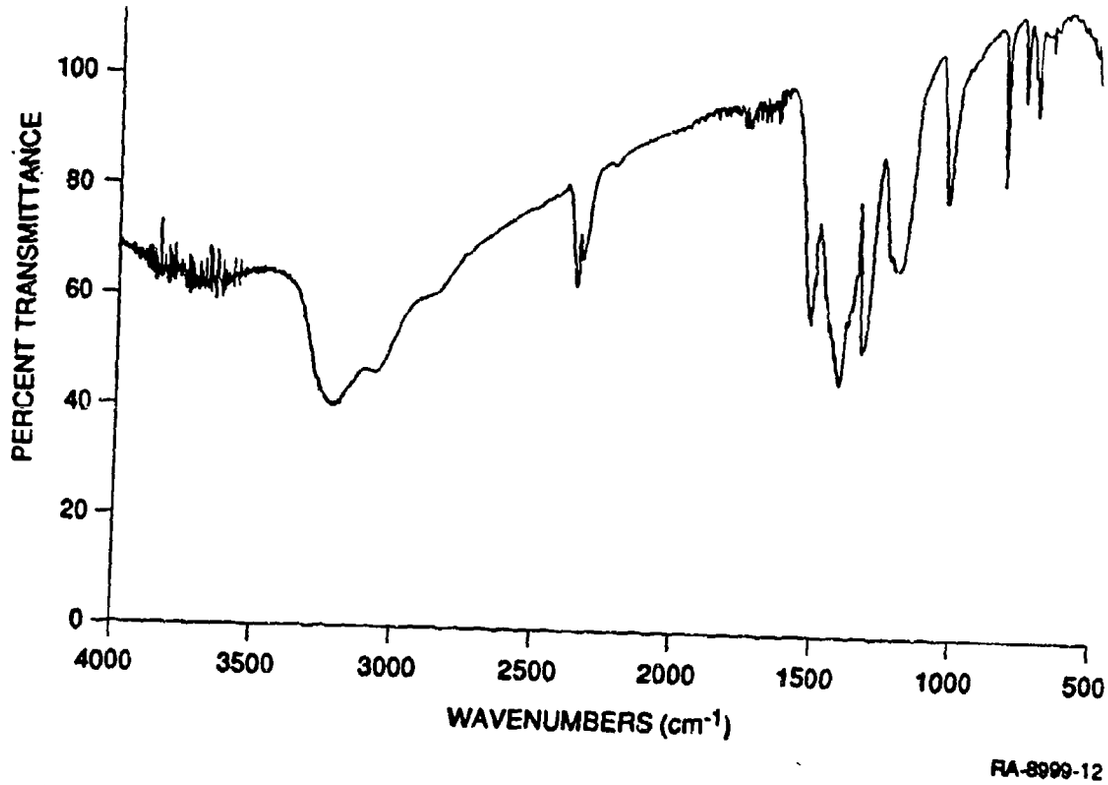

Figure 15. FTIR transmission spectrum of a vapor-deposited $NH_4N(NO_2)_2$ after warming of cryostat to -60°C.

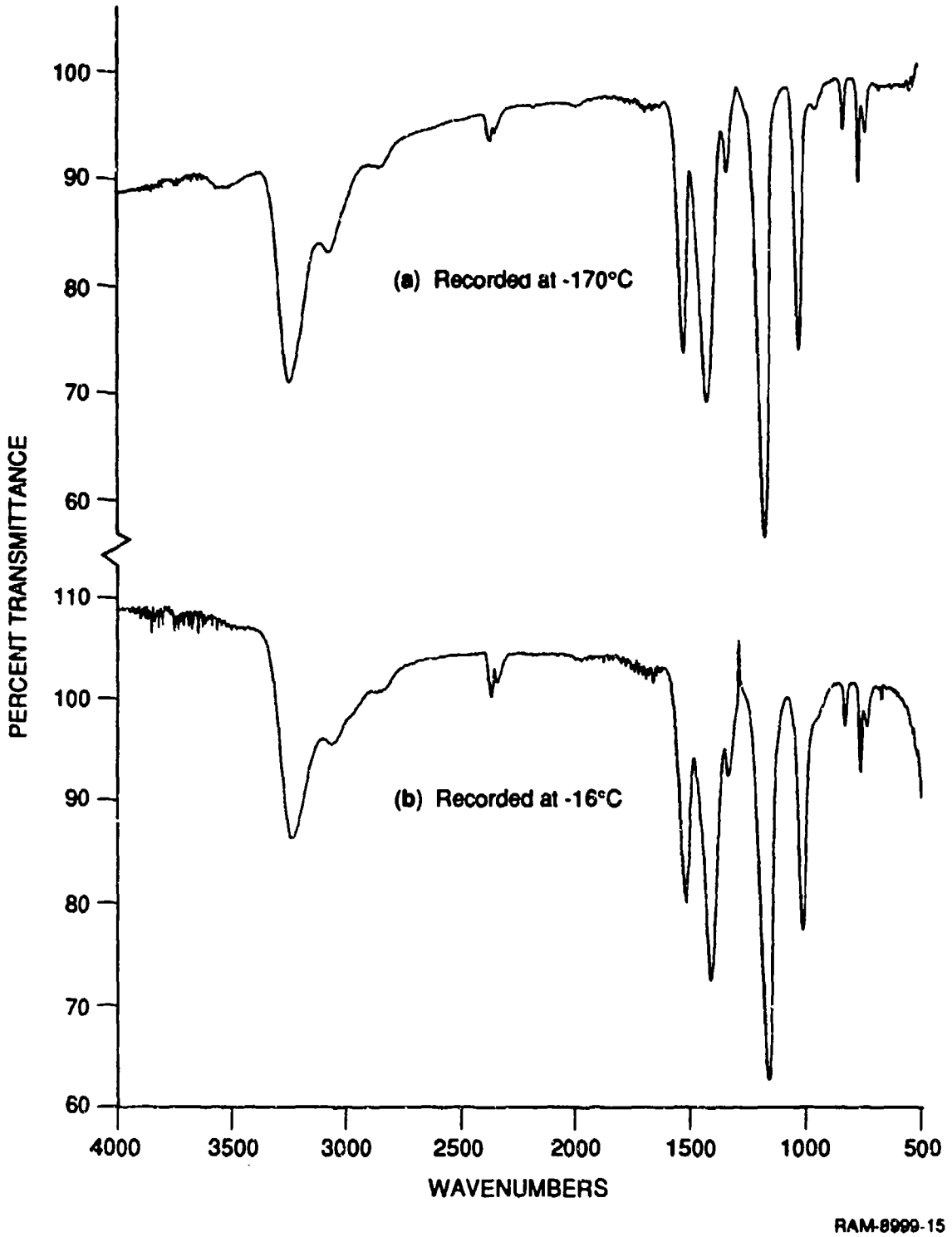

Figure 16. FTIR spectra of SRI-12 decomposition products condensed at -170°C.

The above observations involving deposition and removal of the film deposited from ADN pyrolysis with the cryostat held at close to liquid nitrogen temperature allow us to draw the following conclusions:

- An FTIR absorption spectrum that is identical to that for crystalline ADN (except for small differences such as can be attributed to trace amounts of water and different crystal structure) and is invarient when deposited over a wide range of probe temperatures indicates that the low temperature film is essentially pure ADN.

- Warming of the film from -180°C to ambient results in loss of trace amounts of H_2O, NH_3, and HDN; thereafter, the evolved products are identical with those released from a sample of crystalline ADN heated in the probe.

Pyrolysis with an Ambient-Temperature Cryostat -- FTIR Observations. ADN pyrolysis in the presence of an ambient temperature KCl substrate results in a significantly different FTIR absorption spectrum (displayed in Figure 17) from that observed with a cold cryostat. The spectrum in Figure 17 is quite a bit simpler than that in Figures 12 or 14 above and is characterized by a fairly weak absorption at approximately 3250 cm^{-1}. It retains the characteristic symmetric and asymmetric ONO stretching frequencies in the fingerprint region that are associated with the nitro group. We assign this IR spectrum tentatively to the free dinitraminic acid $HN(NO_2)_2$ with the N-H stretching frequency at 3250 cm^{-1}. Upon close examination, the peak positions of dinitraminic acid, albeit similar, do not correspond exactly to the ones observed for its ammonium salt, ADN, or for the potassium salt. The absorption spectrum in Figure 17 is weaker overall than that from the film deposited on a cooled cryostat because the capture of HDN at ambient temperature is less efficient and/or because the ammonium salt is a stronger absorber. At ambient temperature, the spectrum remains unchanged for at least several hours. Its intensity starts to decrease as the KCl substrate is heated, starting at 70°C, and has disappeared at 140°C, as will be discussed below. We conclude that condensed phase HDN is stable at room temperature under high vacuum conditions (10^{-7} Torr), but does not survive pyrolysis temperatures in excess of 140°C, even for short periods of time.

Pyrolysis with an Ambient-Temperature Cryostat -- Mass Spectra. Figure 18 presents a series of mass spectra obtained during the thermal decomposition of ADN with the cryostat at room temperature and with an unheated vacuum chamber. Five major products were detected, NH_3, H_2O, NO, N_2O, and HNO_3 (and/or NO_2), as indicated by strong signals at m/e 16, 17, 18, 30, and 44 and weaker ones at 28 (over and above the small contribution from background air in the chamber), 46, 60, and 63. In the lower temperature range (ca. 90 to 140°C),

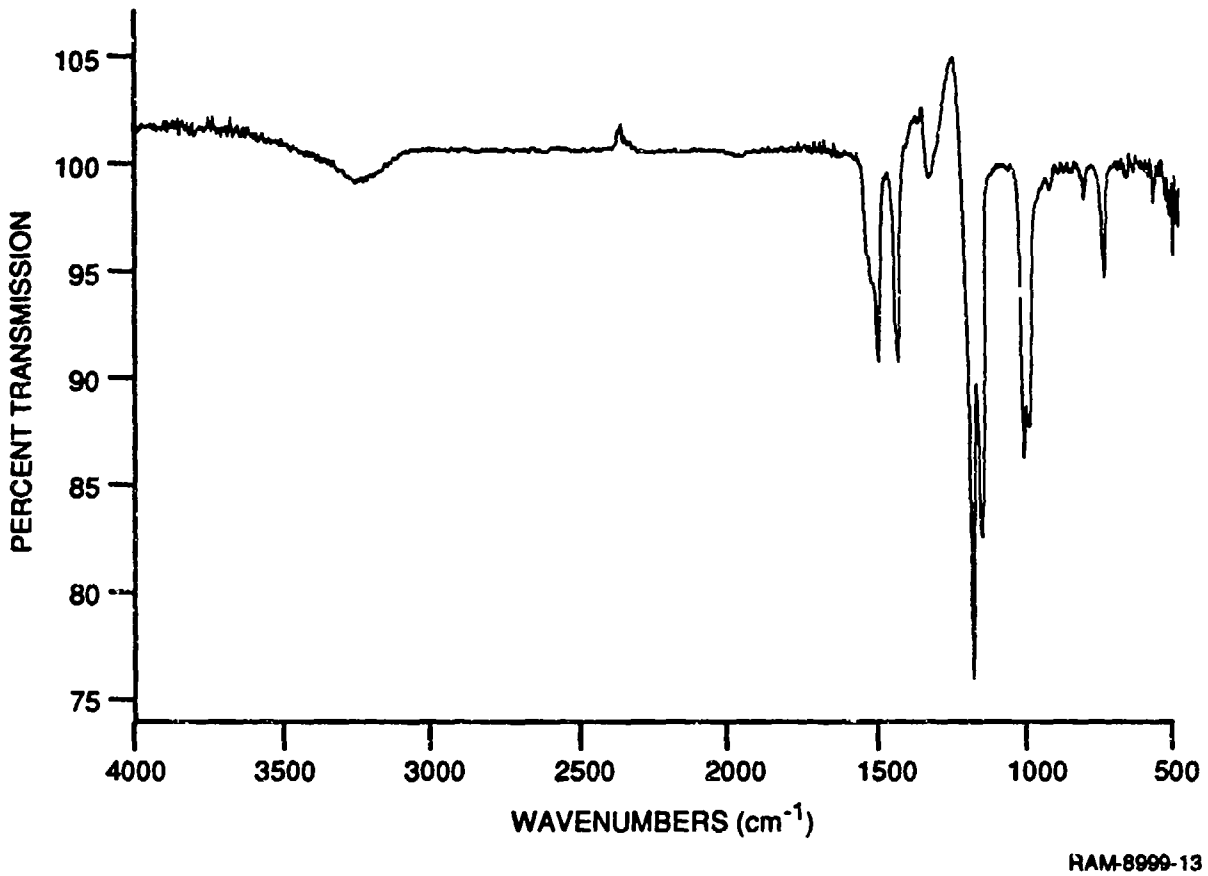

Figure 17. FTIR transmission spectrum of the pyrolysate from $NH_4N(NO_2)_2$ generated from a probe at 196°C, and deposited onto an ambient-temperature KCl window.

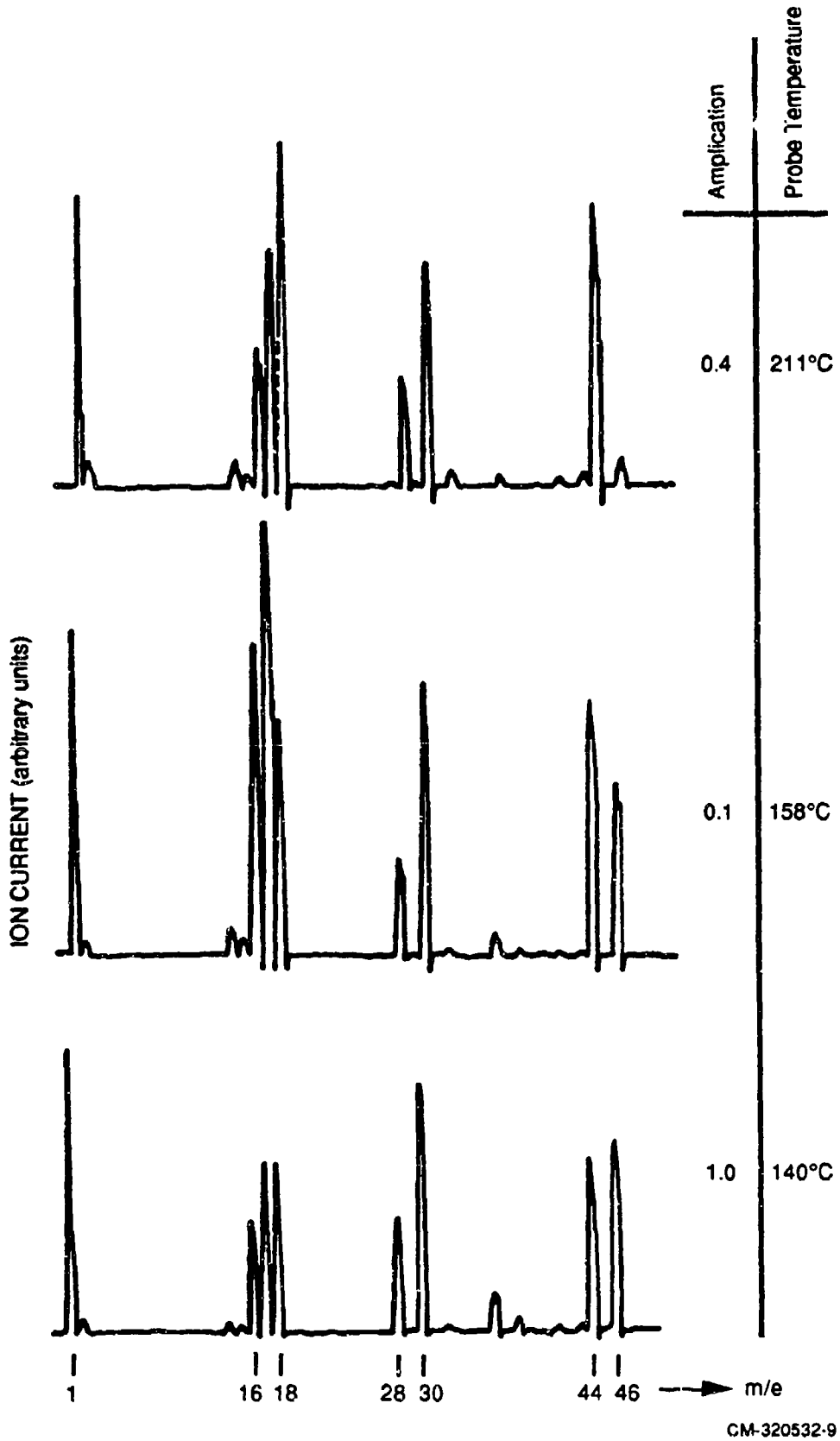

Figure 18. Mass spectra obtained during the decomposition of $NH_4N(NO_2)_2$ with the the cryostat held at ambient temperature.

the predominant products are NH_3, N_2O, and HNO_3. The occurrence of HNO_3 (monitored at m/e 63) is revealing, because it is absent in the thermal decomposition of NH_2NO_2, which was a potential intermediate in the thermal decomposition of ADN. M/e 63 was also absent in the later ADN experiments, where the vacuum chamber was warmed to about 60°C. At probe temperatures above 140°C, the abundance of HNO_3 decreases dramatically, whereas we observe a less dramatic decrease in NH_3. At higher temperatures, therefore, the mass spectrum is dominated by H_2O, N_2O (m/e 44) and m/e 30, which we attribute to NO, presumably due to decomposition of HNO_3 on some surface. In the example of Figure 18, the intensity of m/e 46 is larger than that of m/e 44 at 140°C, slightly below the temperature of maximum rate of release of pyrolysis products. Increasing the probe temperature by only 10° to 20°C results in a substantial shift toward H_2O, NO, and N_2O relative to NH_3 and HNO_3 and/or NO_2. At temperatures beyond 200°-220°C, the sample is spent and background values for masses corresponding to NH_3, NO, and N_2O are attained. In these various decomposition runs, repeated attempts to detect either the parent of ADN at m/e 124 or the parent of HDN at m/e 107 were all unsuccessful.

Pyrolysis of HDN Deposited on Ambient Temperature Cryostat. Following the deposition of HDN onto the ambient-temperature KCl substrate, we proceeded to the pyrolysis of this thin film by heating the cryostat. Immediately after turning on the heat to the heater coils (i.e., at a temperature of 60° to 70°C), we observed strong mass spectrometric signals corresponding to H_2O, NO and N_2O. No intensity was observed at m/e 46 and 60, nor at any masses corresponding to NH_3, in contrast to what occurs during pyrolysis of ADN in the melting capillary. With increasing temperature, the intensity of this mass spectrum decreased steadily, but the peak ratios remained approximately constant until the cryostat temperature approached 200°C. Thus, when a film of HDN is heated (T > ~60°C), there is no detectable NH_3, nor any peaks attributable to NO_2 or intact HDN. These observations from the cryostat film pyrolysis are important and allow the following conclusions to be drawn:

- The base component NH_3 is entirely absent from the ambient-temperature-deposited film.
- The condensed phase acid component (HDN) cannot survive temperatures nearly as high as can ADN (or even gas-phase HDN); no intact gas phase HDN is produced by heating a film of HDN.
- The condensed phase decomposition of HDN under these conditions produces no NO_2.

Slow Heating Rate Probe Decomposition with Heated Cryostat. A slow heating rate experiment was conducted to determine whether heating-rate effects could be observed in ADN pyrolysis, in other words, to determine how the time-temperature history prior to

a given temperature might affect the pyrolysis behavior at that temperature. In this experiment, the KCl window was held above 100°C such that no material was accumulated on KCl surface and only mass spectrometric data were recorded, while the temperature varied at ~0.3°C/min (the normal heating rate in the experiments described above was 5 to 10°C/min). From 40° to 94°C probe temperature we observed a constant mass spectrometric pattern, albeit with rapidly increasing intensity. At 94°C we observed a maximum rate of gas evolution from solid ADN with the products NH_3, H_2O, NO, and N_2O. No intensity was observed at m/e 46, 60, or 63. The 94°C temperature for maximum rate of evolution of gaseous pyrolysis products is much lower than the one measured using a rapid temperature ramp. This is presumably an example of a commonly observed phenomenon, namely that when the heating is slower, less of a sample is left to decompose by the time a given temperature reached. Thus, the maximum decomposition rate will tend to occur at a lower temperature. A smaller temperature lag between the thermocouple and sample at slower heating rate would also tend to make a given "true" temperature appear to be lower, but since the results already discussed indicate that our temperature lag under the faster heating conditions was only about 10° to 15°C, decreasing the temperature lag further could account for an apparent shift of only a few degrees.

Ten degrees below the maximum at 94°C we recorded pressure bursts of H_2O, and probably also NH_3, which we think evolved from pockets of H_2O or NH_3 within the condensed phase material. These pressure bursts have been observed only in slow heating rate experiments, even though the same material has been used for all pyrolysis experiments. They are real in the sense that they are observable both with the mass spectrometer and with the two ion gauges. Beyond 94°C, no pressure bursts have been observed. As discussed before, this phenomenon is encountered predominantly when the sample was aged, that is, when decomposition products have presumably had time to accumulate during storage (see discussion above on preliminary results) and in the present case where decomposition products had time to accumulate during the slow temperature ramp.

To summarize the slow heating rate experiments, we see stable closed-shell molecules such as NH_3, H_2O, NO, and N_2O, but do not see $HN(NO_2)_2$ or HNO_3. As already concluded for the faster heating rate pyrolyses, reaction via NH_2NO_2 and NH_4NO_3 constitutes, at most, minor pathways. Neither of these intermediates would give NO, and NH_2NO_2 gives no NH_3. Under these vacuum decomposition conditions, NH_4NO_3 exhibits an abundant ion at m/e 46, which is totally absent with ADN. Also absent under the slow heating conditions is m/e 60. Since 46 and 60 are characteristic in fragments of HDN, this means that even though the maximum volatiles formation rate is now observed at a probe temperature more than 50°C below temperatures at which $HN(NO_2)_2$ is known in the faster heating experiments to exit the sample capillary intact (~200°C),

no significant fraction of these volatiles produced under slow heating rate conditions is constituted by $HN(NO_2)_2$. We are forced to conclude either that HDN decomposes upon having only one (or a few) collisions with a ~100°C KCl surface or that conditions are such within the remaining ADN sample that HDN is not stable. This may be because HDN is no longer merely forming at the surface —the interface with the low pressure environment — but is forming in the bulk through a hydrolytic process.

Attempted Regeneration of ADN from $HN(NO_2)_2$ + NH_3. A last set of experiments involved the attempt to reconstruct an ADN from a film of $HN(NO_2)_2$ that had been previously deposited on an ambient KCl window. This $HN(NO_2)_2$ film was dosed repeatedly with HN_3 at pressures of 6×10^{-6} Torr for 10 minutes periods (at ambient temperature and slightly above) without measurable conversion. This result is puzzling. It may simply indicate that, although the chamber pressure of NH_3 in these experiments was about 10 times the nominal partial pressure of NH_3 observed during probe pyrolysis when ADN is being reformed on a cold cryostat, the actual partial pressure of NH_3 in the plume between the pyrolysis probe and the cryostat was really significantly higher. Alternatively, the inability to transform a layer of HDN to ADN may indicate that transport properties of NH_3 across a film of $NH_4N(NO_2)_2$ are important limiting factors, given that the residence time of NH_3 on an ambient temperature surface exposed to high vacuum will be very short. In other words, it appears that the formation of the ammonium salt must occur **while** the condensed phase is being built up on the cold surface. The failure to regenerate ADN from a previously-formed film of HDN is surprising, but is perhaps consistent with the fact that the film formed on a cold cryostat, while predominantly ADN itself, has free HN_3 and HDN trapped in it.

It is possible that the film we have identified as HDN is in reality the potassium salt formed through ion exchange on the ambient temperature KCl window.[8] In this case, there of course would be no regeneration of ADN upon exposure of this film to NH_3. As indicated above, however the "HDN" spectrum of Figure 17 does not match an authentic potassium dinitramide spectrum. Furthermore, the authentic potassium dinitramide is slightly *more* stable than ADN, whereas the film we have identified as HDN is distinctly *less* stable.

C. RDX THERMAL DECOMPOSITION EXPERIMENTS AT LOW PRESSURES.

Experiments were performed in which residual gas analysis mass spectra were recorded while vaporized/decomposing RDX was effusing from the heated sample capillary in front of the cooled cryostat and the FTIR spectrum of the material condensing on the cryostat was being repeatedly recorded. One of the difficulties commonly encountered[9] in RDX studies using mass spectrometry is an uncertainty as to which part of the electron impact mass spectrum corresponds, as the temperature of the probe is increased, to parent ions of thermal decomposition products and which part corresponds to ion fragmentation products of undecomposed RDX. Our hope in this series of experiments was to combine the mass spectral and infrared absorption information to help make this distinction and perhaps obtain infrared evidence for the long-postulated[10,11] intermediacy of N-nitromethyleneimine (CH_2=NNO_2) in the decomposition of HMX and RDX.

In view of the rather low volatility of pure RDX, the vacuum chamber housing the mass spectrometer and the cryogenic window were heated to between 60° and 80°C, depending on the location. The heating became necessary to counteract a memory effect that was apparent after several runs with RDX. The purity of the RDX was checked by differential scanning calorimetric experiments on a small quantity of pure substance as-received. A typical plot shows the onset and peak of the melting endotherm at 204.5°C and 205.7°C, respectively, which corresponds very closely to the literature value of 205.5 for the melting point. Thus there can be no doubt that we were investigating a very pure sample of RDX.

The residual gas electron impact mass spectrum of RDX, as observed with the quadrupole mass spectrometer, consisted of the following masses in order of decreasing mass number: m/e 148, 128, 120, 102, 98, 75, 71, 56, 46, 44, 43, 42, 30, 29, 28, together with a few lower masses. Thus, one expects that most, if not all of the ions that one might expect from thermal products will already appear as ion fragments of RDX itself. The above mass scan was performed with the sample at 160-168°C, and after the sample was spent, no non-volatile residue could be detected by visual inspection of the melting tube capillary, in agreement with Behrens.[11] Despite our efforts, we did not see the molecular ion at m/e 222, in contrast to Lee and coworkers who report[2] the observation of a molecular ion by electron impact quadrupole mass spectrometry. On the other hand, we observed the ion at m/e 128, which was not reported by Lee and coworkers,[2] and and also see ions at m/e 75 and 71, whereas Lee and coworkers observe ions at m/e 74. As discussed by Yinon and Zitron,[12] the relative abundances of high-mass ions in electron-impact RDX spectra vary somewhat from instrument-to-instrument, apparently as a result of different

ion-source and probe temperatures, as well as ion-source pressures. In high-resolution work discussed by Yinon,[13] 75, 120, 128, and 148 were the major high-mass ions. Sometimes the molecular ion was not reported, and sometimes it is seen at very low levels (<0.1%).

We found that when a pure RDX sample is slowly heated from ambient temperature up to 147°C, there are significant changes in the mass spectrum. The major change is that the higher masses characteristic of RDX (e.g., m/e 75, 120, 128, 148) become more prominent as the temperature increases. It is important to note that this is not simply a result of equal fractional increases at all masses, but is due also to significant changes in intensity ratios. This was surprising, since generally heating RDX in high vacuum to temperatures less than ca. 200°C is expected to produce mainly intact RDX in the gas phase.[2,9,11] On the other hand, one might expect some variations in the onset of thermal decomposition, since the extent of the autocatalytic behavior of RDX has been shown to depend on the size and shape of the bulk RDX sample.[14]

Masses 128 and 148 were shown by Yinon[13] to correspond (as ion-fragmentation products) to RDX - (2 HONO) and RDX - (CH_2=NNO_2), respectively. Because of changes in the relative intensity of these and other ions observed as the temperature of the sample holder was increased, we had tentatively concluded that we were seeing small extents of thermal decomposition even at these low temperatures, and therefore, that some fraction of the mass 128 and 148 ions, for example, might be due to thermal decomposition. However, after further consideration, we now judge that the variations shown in Table 1 (occurring at less than 150°C) probably result from changing pressure in the ion source and therefore from changing importance of ion fragmentation via adduct ions formed in the mass spectrometer ion source. For instance, Yinon has shown[13] that m/e 128 results not from fragmentation of the RDX $M^{\cdot+}$ species but from $[M+NO_2]^+$. Thus, the relative intensity of ion 128 would be expected to rise as the RDX vapor pressure rises, even if there is no thermal decomposition. This assessment is consistent with the other results discussed below.

Next, we monitored a given mass as the probe temperature was slowly increased. These experiments were designed to help distinguish those masses originating from RDX from those due to its thermal fragments. Samples of roughly the same size (2-3 mg) were loaded into the sample tubes, and a given mass was continuously monitored as the temperature slowly rose after the H_2O signal returned to its background level. Table 1 presents some of the results obtained in this manner.

Qualitatively, the behaviors of masses 148, 132, 128, and 120 were all similar. The evolution of the ion signal with temperature went through a relative maximum at 133°-142°C, then declined and at higher temperature showed a spike that represented a sudden or "explosive" event

sufficient to saturate the mass spectrometer signal and cause a substantial pressure surge in the vacuum system. Visual inspection of samples that were withdrawn after the relative maximum, but before the spike, showed no obvious signs of mass loss. We concluded therefore that >95% of the sample vaporized/decomposed beyond 140°C. These "sudden events" occur over a wide range of temperatures (171°-199°C), and these well below the melting point at 205°C. This is in agreement with the results of Behrens,[11] who found that most of the decomposition took place between 20 degrees below and up to the melting point. (Since our earlier studies with NH_4NO_3 in this project had indicated a lag of roughly 10°C between the thermocouple temperature and the actual sample temperature in the probe under these heating conditions, an onset of sudden decomposition at an apparent temperature of 170 to 175°C in our experiments would seem to be in exact agreement with finding of Behrens.) Unfortunately the variability of the temperatures that mark the various stages of decomposition (T_i, T_{rel}, and T_{max}, as shown in Table 1) prevented us from determining to what extent some of the characteristic RDX peaks may have had contributions from thermal fragments (in addition to ion fragmentation). This variability should not be surprising, in view of the earlier results of Batten [14] who reported that the autocatalytic behavior of RDX depended on the size and shape of the "pile" of RDX.

Table 1

Temperatures of Onset and Maxima of Ion Current for RDX Decomposition.

M/Z	T_i (°C)[a]	T_{rel} (°C)[b]	T_{max} (°C)[c]
128	121	—	199
148	148	—	181
120	—	—	187
120	110	142	181
120	99	135	186
120	97	133	187
128	99	135	187
132	103	130	171
148	115	141	193

a T_i is the temperature of the onset of significant ion current.

b T_{rel} is the temperature at which a local or relative maximum occurs (as a shoulder) on the rising curve of ion current vs. temperature.

c T_{max} is the temperature at which the maximum ion current is observed (and after which the sample is totally spent. $T_{max} - T_{rel} = 40 \pm 8$°C.

We performed another series of experiments in which the RDX loading in the sample capillary was only 10% to 50% of the 2-3 mg used in the series discussed above. In these experiments, no pressure burst was observed, and the persistent mass flux at m/e 148 was measured as a function of temperature. This behavior is entirely consistent with the shape-dependent behavior of Batten[14] referred to above. Moreover, when the heating rate was slowed significantly, no autocatalytic behavior was observed. Also, we obtained the curious result that, when RDX with slight impurities (as measured by DSC) was used, that also seemed to inhibit the autocatalytic behavior. These observations underscore the need to perform kinetic experiments on thermal decomposition of bulk RDX under very carefully controlled conditions. Unfortunately, such control was not possible in this short study of RDX.

In our final series of experiments with RDX, we concentrated on the nature of the deposit that formed on the cryogenic KCl window during partial or complete evaporation/decomposition of RDX. We cooled the window to -170°C and slowly raised the temperature of the probe until after the explosive decomposition of the sample had occurred, after which we examined the FTIR spectrum of the film deposited on the cryostat. An RDX reference spectrum was obtained by grinding RDX between two KCl plates and recording the FTIR spectrum at ambient temperature. Another reference spectrum obtained by preparing a saturated solution of RDX in absolute ethanol, spreading the solution onto the KCl plate, and letting the solvent evaporate. The two "reference" spectra were essentially identical to each other. The spectrum of the film on the -170°C cryostat was slightly different in the intensity distribution of the intense bands. Because this slight intensity variation is a feature often observed in other instances where spectra of pure substances at vastly different temperatures are compared, and because no new IR absorption bands appeared in the spectrum of the film on the cryostat, we conclude that either the extent of decomposition occurring during these vacuum heating experiments was insignificant, and thus we were observing essentially only material transport from the sample tube to the cryogenic substrate, or that no condensible products were produced in the decomposition. The latter alternative is unlikely. Decomposition to N_2O and CH_2O would have resulted in the deposition of the latter; even full decomposition to N_2, CO, and H_2O, highly unlikely under these circumstances of low confinement, would have resulted in deposition of H_2O.

The absence of any significant decomposition under these circumstances was disappointing and somewhat surprising, given the changes in relative peak intensities during heating that were described above, and the conclusion we had earlier made that the sudden "events" that occurred from 171° to 199°C were something other than accelerated vaporization upon melting of the sample. We had concluded that the shifts in relative mass spectral intensities we observed during heating to 200°C could *not* have been due either to changes in ionizer temperature or to changes in

temperature of the RDX as it entered the ionizer, since this is residual gas analysis and the mass spectrometer is thermally isolated from both the sample probe and the cryostat. Similarly, we had ruled out simple accelerated vaporization following melting because these events began as much as an apparent 34°C below the melting point of *this particular sample* of RDX, seemingly too much to be attributed merely to a lag in sample temperature and accelerated heat transfer (and vaporization) upon sample melting. However, given the FTIR evidence showing nothing but RDX in the cryostat films, we conclude that *most* of the shift in mass spectral intensities observed during heating was in fact due to varying contributions of adduct ions (which can be formed from RDX in the ionizer, as earlier reported by Yinon[13]) to ion fragmentation, rather than to significant contribution of thermal decomposition.

In any event, it is clear that experiments at higher pressures or much higher heating rates are required to achieve thermal decomposition rates that compete with simple vapor transport. This result was somewhat to be expected, and we had anticipated moving from an open sample capillary to one with a restricted opening (in effect a mini-effusion cell), but a limit in time and funds, as well as the experiments with ADN and related materials, prevented us from reaching this stage. The difficulty encountered here is simply another example of the difficulty of understanding the detailed chemistry of energetic materials functioning in general and RDX in particular. If the pressure or (degree of confinement) is raised to bring about substantial fractional reaction at some step in the sequence of rapid reactions that constitute functioning of an energetic material, then it is very difficult to avoid having the identity (and amount) of the product of that particular stage obscured by rapid progression to the next stage of reaction.

D. THERMAL DECOMPOSITION OF $AgN(NO_2)CH_2CN$ AS A PRECURSOR TO $CH_2=N-NO_2$

N-nitromethyleneimine (NMI), CH2=N-NO_2, is thought to be an important intermediate in the decomposition of nitramines such as RDX and HMX. To date the thermal stability, kinetics of thermal decomposition, and spectroscopic signatures of this species are essentially unknown, with the only reported observation being the molecular beam experiments of Lee and coworkers. Thus, the synthesis and characterization of this important intermediate represent a continuing challenge to the scientific community dealing with explosives. J. Bottaro of SRI's Chemistry Laboratory has developed several approaches to the synthesis of an NMI precursor.[15]

The precursor tested in this work is $AgN(NO_2)CH_2CN$. This compound was synthesized because it has a high driving force to eliminate AgCN, a white high melting solid , according to equation (10):

$$AgN(NO_2)CH_2CN \rightarrow AgCN + CH_2=N=NO_2 \qquad (10)$$

The original strategy was to conduct the pyrolysis of the Ag-containing precursor in the melting capillary and try to trap NMI onto the cold KCl substrate. The residual gas mass spectrum would be followed as a function of time and temperature.

If NMI were formed under our experimental conditions, we expected either (or both) of the following reactions might take place before the NMI could be trapped on the -180°C cryostat:

$$CH_2{=}N\text{-}NO_2 \rightarrow HCN + HONO \quad (11a)$$

$$CH_2{=}N\text{-}NO_2 \rightarrow N_2O + H_2CO \quad (11b)$$

If the decomposition were to take place according to equation (11a), we would expect mass spectral intensities at m/e 27, 46, and/or 47. For the mode of thermal decomposition according to equation (11b), m/e 44, 29, and 30 should be prominent.

We proceeded to take fast-temperature-ramp mass spectral survey spectra with the cryostat at ambient temperature. First, we were unable to observe m/e 74, the parent ion of NMI. When the mass scan was initiated at 115°C probe temperature, we observed a prominent m/e 44 (N_2O) and some m/e 46. At 127°C the importance of m/e 44 decreased, and m/e 27, 28, 29, 30, and 46 increased in importance. Qualitatively, the mass spectrum looked like a superposition of C_2H_4 (m/e 27, 28), H_2CO (29, 30), and N_2O, with m/e 46 not accounted for. Possible parents for the m/e 46 ion include NO_2, HONO, HNO_3, and N_2O_5, with the latter two being the least probable. Often, the presence of HCN in thermal experiments is associated with the occurrence of m/e 81, the HCN trimer. Neither m/e 81 nor 74, the parent ion of NMI, could be observed in preliminary experiments on the thermal decomposition of $AgN(NO_2)CH_2CN$.

Next, three individual masses (m/e 44,46 and 30) were monitored as the probe temperature was increased in identical and monotonic fashion in order to compare the evolution of the decomposition products with time. In all three instances explosive decomposition was observed, and in all cases several smaller "events" were registered after the main explosive event. These "explosions" consisted of violent pressure bursts monitored using both the mass spectrometer as well as both total pressure ion gauges. The peak decomposition temperatures for the three masses mentioned were 117°, 113°, and 114°C . That is, within experimental uncertainty, all three masses peaked at the same temperature. The special feature of this compound seems to be its rather sharp threshold, which makes the whole sample "go" within a narrow temperature range. Usually, all the action was contained within two to four degrees around the mean indicated above.

Subsequently, slow temperature ramp experiments were conducted to further explore the thermal behavior of $AgN(NO_2)CH_2CN$. The cryostat was again held at ambient temperature. The slow temperature ramp experiments resulted in slow decomposition without any "explosive"

events, analoguous to the case of ADN. Between 86° and 94°C probe temperature, the mass spectrum was dominated by the evolution of N_2O (m/e 44). Masses 56, 29, and 30 also increased but were of lower intensity. Mass 56 was tentatively assigned to NCNO, a known, albeit fragile gas phase molecule. Mass 29 and 30 do seem to originate only partly from H_2CO because the ratio of these two masses is not characteristic of H_2CO. Therefore, to explain the "excess" intensity at m/e 30, we suggest that NO is also formed . At 106°C probe temperature, the peak at m/e 44 attributed to N_2O is of equal intensity to m/e 28, and m/e 30 is about 20% of m/e 28. Mass 56 (NCNO) also decreased at this slightly higher temperature. At 109°C, the maximum rate of evolution of gaseous products is reached. In addition to the products already mentioned, we observe an increase in the unusual mass at m/e 31 starting at 106°C.

From the above results, we conclude that the most important gaseous products of the thermal decomposition of $AgN(NO_2)CH_2CN$ seem to be N_2O, N_2 (or CO), NO, CH_2O, and NCNO with no indication of the presence of free gas phase NMI under our experimental conditions. Under slow heating rate conditions, we seem to obtain less m/e 46, 27, 28, 29, and 30, that is, less C_2H_4 and H_2CO. By contrast, we seem to obtain more N_2O, N_2 and/or CO. In neither type of experiment did we observe substantial amounts of HCN (27) or any of its trimer (81), or HONO (46, 47), or CH_2NNO_2 (74) itself. The mass spectrometric evidence, taken together, indicates mainly decomposition products of either the Ag-precursor or NMI itself. In all cases we observed a black residue inside the melting tube capillary after thermal decomposition of the Ag-precursor suggesting a coat of finely divided elemental Ag. The formation of NCNO is somewhat surprising, but could arise either from the Ag-precursor or free NMI. The former route, of course, would mean that the Ag-precursor did not function as intended according to equation (10) and that no AgCN is formed during thermal decomposition.

The next experiment consisted in condensing these pyrolysis products onto a cold cryogenic surface (-150°C) and investigating both the FTIR absorption spectrum of the condensate as well as the mass spectrum of products generated in its subsequent thermal desorption. The FTIR absorption spectrum displayed in Figure 19 shows considerable scattering of the deposited film. Inspection of the KCl window after thermal desorption of the products revealed a black coat of finely divided material very similar to the residue inside the melting tube capillary. We conclude that this finely divided nonvolatile material is responsible for the scattering properties of the film. The absorption spectrum was inconclusive, and no attempt was made at interpretation. The mass spectrum during deposition of this film showed essentially the same features as the thermal decomposition of $AgN(NO_2)CH_2CN$ in the presence of an ambient temperature KCl window; thus no new information was obtained.

In conclusion, it appears that although we see substantial amounts of N_2O (as would be expected from subsequent decomposition of NMI) and lesser amounts of its product pair CH_2O, we are witnessing extensive direct thermal decomposition of the Ag precursor to something other than the intended AgCN elimination product. It seems that elemental Ag is deposited more easily than AgCN is eliminated. Thus a different precursor to NMI must be sought.

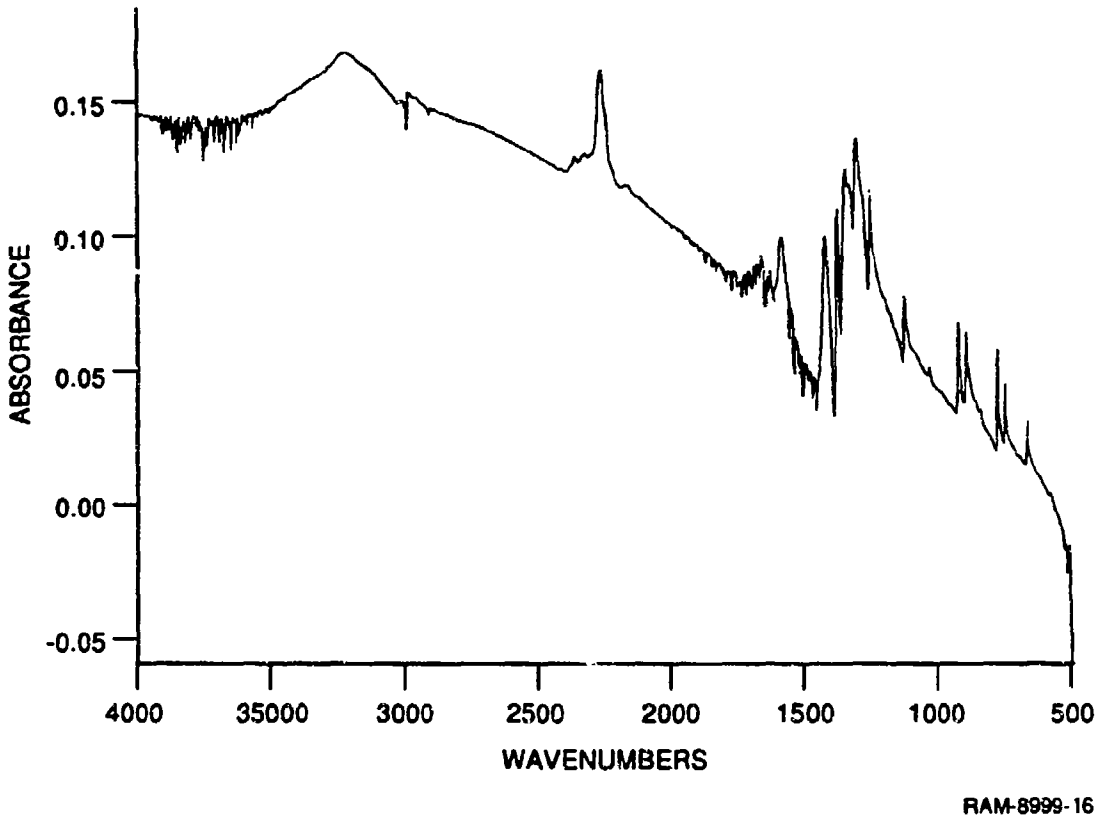

Figure 19. FTIR absorption spectrum of -147°C condensate from decomposition of $AgN(NO_2)CH_2CN$ with probe temperature ranging from 80° to 120C.

SUMMARY AND CONCLUSIONS

ADN Evaporation/Decomposition Scenario. The observations in the foregoing sections lead to the following picture of the molecular processes occurring during ADN evaporation/decomposition.

Dissociation/Pyrolysis of ADN:

$$NH_4N(NO_2)_2 \rightarrow NH_3 + HN(NO_2)_2 \quad (4)$$

$$HN(NO_2)_2 \rightarrow N_2O + HNO_3 \quad (9)$$

$$2\,HNO_3 \rightarrow\rightarrow 2\,NO + H_2O + 1.5\,O_2 \quad (12)$$

Thermal Decomposition of HDN:

$HN(NO_2)_2$ No Desorption of Intact HDN Molecules takes place.

$$2\,HN(NO_2)_2 \rightarrow 2\,N_2O + 2\,NO + H_2O + 1.5\,O_2 \quad (13)$$

The major distinction between ADN pyrolysis onto a cold substrate versus an ambient temperature substrate is that in the former case significant quantities of NH_3 are trapped on the cold substrate as ADN is reformed. In the case of pyrolysis in the presence of an ambient temperature cyrostat, none of the NH_3 released into the gas phase is retained on the surface with the acid component ADN. Thus, the complete absence of NH_3 during subsequent thermal desorption/decomposition of the ambient-temperature-deposited film supports our identification of it as pure $HN(NO_2)_2$. The absence of not only mass 63, but also mass 46, means that HNO_3 and NO_2 were not present. Thus the well known[16] HNO_3 decomposition pathway for HNO_3 shown in reaction (14) cannot describe the loss of any HNO_3 that is formed from $HN(NO_2)_2$.

$$2\,HNO_3 \rightarrow 2\,NO_2 + H_2O + 1/2O_2 \quad (14)$$

Heterogeneous decomposition of HNO_3 evidently occurs in our system primarily to products that do not include NO_2. The most probable reaction site is the wall of the stainless steel vacuum chamber that was exposed to many other molecular environments. In the absence of any major amounts of NO_2, we postulate that the heterogeneous decomposition of HNO_3 proceeds instead to

NO, H_2O, and a larger yield of O_2, as shown above in reaction (12). An alternative that cannot be ruled out is decomposition of $HN(NO_2)_2$ that does not proceed through HNO_3. An alternative route not involving HNO_3 would be supported by the fact that ADN and HDN decomposition produce strong m/e 30 signals and little or no m/e 46, whereas NH_4NO_3 decomposition, known to proceed through HNO_3, produces the opposite: a week NO signal (m/e 30) and strong m/e 46. However, these differences should not be overweighted: it would be naive to expect HNO_3 to decompose in exactly the same way in the absence and presence of HDN. Thus the exact loss route for HDN remains uncertain at this point. In any case, the m/e 44/m/e 30 intensity ratio is substantially higher in ADN decomposition than we observed with NH_4NO_3 under similar conditions. The details of the secondary decomposition of HNO_3 would be more effectively addressed using a molecular beam sampling variation of mass spectrometry that would better indicate the nature of the primary pyrolysis products emanating either from the sample capillary or from the surface of the KCl window.

The absence of m/e 60 (coupled with the absence of m/e 46) during the thermal desorption of the ambient-temperature-deposited film of dinitraminic acid means that no HDN can be desorbed intact even when the film is more than 50°C below temperatures at which intact HDN is evolved from heated ADN (either polycrystalline or amorphous). Thus the decomposition behavior of the condensed phase free acid is far different from that of isolated HDN molecules, or even HDN molecules in contact with a heated surface. On this basis we speculate that the most facile decomposition pathway for ADN involves dissociation or hydrolysis to free HDN, followed by self-protonation. This is consistent with the fact that HDN appears[17] to be a stronger acid than HNO_3. Thus it seems likely that the usual class of amine inhibitors could be used if necessary to enhance the stability of ADN during storage.

In accord with the above discussion, we suggest the following pathway for HDN decomposition under the present slow heating vacuum conditions. We suspect that this pathway for HDN decomposition may be operative even for decomposition of ADN under confinement, such as occurs during propellant decomposition. Further, it seems likely that such a pathway would proceed from the aci form of dinitraminic acid, since this tautomer, in forming the N-N double bond, has already moved in the direction of N_2O formation. In Scheme 1 we show such an acid-catalyzed decomposition pathway leading to HNO_3 and N_2O.

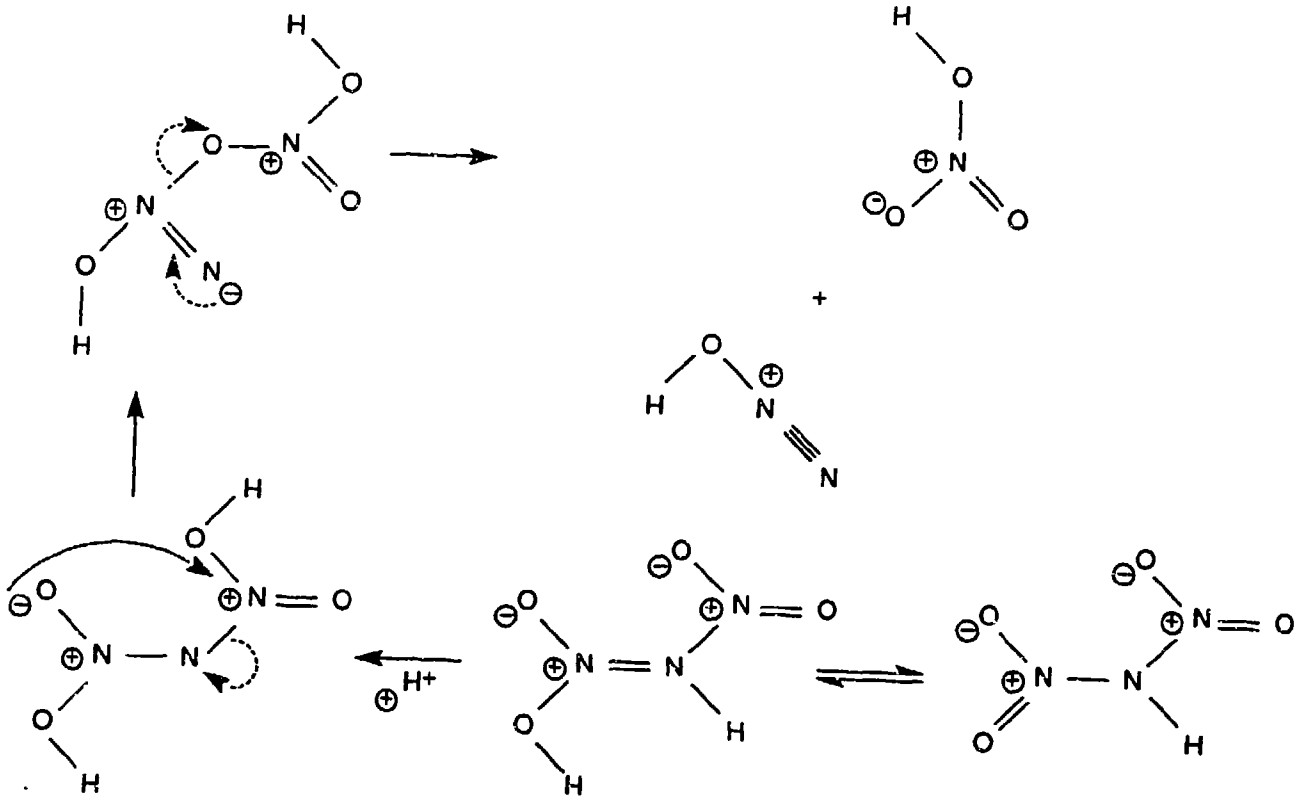

Scheme 1. Potential acid-catalyzed decomposition of HDN via its aci- form.

RDX Decomposition. The objective in this series of experiments was to combine mass spectral and infrared absorption information obtained during low pressure decomposition of RDX in order to distinguish between thermal and ion fragments and to obtain direct infrared evidence for the intermediacy of N-nitromethyleneimine (CH_2=NNO_2). This effort was unsuccessful, in part because of inherent difficulties and in part because experimental control was insufficient in these experiments.

Attempted Generation of an Authentic Sample of CH_2=N-NO_2. The pyrolysis experiments with $AgN(NO_2)CH_2CN$ were at best only partly successful. They were performed in the hope that AgCN would be eliminated and that the long-postulated RDX intermediate, N-nitromethyleneimine (NMI), would be formed . The pyrolysis resulted in the production of N_2O, CH_2O, N_2 (or CO), NO, and NCNO. Although the first two listed products would be expected from decomposition of N-nitromethyleneimine, the molecular ion of NMI itself was not observed, and interpretation of the film deposited on the cryostat was prevented by a black deposit, presumably finely divided elemental silver. Thus, we apparently witnessed extensive direct thermal decomposition of the Ag precursor to something other than the intended AgCN elimination

product. We now conclude that other potential precursors probably offer better routes to the elusive intermediate of RDX decomposition.

RECOMMENDATIONS

Since dissociation of ADN to its acid-base components occurs at moderate temperature in vacuum, and since the condensed-phase free dinitraminic acid is much less stable than ADN or other dinitramide salts, the reactions of HDN almost certainly play a key role in determining the storage stability and combustion behavior of ADN. Moreover, the high acidity of HDN suggests that self-protonation reactions control decomposition of neat HDN, and also means that limiting the hydrolysis of dinitramide salts is key to maintaining the storage stability of ADN. Therefore, the interplay of acid-catalyzed and "thermal" (i.e., non-ionic) decomposition of ADN is an area that warrants a concerted effort. For example, in the present study, we found that slowing the heating rate during vacuum thermal decomposition of ADN to ~0.3°C/min resulted in intact HDN molecules no longer being delivered into the gas phase at 94°C. However, other work by Schmitt and coworkers shows that holding the ADN melt more than 10°C higher (107°C) in flowing N_2 for 22 hours resulted in less than 8% "evaporation" of ADN and in *no* autoacceleratory process. This apparent discrepancy may well result from differing degrees of removal of the base component NH_3 at the two different pressures. We recommend that the decomposition behavior of ADN be thoroughly characterized as a function temperature, acidity, and concentration in aqueous and non-aqueous liquid phase environments. We believe in this case that such studies are even more important than the gas-phase thermal decomposition measurements, which are themselves a baseline for understanding the thermal condensed phase behavior.

REFERENCES

1. Bottaro, J.C.; Penwell, P. E.; Schmitt, R. J., unpublished work, 1991.

2. Zhao, X.; Hintsa, E. J.; Lee. Y. T. *J. Chem. Phys.* **1988**, *88*, 801.

3. Brower, K. R.; Oxley, J. C.; Tewari, M. *J. Phys. Chem.* **1989**, *93*, 4029

4 Rosser, W. A.; Inami, S.; Wise, H. *J. Phys. Chem.* **1963**, *67*, 1753

5 Davies, M.; Jonathan, N. *Trans. Farad. Soc.* **1958** *54*, 469.

6. Arrowsmith, C. H.; Awwal, A.; Euser, B. A. ; Kresge, A.J.; L. Lau, P. P. T.; Onwood, D. P.; Tang; Y. C.; Young, E. C. *J. Am. Chem. Soc.* **1991**, *113*, 172

7. Hughes, M. N.; Lusty, J. R.; Wallis, H. L. *J. Chem. Soc. Dalton Trans.* **1983**, 262.

8. Russell, T. P., Private Communication, 1992

9. Schroeder, M. A. , Proceedings of the 18th JANNAF Combustion Meeting, 1981, Vol. II, p.395.

10. Shaw, R.; Walker, F. E., *J. Phys. Chem.* **1977**, *81*, 2573.

11. Behrens, Jr. R. *Proceedings of the 24th JANNAF Combustion Meeting* CPIA, Baltimore, MD, **1987**, p. 33.

12. Yinon, J.; Zitrin, Z., *The Analysis of Explosives*, Pergamon Press, Oxford, U. K., 1981, p. 189.

13. Yinon, J.; Harvan, D. J.; Hass, J. R. *Org. Mass Spectrom.* **1982**, *17*, 321.

14. Batten, J. J.; Murdie, D. C. *Aust. J. Chem.* **1970**, *23*, 749.

15. Bottaro, J. C., unpublished work, 1990.

16 S. Svensson and E. Ljungstroem, *Int. J. Chem. Kin.* 20, 857 (1988)

17. Ross, D.S. Private Communication 1991.

APPENDIX

THE THERMAL DECOMPOSITION OF THE NEW ENERGETIC MATERIAL AMMONIUMDINITRAMIDE ($NH_4N(NO_2)_2$) IN RELATION TO NITRAMIDE (NH_2NO_2) AND NH_4NO_3.

Michel J. Rossi* Donald F. McMillen, and Jeffrey C. Bottaro
Chemistry Laboratory
SRI International, Menlo Park CA 94025 USA

*To whom correspondence should be addressed at Ecole Polytechnique Fédérale de Lausanne, DGR/Laboratoire de Pollution Atmosphérique, Bâtiment CH/LCT, CH-1015 Lausanne, Switzerland.

To be submitted to the International Journal of Chemical Kinetics

THE THERMAL DECOMPOSITION OF THE NEW ENERGETIC MATERIAL AMMONIUMDINITRAMIDE ($NH_4N(NO_2)_2$) IN RELATION TO NITRAMIDE (NH_2NO_2) AND NH_4NO_3.

Michel J. Rossi,* Jeffrey C. Bottaro, and Donald F. McMillen
Chemistry Laboratory, SRI International, Menlo Park CA 94025 USA

ABSTRACT

This qualitative study examines the response of the novel energetic material ammonium dinitramide (ADN), $NH_4N(NO_2)_2$, to thermal stress under low heating rate conditions in a new experimental apparatus. It involved a combination of residual gas mass spectrometry and FTIR absorption spectroscopy of a thin cryogenic condensate film resulting from deposition of ADN pyrolysis products on a KCl window. The results of ADN pyrolysis were compared under similar conditions with the behavior of NH_4NO_3 and NH_2NO_2 (nitramide), which served as reference materials. NH_4NO_3 decomposes into HNO_3 and NH_3 at 182°C and is regenerated on the cold cryostat surface. HNO_3 undergoes presumably heterogeneous loss to a minor extent such that the condensed film of NH_4NO_3 contains occluded NH_3. Nitramide undergoes efficient heterogeneous decomposition to N_2O and H_2O even at ambient temperature so that pyrolysis experiments at higher temperatures were not possible. However, the presence of nitramide can be monitored by mass spectrometry at its molecular ion (m/e 62). ADN pyrolysis is dominated by decomposition into NH_3 and $HN(NO_2)_2$ (DN) in analogy to NH_4NO_3, with a maximum rate of decomposition under our conditions at approximately of 155°C . The two vapor phase components regenerate ADN on the cold cryostat surface in addition to deposition of the pure acid HDN and H_2O. Condensed phase HDN is found to be stable for indefinite periods of time at ambient temperature and vacuum conditions, whereas fast heterogeneous decomposition of HDN at higher temperature leads to HNO_3 and N_2O. Gas phase HDN also undergoes fast heterogeneous decomposition to NO and other products, probably on the internal surface (ca. 60°C) of the vacuum chamber before mass spectrometric detection.

*To whom correspondence should be addressed at Ecole Polytechnique Fédérale de Lausanne, DGR/Laboratoire de Pollution Atmosphérique, Bâtiment CH/LCT, CH-1015 Lausanne, Switzerland

INTRODUCTION

Nitramines are a familiar class of energetic compounds that are used either pure or in conjunction with other ingredients as propellants or explosives. On the other hand, previous preparations of dinitramines have been very limited and have produced only highly unstable materials of no practical use. Hamel and Olsen describe,[1] in detail, the synthesis of alkyl N,N dinitramines from alkyl nitramines and nitronium fluoborate. These alkyl dinitramines are unstable, decomposing at emperatures of 75°C or less. The unfortunate thermal instability of these materials renders them useless as explosives, propellants, or propellant ingredients. However, the parent dinitramine (or "dinitraminic acid"), $HN(NO_2)_2$, as well as its salts, which were not previously known, display properties vastly different from those of alkyldinitramines. Recently, Bottaro and Schmitt have synthesized a series of salts of dinitramide that have been shown to be promising candidates for halogen-free efficient propellants.[2] The present study provides a qualitative assessment of the properties of the ammonium salt of dinitramide (ADN) under thermal stress in order to gain insight into the modes of thermal decomposition that could be of importance in the explosive decomposition of those materials. It is apparent from our results that experiments at higher heating rates have to be undertaken in order to understand, and hence model, the actual combustion or explosive decomposition of ADN or similar materials. However, our experiments allow us to catch a first glimpse on the possible reaction pathways and reaction products of those novel energetic materials.

We have also examined, under similar experimental conditions, two closely related nitrogen compounds as reference materials, namely NH_4NO_3 and NH_2NO_2, whose thermal decomposition have been studied in some detail previously. Although bulk kinetic studies of NH_4NO_3 have been performed by several authors[3-5], important mechanistic questions remain unanswered, even for this compound. We hope to learn more of the modes of rapid decomposition of the novel energetic materials by comparing their thermal behavior with these "reference" materials.

EXPERIMENTAL APPARATUS AND APPROACH

The apparatus used for this work was constructed to study the decomposition of organic materials by utilizing concurrent mass spectrometeric detection of vapor phase species and FTIR detection of condensible products. Since the decomposition of energetic materials is often characterized by multiple decomposition pathways and fast secondary reactions, heating at low pressures can provide a way to slow down the secondary reactions and facilitate observation of the

initial decomposition steps. Since the branching ratios of the competing secondary reactions will likely change markedly with shifts in phase, concentration, and temperature, we expect low pressure studies by themselves to be insufficient to provide a practical understanding of the behavior of energetic materials. On the other hand, the behavior of these materials is typically so complex that examination under the nominal conditions of propellant combustion, for instance, will seldom, if ever, be sufficient to provide a real understanding of the chemistry that controls the combustion kinetics. Therefore, we have used the experimental apparatus shown schematically in Figure 1 to study and compare the low pressure condensed phase decomposition behavior of NH_4NO_3, NH_2NO_2, and $NH_4N(NO_2)_2$.

The strategy adopted is the following: About 1 mg is heated in a small pyrex capillary housed in a heated direct insertion probe that is located about 5 cm in front of a cryogenically cooled KCl window. The gaseous pyrolysis products hit a cryogenic (liquid N_2 cooled) window whose transmission in the IR is examined at given time intervals by FTIR absorption spectroscopy, at the same time that the gas phase is sampled with a quadrupole mass spectrometer. Due to the fact that the thermal decomposition is taking place at nominal pressures of 10^{-7} Torr, only the gaseous components with an equilibrium vapor pressure smaller than the background pressure will be deposited as an amorphous film onto the cryogenic window. Pyrolysis products that do not satisfy this condition will be monitored by mass spectrometry which is performed in a residual gas mode in this series of experiments. Therefore, such products as N_2, NO and N_2O have been monitored at m/e 28, 30 and 44 essentially *in situ*. The sensitivity of the FTIR absorption measurements is excellent because of the effective integration of the product flux by letting sufficient material accumulate onto the window, and also because of the high signal-to-noise ratios of the FTIR spectrophotometer. Once the sample has decomposed and the growth of the condensed phase on the IR optical window has ceased, the temperature of the cryostat is slowly increased. Thermal desorption of pyrolysis products monitored by mass spectrometry as the temperature of the cryostat is rising gives further insight into the nature and identity of the complex mixture of pyrolysis products.

The main cylindrical stainless steel vacuum chamber housing the cryostat (Figure 1) is pumped by a 2000 l s^{-1} baffled diffusion pump whose base pressure was 10^{-8} Torr. In view of the low vapor pressure of many of the materials investigated in this and other studies, the walls of the vacuum chamber were heated to about 70°C in order to minimize "memory effects" of the samples studied. This heating resulted in a final temperature of the cryogenic KCl window (liquid N_2 cooled) of approximately -185 or -180°C, slightly higher than the temperature achieved without heating the chamber walls. Two total pressure ion gauges measure the pressure in the main vacuum chamber at two different locations. One is mounted near the top of the chamber near the

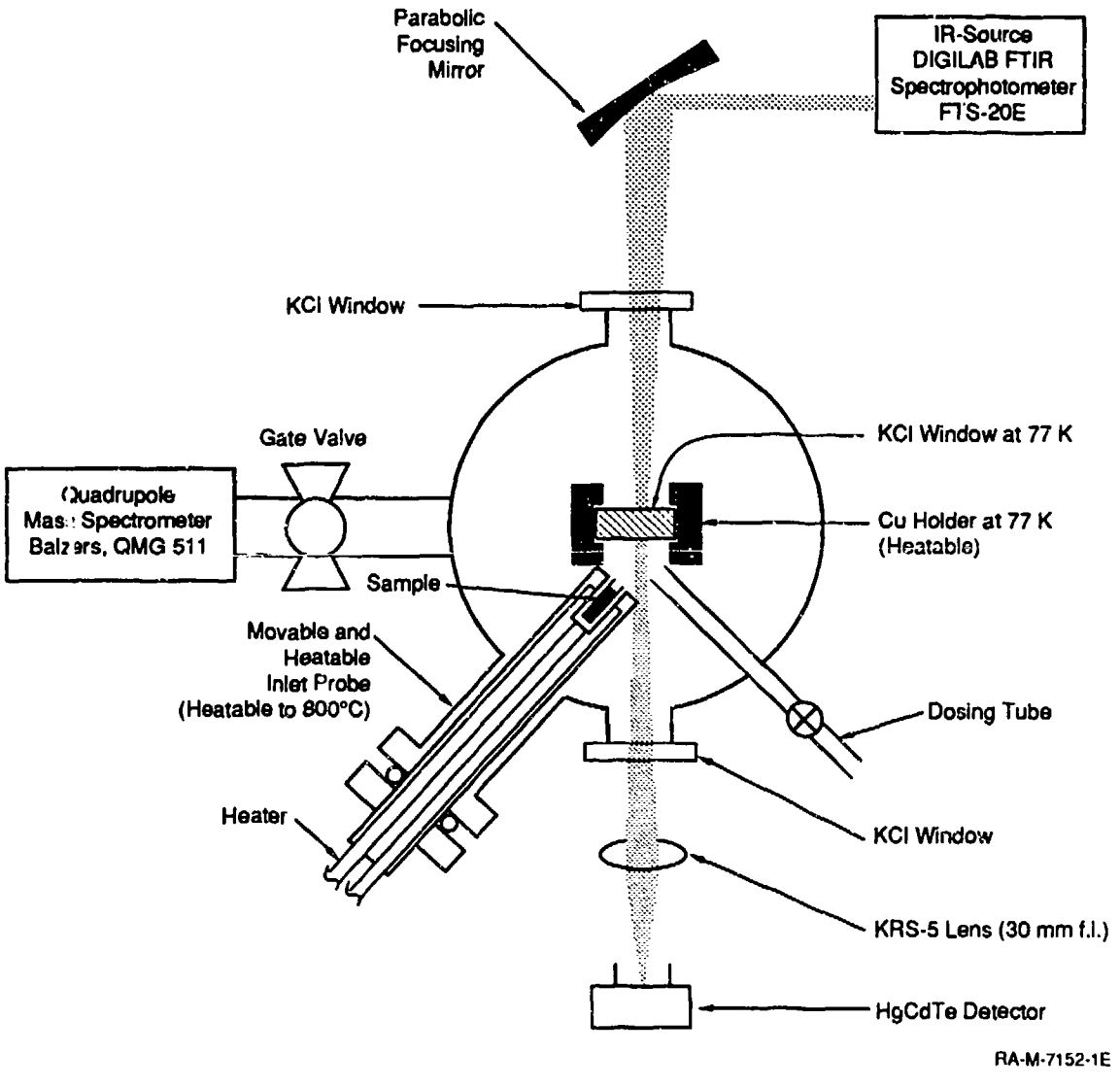

Figure 1. Thin film diagnostic apparatus using FTIR-absorption and mass spectrometry.

cryostat, the second is located in proximity of the inlet to the 8" diffusion pump The mass spectrometry chamber is pumped by a 270 l s^{-1} turbomolecular pump and houses a BALZERS QMG 511 quadrupole mass spectrometer operated in residual gas analysis mode. The mass spectrometer chamber can be isolated from the main deposition/pyrolysis vacuum chamber by a 6" gate valve in case the pressure becomes too high in the mass spectral analysis chamber.

The heatable sample probe is shown in some more detail in Figure 2 and is designed to be inserted through a 0.5 " diameter aperture ball valve. The quartz probe can be completely retracted into the stainless steel sleeve during insertion or removal through the ball valve. The heating of the sample is performed by radiative transfer of energy from the heating wire to the sample across the quartz tubing. Note that the type "K" thermocouple is housed in a well beneath the sample and is separated from the NiCr heating wire by an amount of material (glass) comparable to that which separates the sample (contained in a thin walled pyrex melting capillary tube) from the heating wire.

The material requirements for pyrolysis are minimal in that 0.5 to 2 mg of solid material are placed in the bottom of 1-cm long melting point capillary which is then inserted into the probe tip. This amount is sufficient to obtain intense mass spectra and FTIR spectra of deposited thin films of μm size thickness, resulting in absorption spectra of excellent signal-to-noise ratio (≥100). Typically, the experimental protocol consists of increasing the probe temperature while collecting the pyrolysate on either the cold or ambient temperature KCl window, whose temperature is measured at the distant tip (furthest from the liquid N_2) using a type "E" thermocouple fastened with a screw to the copper frame of the 1" diameter KCl IR transmission window. Once the material in the probe capillary is exhausted and has been collected on the KCl window, the latter is heated in order to desorb the condensate until the original IR transmission of the KCl window has been restored.

The cryostat is a 0.5" diameter stainless steel tube holding liquid nitrogen. The upper portion of the cryostat is surrounded by a vacuum insulated concentric tube in order to ensure ambient temperature at the seal (knife-edge) to the top of the vacuum chamber. The tip of the cryostat is a brazed copper plug to which the copper window holder is fastened. For heating, the cryostat is wrapped on its entire length by a resistive heating element (ARI heaters) clamped to the cryostat by steel clamps. In some experiments temperatures of 300°C had to be attained in order to rid the KCl window of any absorptions in the IR. In this way mass spectra for all the components of the pyrolysate are obtained as a function of temperature, whereas FTIR transmission spectra are obtained for those components that are collected onto the cryogenic window and that are stable with respect to evaporation and/or pyrolysis at a given probe temperature.

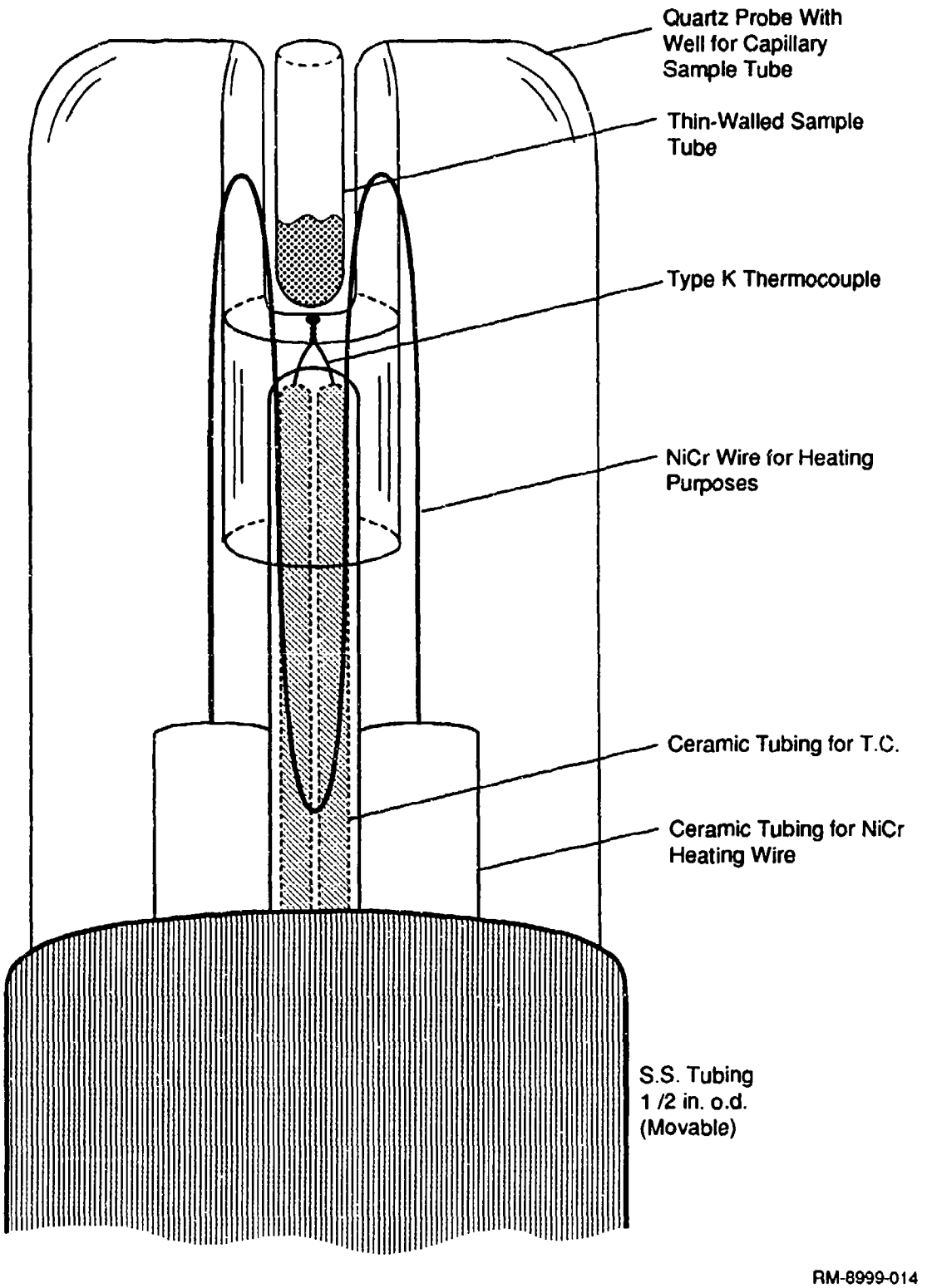

Figure 2. Schematic cross section of the resistively heated fused silica probe tip for holding capillary sample tubes.

FTIR spectra are recorded using a DIGILAB FTS-20E spectrometer, whose external beam was not purged. Therefore, the resulting IR spectra show some presence of atmospheric constituents (CO_2, H_2O), even after spectral subtraction. IR radiation leaving the optics bench of the FTS-20E spectrometer was directed using two flat first surface Al mirrors onto a 3" diameter first surface Al focussing mirror (f. l. 5"). The vacuum system was sealed by two 2" flat KCl windows. After passage through the cryogenic window at the tip of the cryostat, the beam was refocussed onto the wide-band HgCdTe detector (5000-500 cm^{-1}) using a 1" diameter 1" f. l. KRS-5 lens. In some experiments not detailed here, the thickness of the deposited amorphous film was measured using the interference fringes of a HeNe laser using the same focussing mirror as the IR beam (This is not shown in Figure 1).

Nitramide, NH_2NO_2, and ammoniumdinitramide (ADN), $NH_4N(NO_2)_2$ were synthesized by Bottaro of SRI's Chemistry Laboratory.[2] The ammoniumdinitramide appeared to have a purity >99%, with the only significant impurity (apart from water) being evidenced by small contributions at m/e 55 and 57, which originate from a small impurity of n-butanol which was used to recrystallize $NH_4N(NO_2)_2$.

RESULTS AND DISCUSSION

In this paper only qualitative results on the thermal decomposition of ammonium dinitramide will be presented. In order to put these results into the proper context, we will compare the behavior of ADN with that of NH_4NO_3 and NH_2NO_2 under thermal stress. The reason for this procedure is the fact that both NH_4NO_3 and NH_2NO_2 are possible intermediates of the thermal decomposition of $NH_4N(NO_2)_2$, although the connection is more formal than structural. We will present results on the two simpler nitrogen containing compounds prior to the discussion of ADN thermal decomposition. Throughout the discussion, we will usually refer to ammonium dinitramide by the acronym ADN, and for consistency to the free dinitraminic acid as HDN, although in deference to common usage, we will continue to use the name nitramide for NH_2NO_2.

NH_4NO_3

Quantities on the order of a milligram of ground NH_4NO_3 were placed in the probe with the cryogenic window at -190°C (83 K). Upon heating the probe, the effusing gases were monitored by mass spectrometry. Mass spectral scans revealed the presence of NH_3 and HNO_3 in increasing amounts with increasing probe temperature. NH_3 was monitored at masses m/e 16 and 17, whereas HNO_3 was followed at m/e 63, 46 and 30. Quantitative evaluation established these

two gas phase products as the only vapor phase species of importance. The presence of gas phase HNO_3 is somewhat surprising given the fact that the equilibrium vapor pressure is estimated to be significantly smaller than the background pressure in the cryostat chamber of approximately $3*10^{-8}$ Torr. Based on this estimate we expected most of the effusing HNO_3 to "stick" to the cryogenic KCl window and expected therefore a small mass spectrometric signal. NH_3 is a borderline case with a vapor pressure of 10^{-6} Torr at 102 K and 10^{-7} Torr at 96 K. FTIR indicates that NH_3 does not condense on the cryostat under the present experimental conditions by itself, even at the lowest temperatures reached. The abundance of HNO_3 in the gas phase is more surprising. Since the heat of condensation and heat capacity of a microns thick film are insignificant compared to the heat capacity of the KCl substrate, the KCl surface during condensation cannot be more than a few degrees above that of the thermocouple located at the warmest end of the copper substrate holding the KCl window (i.e., farthest from the liquid nitrogen reservoir). Therefore, we judge it likely that the effusing gas is simply partly "missing" the cryogenic surface due to insufficient geometric overlap. Even with the short distance between the exit aperture of the melting capillary and the cryogenic surface (3 cm), a $(\cos)^2$ distribution would have a significant part of the effusing species pass by the 3-cm diameter cryostat assembly.

In order to put the mass spectrometric results into a more quantitative context, a specific mass was followed as a function of probe temperature using identical heating rates and comparable sample sizes. Table I displays the results when the evolution of NH_3 and HNO_3 was followed by monitoring the ion current as a function of temperature.

TABLE 1.

Temperatures of Rapid Gas Evolution during NH_4NO_3 Decompositon.

Species Monitored	M/e Monitored	T°C of maximum evolution rate
NH_3	17	187
NH_3	17	190
HNO_3	63	174
HNO_3	63	181
HNO_3	46	182
NH_3	17	185
HNO_3	46	177
		Avg. 182.3

The characteristic feature of every one of the curves thus obtained is the presence of a single sharp spike indicating a single "explosive" event after which the sample was spent. This explosive decomposition was observed also by monitoring the total pressure (ion gauges) whose readout resulted in a similar sharp spike at the same probe temperature as the mass spectrometric observation. Although the individual ion current vs. temperature curves vary sometimes significantly as to their precise shapes, their characteristic parameters such as onset, width and maximum agree remarkably well within certain limits. The maximum evolution of both constituents is measured at 182±5°C which is nominally about 10°C higher than the measured melting point at 169.9°C. Under these vacuum conditions, the decomposition of NH_4NO_3 is clearly dominated by the simple dissociation into the acid and base components, as in Equation (1):

$$NH_4NO_3 \Rightarrow NH_3 + HNO_3 \qquad (1)$$

The sudden increase in dissociation (an endothermic event) in the absence of any substantial amount of exothermic reaction to drive it very likely results simply from improved heat transfer from the hot capillary walls upon melting of the NH_4NO_3. Based on previous experience with this particular probe design, we expect that a lag in temperature of about 10°C between thermocouple in contact with the bottom of the sample capillary holder and the inside of the capillary itself is not unlikely. (see Figure 2). Consequently, we conclude that the rapid dissociation of NH_4NO_3 under these conditions takes place within a few degrees of (and very probably at) the melting point. In any event, the temperature at which either simple dissociation or exothermic decomposition of NH_4NO_3 take place is not an intrinsic value, but is dependent on the partial pressure of the acid and base species over the condensed phase material.

The current conditions are not those that that we expect to yield irreversible decomposition of the acid and base components of NH_4NO_3. Brower and coworkers[3] concluded in a recent study of NH_4NO_3 decomposition that ionic equilibria were important in the lower temperature range, which is of interest here. It was conclusively shown that HNO_3 had a catalytic effect on NH_4NO_3 decomposition, while H_2O and NH_3 inhibited the formation of N_2O and H_2O, the two principal products of NH_4NO_3 decomposition. This finding is consistent with reaction involving self-protonation of HNO_3 in the condensed phase, because the vapor phase does not support ionic reaction mechanisms. Although the extremes of the temperature ranges overlap in the two studies, the conditions are otherwise radically different. In our low pressure study, the evaporation of NH_4NO_3 is so fast that a molten phase with its considerable vapor pressure can not be sustained. Our study therefore addresses predominantly the behavior of the bulk crystalline phase under thermal stress minimizing secondary bimolecular gas phase reactions and secondary reactions in a

liquid or melt phase. The absence of any "real" chemical decomposition of NH_4NO_3 in our case is evidenced by the absence of any N_2O and H_2O, the known products of NH_4NO_3 decomposition.

FTIR absorption spectra were obtained by heating NH_4NO_3 to temperatures of about 200°C and collecting the effluent on the cold cryostat window, usually at approximately -190°C. Figure 3 shows a FTIR absorption spectrum of a condensate film that has been collected at -190 °C and been allowed to warm up to -50°C. The condensate has been identified as NH_4NO_3 by comparison with a measured absorption spectrum of an ambient temperature authentic polycrystalline sample and by comparison with literature data. By observing the differences in the absorption spectrum upon warming the sample to -50°C, we concluded that a small amount of NH_3, perhaps 10%, was incorporated in the polycrystalline sample of NH_4NO_3. Notably, a characteristic absorption band at 958 cm^{-1} corresponding to the bending mode (umbrella motion) in NH_3, together with other broader absorption bands, disappeared upon warming. Apparently the occluded NH_3 leaves the condensate film in the temperature range -190°C to -50°C. The characteristic bands of NH_4NO_3 are the broad N-H stretch at 3150 cm^{-1}, the asymmetric and symmetric NO_2 stretch at 1440 and 1400 cm^{-1} and the sharp absorption at 825 cm^{-1}. When the identical pyrolysis experiment was performed with the cryostat at ambient temperature, only a very small amount of NH_4NO_3 was observed by FTIR absorption.

The experimental results show that the sublimation of NH_4NO_3 proceeds by way of dissociation of the molten material into its gas phase constituents HNO_3 and NH_3. Subsequently, the gas phase components undergo the acid-base reaction (the reverse of reaction (1)) on the cold surface of the cryostat. In view of the fact that NH_3 does not condense under our conditions, we suggest that the reformation of NH_4NO_3 proceeds by collisions of gaseous NH_3 with solid HNO_3. The presence of small but significant amounts of NH_3 in condensed films of pyrolyzed NH_4NO_3 is due to a loss of HNO_3, presumably by heterogeneous pathways (see below). We suggest that this loss occurs either on the walls of the capillary sample holder or on some other ambient temperature surface of the vacuum chamber. An important conclusion is the fact that no products of the "real" thermal decomposition of NH_4NO_3, such as N_2O, H_2O, and NH_2NO_2, were found. Therefore, sublimation via simple dissociation seems to be the only important pathway of NH_4NO_3 under the present slow-heating, low-pressure conditions.

NH_2NO_2

In contrast to NH_4NO_3 and ADN, solid nitramide is a deliquiescent material and is a molecular crystal whose vapor pressure by far exceeds the background pressure in the vacuum chamber. Therefore, evaporation took place even with the probe at ambient temperature, so that

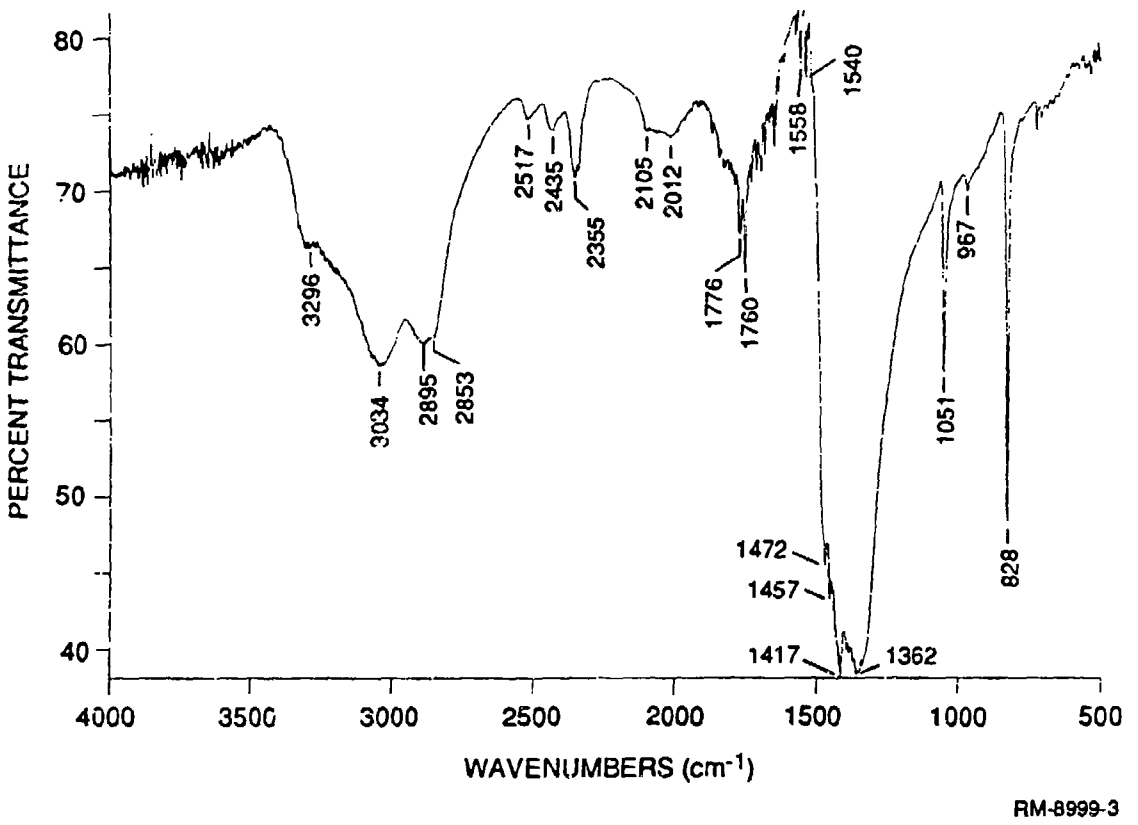

Figure 3. FTIR transmission spectrum after complete evaporation of NH_4NO_3 (probe $\bar{T}$ = 203°C) after the cryostat has been warmed to -50°C.

normal pyrolysis experiments, uncomplicated by simple evaporation, were not possible. Nevertheless, decomposition of nitramide is so facile that significant decomposition took place in competition with evaporation. Figure 4 shows a typical mass scan after the introduction of a NH_2NO_2 sample with the cryostat at low temperature and the probe at ambient temperature. Important mass spectral intensities are registered at m/e 17, 18, 28, 30, 44, and lower but significant intensities at 46 and 62. This latter mass corresponds to the molecular ion of NH_2NO_2 and has about 2 to 3% of the intensity of the base peak at m/e 44. The relative intensity of the peaks in the mass spectrum was essentially independent of the temperature of the cryostat, but did change with time (i.e., as the fractional depletion of the sample in the probe changes). For this reason it is apparent that this mass spectrum does not originate entirely from one single neutral parent species, namely NH_2NO_2. The most noticeable change is in the relative intensity of the fragment masses m/e 18 and 44 and the molecular ion, m/z 62. As shown below, the former are still observed under conditions where m/e 62 has vanished. We conclude therefore, that a condensed-phase or heterogeneous reaction is causing rapid decomposition of NH_2NO_2 according to the following reaction:

$$NH_2NO_2 \Rightarrow N_2O + H_2O \qquad (2)$$

We presume that under these rather mild conditions, this reaction occurs according the accepted base catalyzed mechanism, as recently discussed by Arrowsmith et al.[6] In any case, in the early stages of the sublimation, Reaction 2 is simply not rapid enough to destroy all of the NH_2NO_2, and some residual intensity is observed at m/e 62.

Reaction 2 is exothermic by 16.8 kcal/mol (in the gas phase) if one assumes a sublimation enthalpy of 10.0 kcal/mol for NH_2NO_2. The fact that the observed mass spectrum is independent of the cryostat temperature means that: (a) the heterogeneous decomposition must take place either in the condensed phase or on the walls of the melting tube capillary (probe) or some ambient temperature internal surface of the vacuum vessel, and (b) none of the products are substantially condensible.

Measurements of ion current at m/e 18 (H_2O), 44 (N_2O) and 62 (NH_2NO_2) as a function of probe temperature revealed totally erratic behavior of the ion current with increasing temperature, in that irregular bursts of H_2O and N_2O were monitored using both the mass filter as well as measuring the total pressure (ion gauges). Qualitatively the same erratic behavior was observed for m/e 62 This effect was especially pronounced when older samples that had time to undergo thermal decomposition prior to pyrolysis were used. This behavior stands in contrast to the one observed with NH_4NO_3, in that for the latter, the consistent observation was of a single

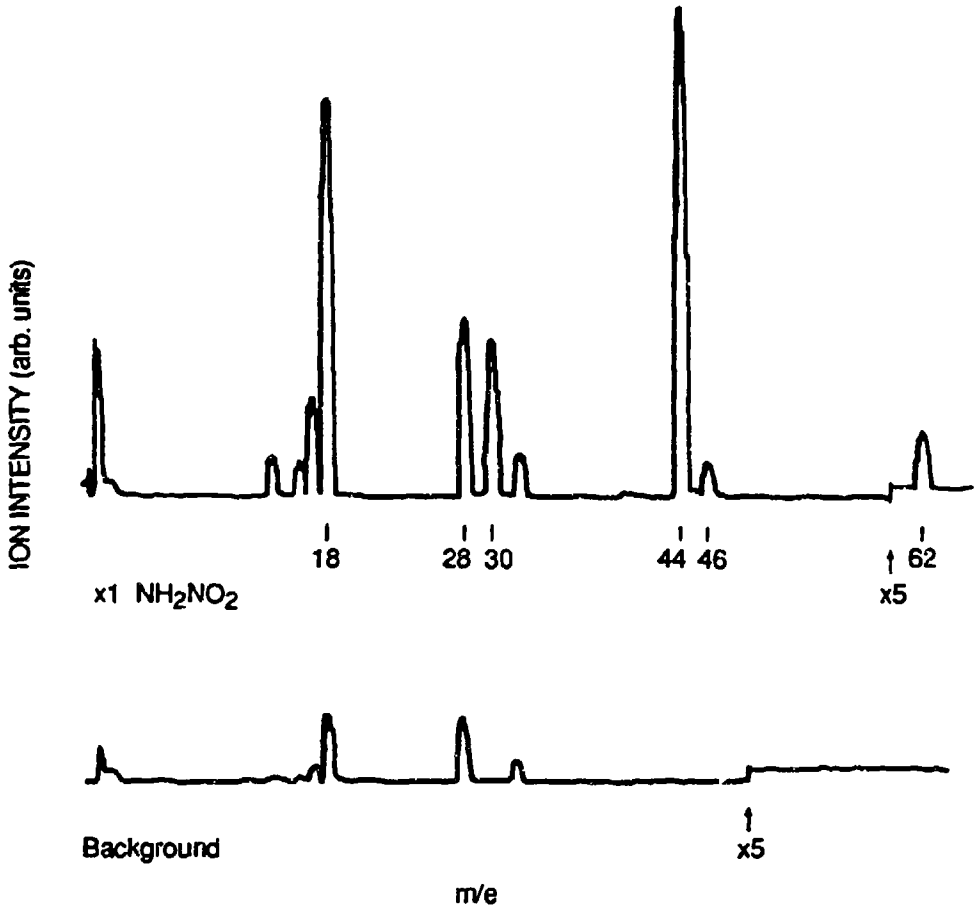

Figure 4. Mass spectrum of material desorbing/decomposing from an ambient temperature probe containing NH_2NO_2, with the cryogenic window held at -180°C.

"energetic event" occurring at a reproducible temperature very close to the melting point. Furthermore, with NH_4NO_3, the only ions observable were the acid-base components (i.e., products that are endothermically generated, and which cannot be responsible for autoacceleratory decomposition.

The fact that parts of the bulk sample have already undergone (partial) thermal decomposition at ambient temperature is not surprising in view of the thermal instability of NH_2NO_2. We postulate that small bubbles of NH_2NO_2 decomposition products form throughout the bulk material storing H_2O and N_2O under pressure. While evaporation occurs layer-by-layer, occasionally a "bubble" close to the surface bursts, releasing its content into the gas phase.

Figure 5 displays a FTIR absorption spectrum obtained from an evaporating NH_2NO_2 sample. The effluent was collected at about -190°C (which is still too warm for N_2O to condense in view of the low background pressure). Even if major amounts of NH_2NO_2 heterogeneously decomposed according to equation (2) in the probe, we would still expect a significant IR absorption due to NH_2NO_2 because cryogenic films of amorphous H_2O are relatively weak absorbers. They absorb around 3220 cm^{-1} with shoulders at 3360 and 3150 cm^{-1}. In addition, weaker bands at 2220, 1690 and 800 cm^{-1} can be observed for thick amorphous films of H_2O. The spectrum displayed in Figure 5 is simple and shows the asymmetric and symmetric NH_2 stretch vibrations at 3435 and 3291 cm^{-1} as well as the strong asymmetric and symmetric NO_2 stretch vibrations at 1535, 1491 (doublet) and 1396 cm^{-1}, respectively. The agreement with the literature spectrum obtained by Davies and Jonathan[7] is good, considering that they recorded an absorption spectrum of a crystalline film at ambient temperature, whereas the spectrum of Figure 5 is from a low temperature amorphous thin film. The simplicity and intensity of the spectrum are very suggestive of the existence of relatively isolated units in a disordered solid.

After deposition of the NH_2NO_2 film shown in Figure 5 above was complete, the cryostat was allowed to slowly warm up, and at -113°C large amounts of desorbing H_2O were recorded by mass spectrometry at m/e 17 and 18. Upon further warming, the rate of H_2O desorption reached a minimum at -82°C with m/e 30, 44, 46 and 62 steadily increasing. Apparently, the large H_2O desorption rate was due to the presence of an amorphous water film deposited in the course of evaporation of NH_2NO_2 and its concurrent heterogeneous decomposition to H_2O via Reaction (2). The surge in the masses at m/e 30, 44, 46 and 62 stems obviously from evaporation /decomposition of the intact NH_2NO_2 in the cryogenic film. Upon further warming, m/e 17, 18, 28, 30, 44, 46 and 62 all increased dramatically to a maximum at -46°C cryostat temperature. From the decrease in the intensity ratios m/e 62 ($NH_2NO_2^+$) vs. 46 (NO_2^+), 18, 30, and 44 with increasing cryostat temperature in the range -56°C to -38°C (above which m/e 62 virtually

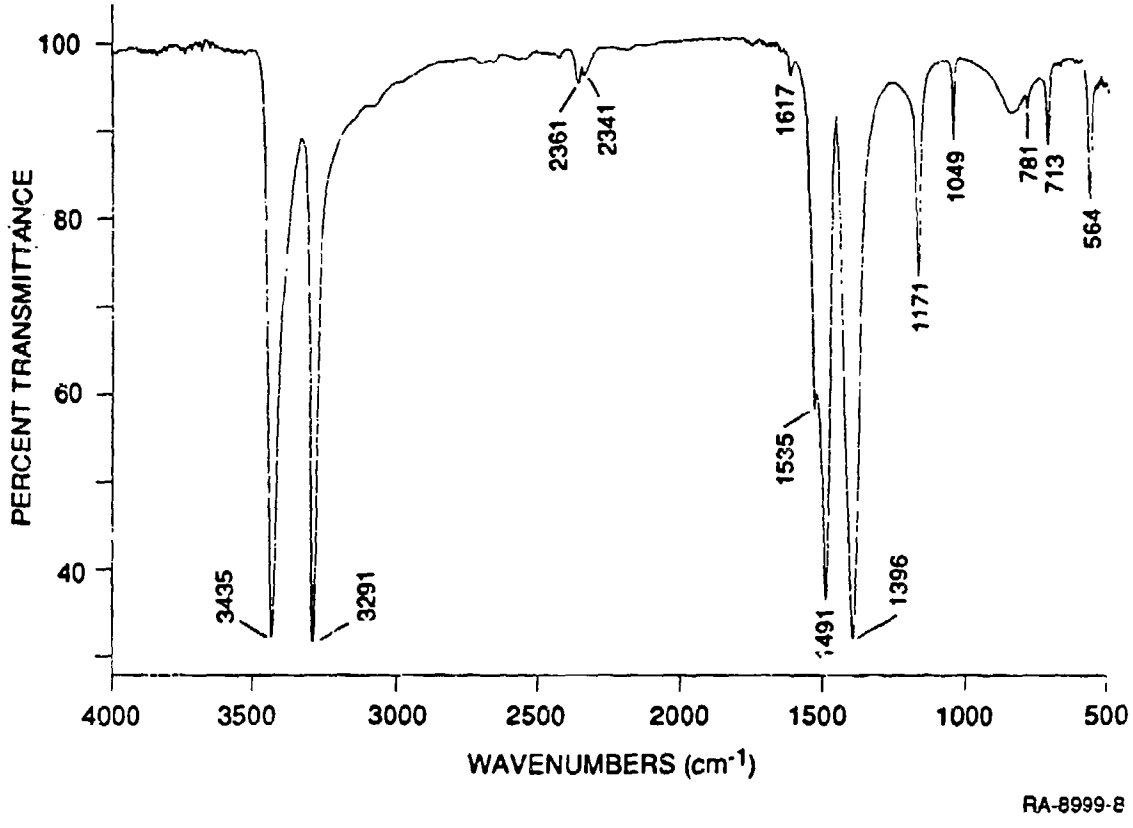

Figure 5. FTIR transmission spectrum of NH_2NO_2 obtained from a thin film deposited onto a -190°C KCl window by evaporation from an ambient temperature probe.

vanishes), we see that Reaction (2) is facile even at very low temperatures. Furthermore, this observation establishes the existence of different parents on the one hand for m/e 62, the molecular ion of NH_2NO_2, and on the other hand for some portion of all the other important fragment ions.

In view of a high $\Delta H°$of 63.5 kcal/mol for dissociation[8] of NH_2NO_2 into NH_2 and NO_2 (assuming a sublimation enthalpy of 10.0 kcal/mol for nitramide) we assume that reaction (2) follows another, heterogeneous route leading directly to N_2O and H_2O. From the recent work of Arrowsmith, et al.[6], and earlier work,[9] we expect that this heterogeneous process is a base-catalyzed reaction. We interpret the occurrence of m/e 46 as due to reaction (3), occurring as a minor reaction pathway under the present conditions :

$$NH_2NO_2 \Rightarrow 0.5\ N_2O + 0.5\ HNO_3 + 0.5\ NH_3 \qquad (3)$$

In this interpretation, m/e 46 is due partly to the evolution of HNO_3, whose base peak is m/e 46. Small amounts of NH_3 are obscured due to the abundance of H_2O.

To summarize our observations with NH_2NO_2, under the low-pressure conditions of this experiment, the high vapor pressure of nitramide results in substantial sublimation from the probe, even at ambient temperature, as evidenced by the molecular ion at m/e 62, and by redeposition of an apparently amorphous film of NH_2NO_2 on the cold cryostat, together with some water. Nevertheless, the decomposition pathway to produce N_2O and H_2O (Reaction 2) is so facile that there is substantial decomposition of material evaporated from the cryostat while it is still at -40°C, apparently as a result of catalysis on the chamber walls (which are normally heated to ~40°C above room temperature). A parallel, but minor, reaction channel leading to HNO_3 is also observed. What stands out is the high rate of both Reactions (2) and (3) at the observed low temperatures.

$NH_4N(NO_2)_2$ (ADN)

Although ADN is, in a formal sense, the dimer of NH_2NO_2, there is no great expectation that ADN will behave substantially like nitramide itself. Reactions (4), (5) and (6) describe several stoichiometric decomposition possibilities:

$$NH_4N(NO_2)_2 \Rightarrow NH_3 + HN(NO_2)_2 \Rightarrow NH_3 + HNO_3 + N_2O \qquad (4)$$

$$\Rightarrow 2\ NH_2NO_2 \Rightarrow 2\ N_2O + 2\ H_2O \qquad (5)$$

$$\Rightarrow NH_4NO_3 + N_2O \qquad (6)$$

This formal relationship of NH_4NO_3 and NH_2NO_2 with ADN is the reason for including the simpler nitrate and nitramide in this study under similar experimental conditions. We will present and discuss the results on ADN in two parts. The first involves pyrolysis experiments of ADN with the cryostat at ambient temperature, at which only the less volatile thermal decomposition products will condense onto the KCl window. The second part involves ADN pyrolysis with a cold cryostat, where only gas phase components not condensing on the cryostat, such as N_2O, NO and NH_3, are monitored by mass spectrometry. The comparison between these two modes has allowed us to draw some important mechanistic conclusions on the thermal behavior of ADN. In addition, the subsequent evaporation or thermal decomposition of the thin film condensate deposited on the cryostat, leads to some further insights.

ADN Pyrolysis with ambient temperature cryostat. Figure 6a presents a mass scan during the pyrolysis of ADN at 169°C. We observe large mass spectrometric signals at m/e 16, 17, 30, 44, and weaker ones at 28 (in addition to the contribution from background air), 46 and 60. We interpret the mass spectrum in terms of evolution of NH_3, NO and N_2O together with smaller amounts of free $HN(NO_2)_2$ monitored at m/e 46 (NO_2^+) and 60 (NNO_2^+). This latter fragment is also observed in electron-impact mass spectra of dimethylnitramine ($(CH_3)_2NNO_2$), a frequently used model compound for explosives studies. Within experimental uncertainty we did not observe the evolution of HNO_3, with the exception of the very first few, lower temperature runs at the beginning of the study, where the vacuum chamber was not warmed to the ca.70°C used throughout the rest of the study. Under those earlier conditions, m/e 46 was more intense than m/e 44 (see Figure 6b) and m/e 63 was observed as an unambiguous marker for the presence of HNO_3. Figure 6c shows the significant decline of m/e 46 that results from increasing the temperature less than 20°C. In evaluating this result one has to keep in mind that the neutral parent species collides many times with the walls of the stainless steel walls before being ionized (residual gas analysis). The absence of HNO_3 in the later ADN decomposition runs most likely has to do with its heterogeneous decomposition on seasoned metal walls (which were then being heated to about 70°C), a fact alluded to earlier in the discussion of the sublimation of NH_4NO_3. At 170°C, NH_3 and NO evolution increase, whereas m/e 46 and 60 decrease substantially. This decrease apparently signals the thermal decomposition of $HN(NO_2)_2$ becoming important at temperatures around 170°C.

When ADN is heated under our conditions, it exhibits "explosive" behavior similar to NH_4NO_3, in that it gives a single pressure burst observed at several masses. The measurement of the time dependent evolution of NH_3 at m/e 17, of H_2O at m/e 18, and of N_2O at m/e 44 as a function of temperature revealed an onset of thermal decomposition of about 90°C and a maximum

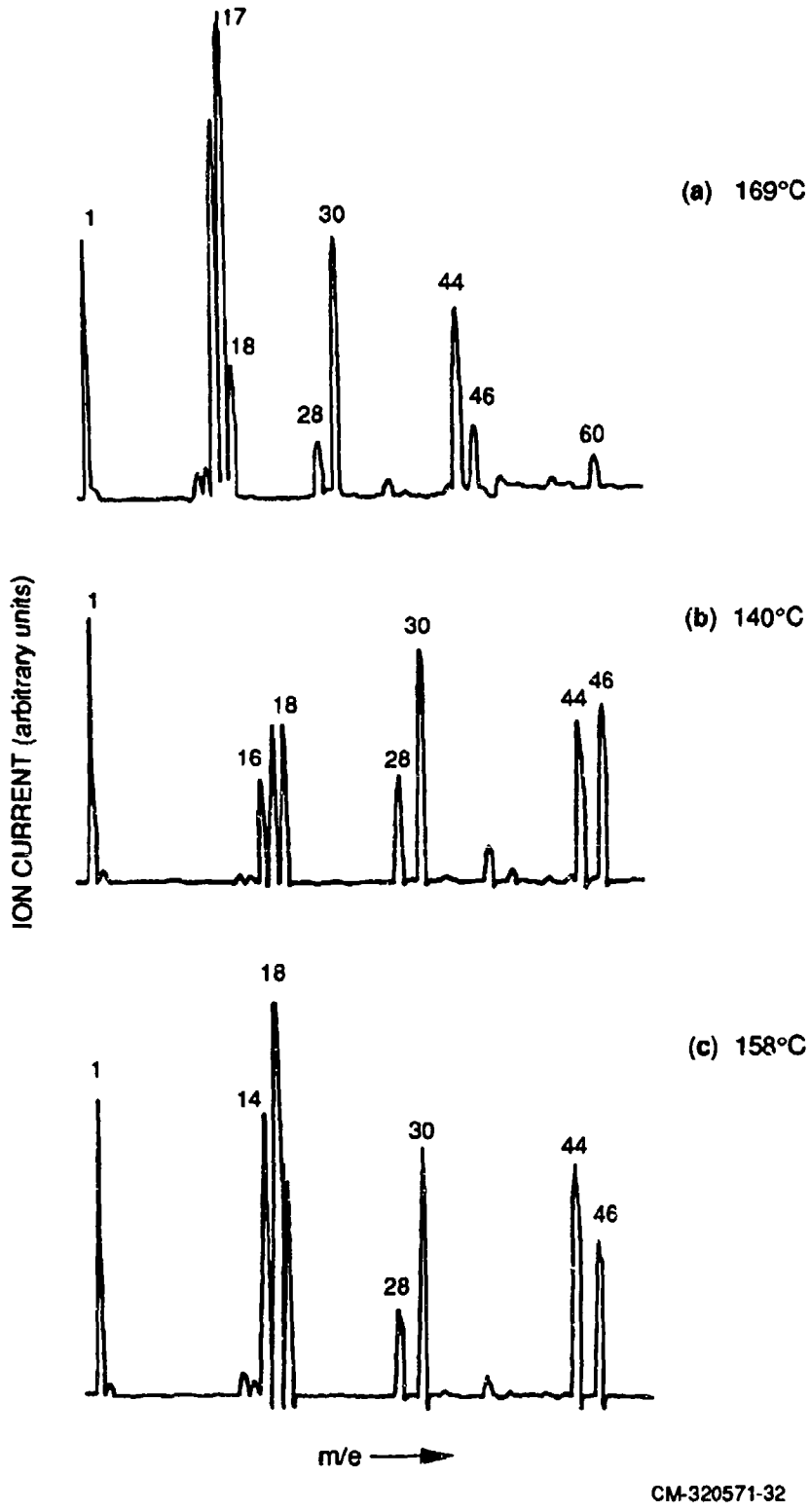

Figure 6. Mass spectra of $NH_4(NO_2)_2$ (ADN).

(a) 169°C probe temperature and ambient temperature cryostat.
(b) 140°C probe temperature taken at beginning of the study.
(c) Same as (b) except probe temperature of 158°C.

in decomposition rate at about 155°C. The exact numbers depend somewhat on the heating rate, but the temperature dependent evolution occurs over a significantly narrower temperature range than NH_4NO_3 dissociation (onset at 74°C, maximum rate at 182°C). This difference is thought to have important ramifications in applications of ADN. As with NH_4NO_3 and NH_2NO_2, we observed bursts of H_2O released into the gas phase before the onset of NH_3 release. The importance of this effect again correlates with the quality (purity) and age of the sample. However, our limited set of data does not distinguish between H_2O as a product of a particular decomposition reaction (such as Reaction 2 or 5) or as a result of water-uptake due to the hygroscopic nature of the sample.

Figure 7 presents a FTIR absorption spectrum of the pyrolysate of ADN from a probe heated to 196°C and condensed on an ambient KCl window. We conclude that it corresponds to pure dinitraminic acid ($HN(NO_2)_2$) or "HDN" by virtue of the pyrolysis results discussed below and the simplicity of its IR absorption spectrum. The weak absorption at 3250 cm^{-1} corresponds to the N-H stretching mode. The lineshape of this band suggests an isolated vibrational mode pertaining to a molecular crystal, analogous to the situation encountered in NH_2NO_2. Upon closer examination, the peak positions of HDN (Figure 7, lower part) do not correspond exactly to those of ADN (Figure 7, upper part), which indicates that the fundamental frequencies are significantly perturbed in going from HDN to its ammonium salt (ADN). The IR absorption spectrum is characterized by the symmetric and asymmetric NO_2 stretching and bending motions, the latter being split into doublets indicating degenerate interaction of the two NO_2 groups. A more detailed interpretation of the FTIR absorption spectrum lies beyond the scope of this paper and will be presented elsewhere.[10] The condensate on the ambient temperature KCl window resulting from the pyrolysis of ADN seems to be *pure* HDN in, view of the identity of the other pyrolysis products, namely N_2O, H_2O and NH_3 which do not condense under these experimental conditions. Obviously the sticking coefficient of NH_3 onto what is, at least in the bulk, condensed molecular HDN, is too low at ambient temperature to allow regeneration of ADN, in contrast to the case of NH_4NO_3 discussed above, where small amounts of NH_4NO_3 are re-formed at ambient temperature. This is clearly a kinetic effect since ADN is a stable crystalline solid at ambient temperature and the pressures that pertain in this apparatus.

We attempted to regenerate ADN *in situ* from a deposited film of HDN by exposing the film to various pressures of NH_3 for variable lengths of time at and slightly above ambient temperature. The high vacuum system was backfilled with NH_3 at 6×10^{-6} Torr for 15 minutes without measurable change in the FTIR absorption spectrum or decrease in the partial pressure of NH_3. Thus, we did not observe any sign of conversion of the thin HDN film to ADN, whose absorption spectrum will be discussed below. (This NH_3 pressure is substantially higher than the

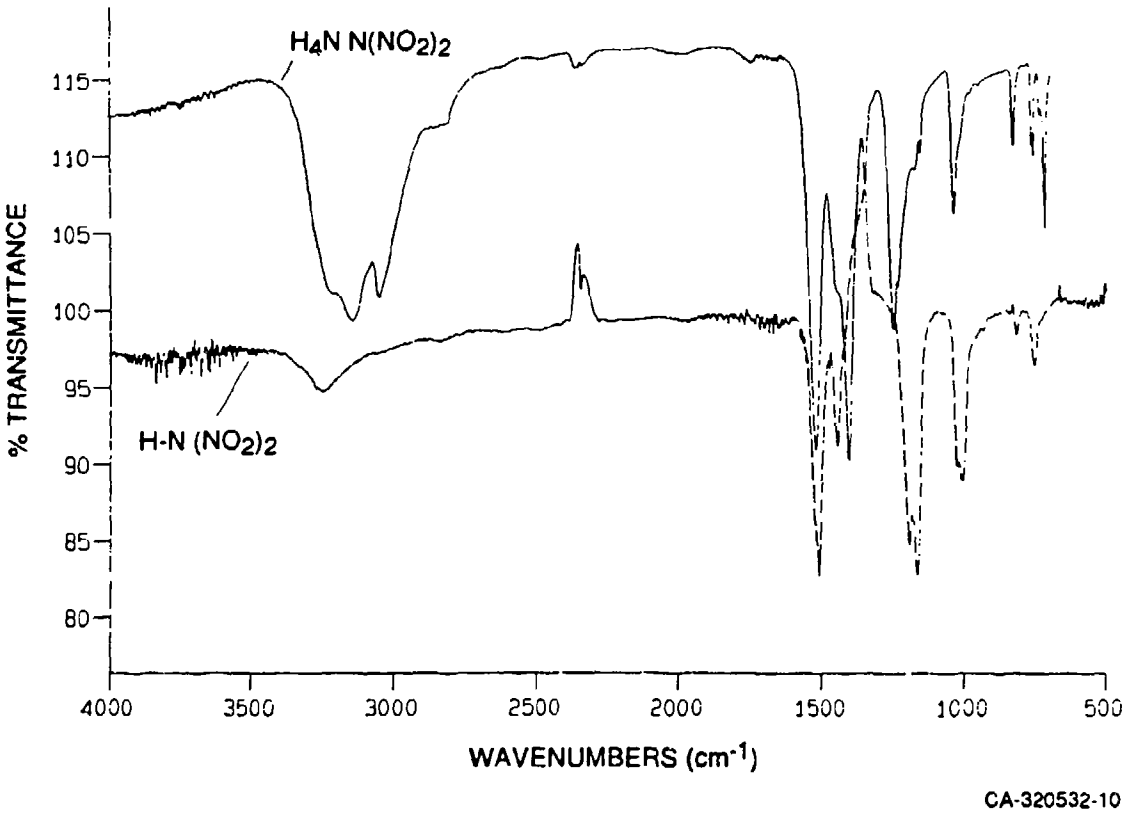

Figure 7. Comparison of FTIR absorption spectrum of $HN(NO_2)_2$ deposited on ambient temperature KCl window from pyrolysis of ADN (probe temperature up to 196°C) with FTIR spectrum of an authentic $NH_4N(NO_2)_2$ sample.

chamber pressure during the course of re-formation of ADN on a cold cryostsat; it presumably results in at least a NH_3 partial pressure in the immediate vicinity of the cryostat comparable to that which exists during effusion of the ADN components from the pyrolysis probe). This inability to convert HDN to ADN suggests that transport of NH_3 across a thin solid film of ADN is an important limiting factor. Apparently, the regeneration of a solid film of ADN occurs most readily when the components strike the surface together. By microscopic reversibility, the acid-base dissociation of ADN has to occur sequentially, that is layer-by-layer. However, an obvious exception is the result of "bubble" formation in the interior of the bulk phase at slow heating rates or over long time intervals, as discussed above. For these solid state kinetic phenomena, questions of sample crystallinity and crystal defects are of obvious importance and are not discussed here. An alternative explanation for the inability to regenerate ADN from an already-deposited film of HDN is that the latter film is in reality potassium dinitramide, KDN, formed by ion-exchange on the ambient-temperature cryostat. We consider this less likely because the "HDN" film (Figure 7) differs significantly in the 700-800 cm^{-1} region from a spectrum of authentic KDN. Furthermore, the authentic potassium dinitramide is *slightly* more stable than ADN, whereas the film we have identified here as HDN, is distinctly *less* stable.

The pyrolysis of this thin film of deposited HDN resulted in the rapid evolution of H_2O, NO and N_2O beginning at ~70°C (immediately after turning on the cryostat heater). Most importantly, no NH_3 was evolved, consistent with our earlier conclusion that ADN pyrolysis yielded pure HDN containing no trapped NH_3 upon condensation. Furthermore, no gas phase HDN was observed (m/e 46, 60) indicating that HDN decomposed on the very modestly heated KCl surface before evaporation, in contrast to pyrolysis of ADN in the melting tube capillary at ca. 150°C. Using the FTIR absorption spectrum as a monitor for the pyrolysis of HDN, we could see that it began to decompose at 70°C and was consumed by 140°C. This result puts an upper limit of ~70°C for even short-term stability of *condensed phase* HDN. However, at ambient temperature (50-60°C) HDN was stable under vacuum for at least 4 hours. Interestingly, there was no increase in optical density of HDN (on an ambient-temperature cryostat) upon ADN pyrolysis at probe temperatures in excess of 140°C, even though ADN could be redeposited on a cold cryostat for probe temperatures approaching 200°C. Apparently, the plume of products emanating from a probe at 140°C or above contains enough decomposition products to promote destruction of any remaining intact vapor phase HDN as it strikes the ambient-temperature cryostat, but not enough to promote decomposition of HDN as it strikes a cold cryostat.

The results presented so far lead to the following conclusions regarding the fate of ADN under thermal stress in vacuum. The pyrolysis of ADN performed in a Pyrex melting tube capillary occurs according to reactions (7), (8) and (9):

$$NH_4N(NO_2)_2 \Rightarrow NH_3 + HN(NO_2)_2 \quad (7)$$

$$HN(NO_2)_2 \Rightarrow N_2O + HNO_3 \quad (8)$$

$$HNO_3 \Rightarrow 0.5\ H_2O + NO + 0.75\ O_2 \quad (9)$$

Reaction (7) describes a dissociation of ADN analogous to NH_4NO_3. Subsequently, HDN partially condenses on the cryostat, while NH_3 is pumped away. The other part of free HDN decomposes on the chamber walls or in the probe according to Reactions (8) and (9). In early experiments we obtained unambiguous proof of gas phase HNO_3, whereas in later experiments reaction (9) was apparently much faster than reaction (8), precluding mass spectrometric detection of HNO_3. We believe reaction (9) to be occurring heterogeneously on the walls of the warmed stainless steel vacuum chamber, as discussed earlier. It is well known[11] that HNO_3 can decompose heterogeneously according to reaction (10).

$$HNO_3 \Rightarrow NO_2 + 0.5\ H_2O + 0.25\ O_2 \quad (10)$$

However, if Reaction 10 were occurring here, we should have seen NO_2 as a major reaction product, but it was not observed in significant quantities. On the other hand, we observed large amounts of NO consistent with reaction (9), which we believe is the major heterogeneous destruction pathway for HNO_3. The exact mechanism of the heterogeneous reactions (9) and (10) is not known. They are both endothermic, by 11.1 and 24.8 kcal/mol, respectively, but are both exoergic at 300°C by 5.9 and 2.7 kcal/mol, respectively.[12] High temperature favors reaction (9) over reaction (10) in view of the significantly higher reaction entropy of 45.9 e.u. vs. 28.4 e.u.. In the absence of more accurate mechanistic information and measured temperature profiles (that might indicate hot spots) we will postpone any more quantitative explanations.

The pyrolysis of a thin solid film of HDN on the surface of the KCl substrate occurs according to equation (11), which is the sum of reaction (8) and (9):

$$2HN(NO_2)_2 \Rightarrow 2\ N_2O + 2\ NO + H_2O + 1.5\ O_2 \quad (11)$$

We prefer in this case to express the molecular processes using Reaction (11) because HNO_3 was not itself observed during decomposition of pre-deposited HDN films. Presumably, HNO_3 is a reaction intermediate but is not observed due to its rapid decomposition on the walls of the warm vacuum chamber. The high sensitivity of HDN to decomposition in the condensed phase is suggestion of reaction via self-protonation. Protonation could then quite reasonably lead to

formation of HNO_3, as is suggested in Scheme 1. However, we note that direct decomposition to N_2O, NO, and H_2O, and O_2 bypassing HNO_3 formation entirely, cannot be ruled out for a substantial portion of the HDN.

ADN Pyrolysis with a Cold Cryostat. Essentially identical experiments were performed as described in the previous section with the exception that the cryostat was cooled, usually to between -160°C to -180°C before the start of the pyrolysis experiment. The gas evolution starts with the appearance of NH_3 and N_2O at a probe temperature of 90°C, together with some NO. At 130°C probe temperature, the transmission of the cryogenic KCl window starts to drop by forming an amorphous H_2O film. NH_3 and N_2O are the dominant species in the mass scans with H_2O starting to appear and a small but significant amount of NO appears. At 150°C, NH_3 and N_2O are still dominant, NO and H_2O are significant and m/e 46 and 60 indicate the presence of gas phase HDN. The surprising occurrence of gas phase H_2O despite a cold cryostat is probably due to the fact that HNO_3 decomposes somewhere on the walls of the vacuum chamber (i.e., downstream from the cryostat), releasing NO and H_2O according to reaction (9). At a nominal temperature of about 170°C, NH_3, N_2O, NO and H_2O are all of comparable magnitude with HDN evolution reaching a maximum. However, the presence of small amounts of HNO_3, which was observed in significant amounts in the early experiments, cannot be excluded. Finally, as 200°C is approached, the maximum rate of evolution of NH_3, H_2O, NO and N_2O is observed, but by this temperature the HDN flux has decreased significantly. By 220°C, the sample is totally expended, and all signals have fallen to near background levels.

These results are essentially identical to the ones obtained with the ambient cryostat, with the exception perhaps of the abundance of H_2O. Referring to reactions (7), (8) and (9), the presence of NH_3 unambiguously points to the dissociation of ADN into its acid and base components. The pronounced abundance of NH_3 in the presence of a cold cryostat is perhaps surprising and is in contrast to the NH_4NO_3 case which shows more modest amounts of NH_3. We take this large amount of NH_3 as an indication of a large extent of decomposition of HDN without which NH_3 is "orphaned" in that it lost its anchor to form ADN on the cold cryostat surface, and/or as an indication of kinetic difficulty in reforming ADN. Consistent with this scenario, we observe the products of the heterogeneous decomposition of HDN, namely N_2O (reaction (8)), and the secondary decomposition products of HNO_3: NO and H_2O (reaction (9)). The present experiments do not address the question of the mechanism by which the heterogeneous decomposition of HDN and HNO_3 occurs. This question can only be addressed by experiments with variable surface-to-volume ratios.

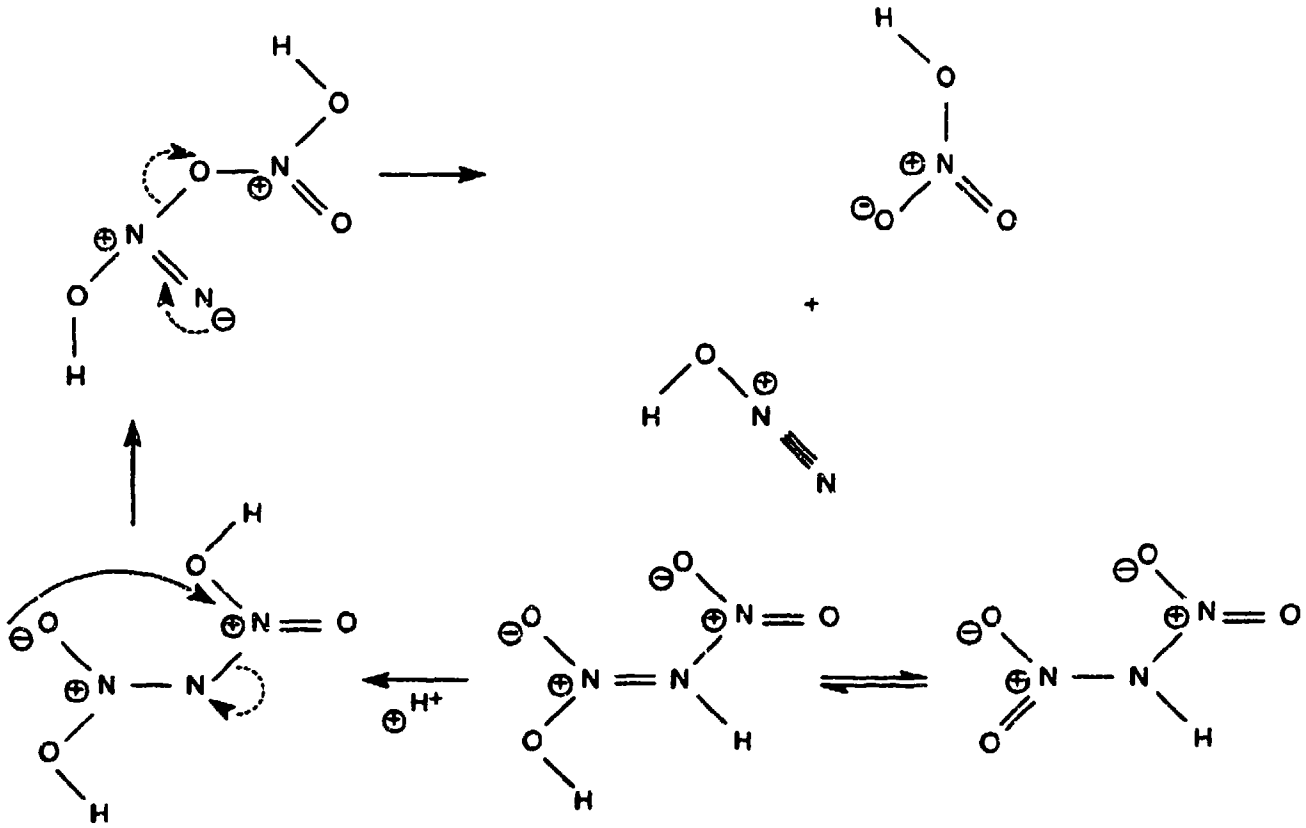

Scheme 1. Potential acid-catalyzed decomposition of HDN via its aci- form.

Figure 8 displays a FTIR absorption spectrum of the ADN pyrolysate, where the probe had been heated to T<200°C and the sample collected on the cryostat. A comparison of the absorption spectrum with an authentic polycrystalline sample of ADN dissolved in ethanol and spread over a KCl window revealed that the major component of the condensate was indeed ADN, which had been regenerated from the gas phase components. In comparing the vapor deposited with the polycrystalline ADN (Figures 8 and 7, respectively), one observes that the intensity of many absorption bands have changed significantly, but the band positions are usually identical within experimental error. A comparison with an ADN sample dispersed in a KBr pellet leads to similar observations. Apparently, ADN is regenerated from its vapor phase components on the cold surface in exactly the same manner as NH_4NO_3. In the microscopic process of ADN regeneration, NH_3 hits an already adsorbed HDN to form the ammonium salt. We have some indications (see below) that the condensed phase also contains some "free" HDN despite the presence of the observed large amounts of NH_3. An investigation of the morphology of the condensed film would be of great interest here because of the differences in the ease of decomposition of ADN and HDN and the consequent implications for storage stability of ADN.

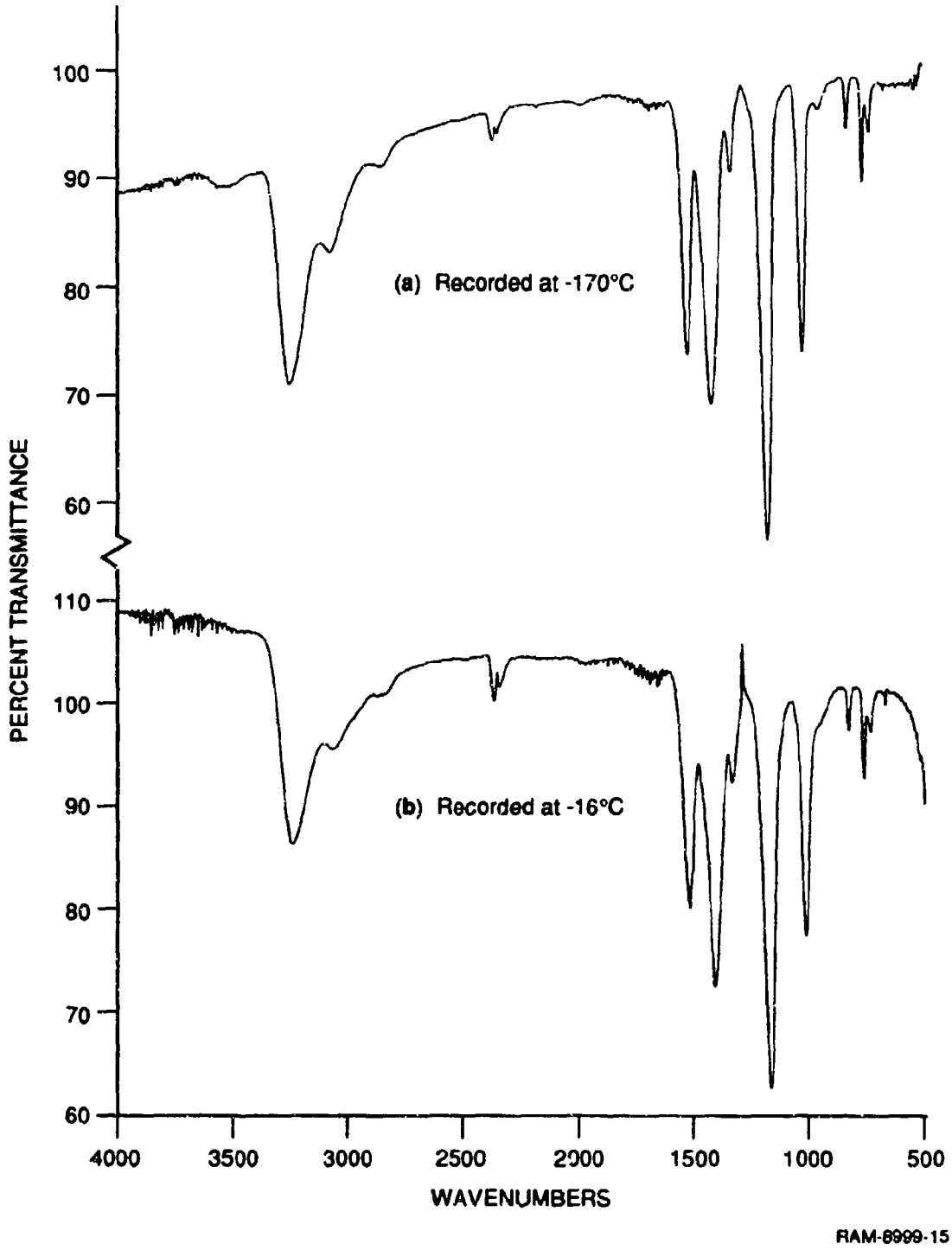

Figure 8. FTIR spectra of SRI-12 decomposition products condensed at -170°C.

The first increase in IR absorption of the cryogenic KCl window after the start of ADN pyrolysis is caused by the deposition of a pure amorphous H_2O film characterized by a broad peak at 3250 cm^{-1} with two shoulders, as discussed above. At higher pyrolysis temperatures (130°C), a similar broad absorption at 3500 cm^{-1} grows in in conjunction with the broad and complex IR absorption at lower frequency due to the presence of the NH_4 ion in regenerated ADN. This higher frequency absorption at 3500 cm^{-1} is also associated with the presence of condensed phase H_2O, as can be seen from mass the spectrometric evidence (see below). From 130° to 200°C probe temperature, after which the ADN sample is spent, the FTIR absorption spectrum does not change qualitatively except that it grows in intensity.

If the cryostat is subsequently slowly heated up, a H_2O burst is observed at approximately -110°C cryostat temperature without much change in the FTIR spectrum. The H_2O that condensed first on the KCl window giving rise to the amorphous water layer evaporates first, apparently moving through the condensed layer of ADN. The next "wave" of H_2O is released in the temperature range -77° to -61°C and is accompanied by the disappearance of the 3500 cm^{-1} absorption, but otherwise by little change in the FTIR spectrum, as can be seen in the spectrum in Figure 8b. In some cases, when H_2O is desorbed from the film, a sloping baseline appears in the FTIR absorption spectrum, with increasing absorption at higher frequency. Such a change is typical of an increase in surface roughness that increases the scattering properties of the amorphous matrix, and could easily result from the loss of a portion of the matrix.

From about -30°C to ambient cryostat temperature, the only products evaporating are NH_3 and HDN, at a small rate. At the same time, the optical density around 3250 cm^{-1} due to the N-H stretching mode in NH_3 decreases noticeably. This can be described as an annealing process that purifies the ADN layer of those constituents (NH_3 and HDN) that were isolated in the matrix. Concomitantly, the structure of the remaining ADN matrix is annealed, leading to an intensity enhancement of the characteristic ADN absorption. However, we want to point out that HDN condensed on an ambient temperature KCl window is relatively stable at ambient temperature as demonstrated by the persistence of its FTIR absorption spectrum (Figure 7). With the cryostat returning to ambient temperature, the evolution of NH_3 and N_2O pick up, and beyond that temperature, the pyrolysis products are identical to the case of ADN pyrolysis with ambient temperature cryostat. Concomitantly, the optical density of the KCl window decreases until the original percent transmission is reached at about 200°C.

SUMMARY

The results of ADN pyrolysis show that the behavior of ADN at slow heating rates under high vacuum is controlled by dissociation into its components NH_3 and HDN. On an ambient temperature cryostat, HDN can be trapped and stored indefinitely under high vacuum, whereas it regenerates ADN on a cold cryostat (-190°C) in the presence of gas phase NH_3. This behavior is analogous to the response from NH_4NO_3 in the same type of experiment. The regeneration of ADN must occur by collisions of gas-phase NH_3 onto condensed HDN, similar to the regeneration of NH_4NO_3. In addition, fast secondary (presumably heterogeneous) decomposition of HDN both in the probe as well as on the heated cryostat yields N_2O and HNO_3. The latter secondary pyrolysis product also undergoes fast heterogeneous decomposition in our apparatus, producing mostly NO, which served as a marker for the heterogeneous decomposition of HNO_3. This aspect is also analogous to NH_4NO_3, where an "excess" of NH_3 was observed in thin condensed films of NH_4NO_3 due to HNO_3 decomposition. Decomposition of condensed phase HDN is evidently much more facile than of isolated HDN molecules (either gas phase or in contact with a surface): marked decomposition of HDN condensed on the cryostat occurs below 70°C, but gas phase HDN survives transit from the heated capillary at temperatures up to 200°C. This behavior is consistent with decomposition via self-protonation.

The morphological and optical properties of evaporating condensate films from ADN pyrolysis are interesting and annealing studies could lead to increased mechanistic understanding of ADN thermal decomposition. In particular, understanding the kinetic barriers that make it difficult to convert a preexisting HDN film to ADN may provide insight into factors that hinder the reverse process -- dissociation -- and thus inhibit the outright chemical decomposition of ADN. Pyrolysis of ADN under our experimental conditions does not lead to observation of potential intermediates such as NH_4NO_3 (Reaction (6))or NH_2NO_2 Reaction (5)). Therefore a scission of ADN into its "monomer" NH_2NO_2 does not take place under the present experimental conditions.

REFERENCES

1. Hamel, X. X.; Olsen, X. X., U.S Patent 3,428,667, Feb. 18, 1969.
2. Bottaro, J. C.; Schmitt, R. J. Unpublished work, 1991.
3. Brower, K. R.; Oxley, J. C.; Tewari, M. *J. Phys. Chem.* **1989**, *93*, 4029
4 Rosser, W. A.; Inami, S.; Wise, H. *J. Phys. Chem.* **1963**, *67*, 1753
5. L. Friedman and J Bigeleisen, *J. Chem. Phys.* 18(10), 1325 (1950).
6. Arrowsmith, C. H.; Awwal, A.; Euser, B. A. ; Kresge, A.J.; L. Lau, P. P. T.; Onwood, D. P.; Tang; Y. C.; Young, E. C. *J. Am. Chem. Soc.* **1991**, *113*, 172
7. Davies, M.; Jonathan, N. *Trans. Farad. Soc.* **1958** *54*, 469.
8. Ray, J.O.; Ogg, R. A., Jr., *J. Phys. Chem.* **1956**, *60*, 1956.
9. Bronsted, J. N.; Pedersen, K. *Z. Phys. Chem.* **1924**, *108*, 185.
10. Rossi, M. J., in preparation, 1991.
11. Svensson, S. and Ljungstroem,E. *Int. J. Chem. Kin.* **1988** *20*, 857
12. Stull, D. R.; Prophet, H. *JANAF Thermochemical Tables*, National Standard Reference Data Series, NSRDS-NBS37, Nat. Bur. Stand., Washington D.C., 1971.

ACKNOWLEDGEMENT

Support of this work by the Energetic Materials Program of the Office of Naval Research, administered by Dr. Richard S. Miller under Contract N00014-90-0115, is gratefully acknowledged.